

Master's Programme in Advanced Energy Solutions

Integrating Battery Energy Storage Systems for Wind Power Imbalance Management and Market Participation in Nordics

Saku Snabb

Copyright ©2025 Saku Snabb

Author Saku Snabb

Title of thesis Integrating Battery Energy Storage Systems for Wind Power Imbalance Management and Market Participation in Nordics

Programme Advanced Energy Solutions

Major Energy Conversion Processes

Thesis supervisor Prof. Sanna Syri

Thesis advisor D.Sc. Ilari Alaperä

Collaborative partner Fortum Oyj

Date 19.09.2025 **Number of pages** 141 **Language** English

Abstract

Nordic countries are attracting investments in large electricity-consuming facilities, such as data centres, green hydrogen, and electrification of heavy-industry. As consumption increases, generation must also grow, mainly through new wind power. However, wind power challenges the balancing and reliability of the power system, and causes imbalance-related costs for operators due to its intermittent generation. Flexible balancing is essential, and Battery Energy Storage Systems (BESS) have proven most promising for addressing imbalance challenges. BESS have shown significant value in reserve markets, but little study has examined the value in imbalance management alongside multi-market optimisation in the Nordic market environment.

This thesis investigates the potential of co-located BESS optimised to operate simultaneously in imbalance management and market participation. Its objective is to evaluate how imbalance management affects the profitability of BESS investments and how capacity is allocated in multi-market optimisation. A simulation model was developed for a 10 MW lithium-ion battery with 20 MWh and 40 MWh energy capacities, accounting for battery degradation. The simulation uses market data from 2024, and profitability was assessed through capital budgeting methods in Finnish, Swedish, and Norwegian market environments.

The results show that a co-located BESS with a share of its capacity reserved for imbalance management can significantly reduce imbalance cost spikes, thereby decreasing overall system costs. However, the reduced capacity available for market participation leads to greater losses in market revenues, which is not fully offset by imbalance cost savings. Therefore, reserving less fixed capacity for imbalance management improves potential profitability. Finland showed the highest value for imbalance management, followed by Sweden, where profitability remained strong for both countries even with 70% of capacity allocated to imbalance management. Solely relying on imbalance management proved to be unprofitable. Most market revenues were generated in capacity markets, mainly in frequency containment reserve markets. Finland showed a well-diversified revenue stream, while Sweden and Norway had less diversification.

Keywords Battery Storage System, BESS, Market Optimisation, Wind Power, Imbalance Management, Reserve Markets, Electricity Markets, BESS Profitability

Tekijä Saku Snabb

Työn nimi Akkusähkövarastointijärjestelmän integrointi tuulivoiman tasehallintaan ja markkinaosallistumiseen pohjoismaissa

Koulutusohjelma Advanced Energy Solutions

Pääaine Energy Conversion Processes

Vastuuopettaja/valvoja Prof. Sanna Syri

Työn ohjaaja D.Sc. Ilari Alaperä

Yhteistyötaho Fortum Oyj

Päivämäärä 19.09.2025 **Sivumäärä** 141

Kieli Englanti

Tiivistelmä

Pohjoismaat houkuttelevat investointeja suuriin sähköä kuluttaviin laitoksiin, kuten datakeskuksiin, vihreään vetyyn ja raskaan teollisuuden sähköistämiseen. Suuremman kulutuksen myötä sähkön tuotanto täytyy kasvaa, pääosin uuden tuulivoiman avulla. Tuulivoima kuitenkin lisää haasteita sähköjärjestelmän tasapainon ja luotettavuuden suhteen sekä aiheuttaa toimijoille tasehallintakustannuksia. Joustava tasapainottaminen on välttämätöntä, ja akkuvarastointijärjestelmät ovat todettu lupaaviksi ratkaisuiksi tasehallinnassa. Akkuvarastointijärjestelmät ovat osoittaneet merkittävää arvoa reservimarkkinoilla, mutta vähän tutkimusta on tehty tasehallinnan taloudellisista hyödyistä multimarkkinaoptimoinnin yhteydessä pohjoismaisilla markkinoilla.

Tämä diplomityö tutkii tuulivoiman oheen sijoitettujen akkuvarastojen potentiaalia, optimoituina samanaikaisesti tasehallintaan ja markkinaosallistumiseen. Tavoitteena on arvioida miten tasehallinta vaikuttaa investointien kannattavuuteen, sekä miten kapasiteetti allokoituu markkinaoptimoinnissa. Simulaatiomalli kehitettiin 10 MW litiumioniakulle, jonka energiakapasiteetit ovat 20 MWh and 40 MWh, huomioiden akun rappeutumisen. Simulaatio hyödyntää vuoden 2024 markkinadataa, ja pitkän aikavälin kannattavuus arvioitiin investointilaskentamenetelmillä Suomen, Ruotsin ja Norjan markkinoilla.

Tulokset osoittavat, että tuulivoiman oheen sijoitettu akkuvarastointijärjestelmä, jonka osa kapasiteetista on varattu tasehallinnalle, voi merkittävästi vähentää kustannuspiikkejä, vähentäen järjestelmän kokonaiskustannuksia. Markkinaosallistumiseen käytettävän kapasiteetin väheneminen kuitenkin johtaa suurempiin tulojen menetyksiin, joita tasehallinnan säästöt eivät täysin kompensoi. Täten tasehallinnan kiinteän kapasiteetin osuutta pienentämällä kannattavuus paranee. Suomi osoitti suurimman arvon tasehallinnassa, toisena Ruotsi, joissa molemmissa kannattavuus säilyi suotuisana, vaikka 70% kapasiteetista oli varattu tasehallintaan. Pelkästään tasehallintaan keskittyvä toiminta osoittautui kannattamattomaksi. Markkinatulot syntyivät pääosin kapasiteettimarkkinoilta, erityisesti taajuusohjatusa käyttö- ja häiriöreserveistä. Suomessa tulot jakautuivat tasaisesti markkinoiden välillä, kun Ruotsissa ja Norjassa hajautus oli heikompa.

Avainsanat Akkusähkövarastointijärjestelmä, BESS, Markkinaoptimointi, Tuulivoima, Tasehallinta, Reservimarkkinat, Sähkömarkkinat, Akuston kannattavuus

Författare Saku Snabb

Titel Integrering av batterienergilagringssystem för obalanshantering av vindkraft och marknadsdeltagande i Norden

Utbildningsprogram Advanced Energy Solutions

Huvudämne Energy Conversion Processes

Ansvarslärare Prof. Sanna Syri

Handledare D.Sc. Ilari Alaperä

Medarbetare Fortum Oyj

Datum 19.09.2025

Sidantal 141

Språk Engelska

Sammandrag

De nordiska länderna attraherar investeringar i stora el konsumerande anläggningar, såsom datacenters, grön vätgas och elektrifiering av tung industri. Med ökande elförbrukning måste elproduktion växa, främst genom ny vindkraft. Vindkraft medför dock utmaningar för elsystemets balans och säkerhet, samt orsakar kostnader inom balanshantering för vindkraftoperatörer. Flexibel balansering är nödvändigt, och batterilagringssystem är ett lovande alternativ för obalanshantering. Batterilagringssystem har visat signifikant värde i reservmarknader, men lite forskning har gjorts om ekonomiska fördelarna inom obalanshantering i kombination med multimarknadsoptimering i Norden.

Denna diplomarbete undersöker potentialen i samlokaliserade batterilagringssystem optimerade för samtidig operation inom obalanshantering och marknadsdeltagande. Syftet är att utvärdera hur obalanshantering påverkar ekonomiska lönsamheten för investering i batterilagringssystem, samt hur kapacitet är allokerat i multimarknadsoptimering. En simuleringsmodell utvecklades för en 10 MW litiumjonbatteri med energikapaciteter av 20 MWh och 40 MWh, med hänsyn till batteridegradering. Simulationen använder marknadsdata från 2024, och den långsiktiga ekonomiska lönsamheten värderades med investeringskalkylmetoder i finska, svenska och norska marknader.

Resultaten visar att samlokaliserade batterilagringssystem, med en del av kapaciteten reserverad för obalanshantering, kan signifikant minska på kostnadstoppar för obalans och därmed minska totala systemkostnader. Den minskade tillgängliga kapaciteten för marknadsdeltagande leder dock till större förluster i marknadsintäkter, vilket inte fullt kompenseras av besparingar i obalanshantering. Därmed, mindre reserverad kapacitet för obalanshantering ger bättre potentiell ekonomisk lönsamhet. Finland visade högsta värdet för obalanshantering, följt av Sverige, där lönsamheten för båda förblev på god nivå även när 70% av kapaciteten var reserverad för obalanshantering. Drift enbart fokuserad på obalanshantering visade sig olönsamt. Marknadsintäkter uppstod huvudsakligen från kapacitetmarknader, främst från frekvenshållningsreserver. Finland visade jämn intäktsfördelning från marknader, medan Sverige och Norge var mindre diversifierade.

Nyckelord Batterienergilagringssystem, BESS, Marknadsoptimering, Vindkraft, Obalanshantering, Reservmarknader, Elmarknader, Batteriets lönsamhet

Table of contents

Symbols and abbreviations.....	8
Symbols	8
Operators.....	10
Abbreviations	10
1 Introduction	12
2 Review on Previous Studies	14
3 Nordic Electricity Markets	18
3.1 Nordic Power System.....	18
3.2 Day-ahead market.....	23
3.3 Intraday market	25
3.4 Frequency Containment Reserve (FCR).....	28
3.5 Fast Frequency Reserve (FFR)	32
3.6 Frequency Restoration Reserve (FRR).....	36
3.6.1 aFRR Markets.....	37
3.6.2 mFRR Markets	38
3.7 Nordic Balancing Model and Imbalance Settlement	40
4 Battery Energy Storage Systems	44
4.1 Energy Storage Systems and Battery Technologies	44
4.2 Overview of Battery Energy Storage Systems	48
4.3 Li-Ion Batteries	50
4.3.1 Battery Components	50
4.3.2 Cathode Materials in Li-Ion Batteries.....	52
4.4 Battery Degradation.....	54
4.5 Economics of BESS	59
4.5.1 CAPEX analysis of BESS	60
4.5.2 OPEX analysis of BESS	62
5 BESS Integration and Wind Power Operation	64
5.1 Wind Power.....	64
5.1.1 Operating principles.....	64
5.1.2 Impact on Power System.....	67
5.2 BESS Applications with Wind Power	70

6	Optimisation Setup	74
6.1	Problem formulation and markets	74
6.2	Simulation input data	75
6.3	Optimisation objective and constraints.....	84
6.4	Economic evaluation.....	89
7	Simulation Results	91
7.1	Results on Operational Performance	91
7.1.1	FI results.....	91
7.1.2	SE2 results	95
7.1.3	NO4 results	98
7.1.4	Summary on operational performance	100
7.2	Economic Evaluation of Scenarios	102
7.2.1	Net cash flow analysis.....	102
7.2.2	Financial summary, NPV and PBT.....	107
7.3	Results of Imbalance Correction	113
7.4	Sensitivity Analysis	118
8	Conclusions and Future Research.....	121
	References.....	124

Symbols and abbreviations

Symbols

RTE	Battery round-trip efficiency
E_{output}	Battery energy output during discharging
E_{input}	Battery energy input during charging
SoC_t	Battery State of Charge at a given moment t
E_t	Battery energy capacity at a given moment t
$E_{battery}$	Nominal energy capacity of battery
SoC_{min}	Minimum State of Charge
SoC_{max}	Maximum State of Charge
L_{cal}	Battery calendar life
f_t	Degradation model function for calendar degradation
\overline{SoC}	Average SoC
\overline{T}_c	Average cell temperature
$t_{el.}$	Elapsed time
L_{cyc}	Battery cycle life
n_i	Indication for full or partial cycle
f_c	Degradation model function for cyclic degradation
DoD_i	Depth of Discharge for cycle i
SoC_i	State of Charge during cycle i
$T_{c,i}$	Cell temperature during cycle i
f_d	Degradation model for calendar and cyclic degradation
D_{cal}	Calendar degradation
a_1, a_2, b_1, b_2, c_1	Fitting parameters
n	Number of equivalent full cycles
$E_{t,p}$	Cumulative energy throughput of battery
E_{kin}	Kinetic energy
m	Mass of air
U	Wind speed
P	Theoretical wind power production
ρ	Density of air
A	Swept area by turbine blades
C_p	Power coefficient of a wind turbine
T_{fee}	Transmission fee
p_h^{DA}	Day-ahead market price for hour h
r_p	Risk premium for calculating transmission fees

F	Margin loss rate for calculating transmission fees
$E_{ch,h}$	Total energy charged for hour h
$E_{ch,h}^{(m)}$	Energy charged for a specific market m for hour h
$E_{dch,h}$	Total energy discharged for hour h
$E_{dch,h}^{(m)}$	Energy discharged for a specific market m for hour h
SoH_h	State of health for hour h
E_h	Degraded energy capacity for hour h
$D_{cal,h}$	Calendar degradation for hour h
$D_{cyc,h}$	Cyclic degradation for hour h
E_{BoL}	Energy capacity at beginning of life
SoC_h	State of charge at start of hour h
$\theta_h^{(m)}$	Committed capacity or energy for a specific market
P_{rating}	Power rating of the battery system
C_{share}	Capacity share reserved for either market participation or imbalance management
$V_{realized,h}^{(m)}$	Real procured capacity volume or energy volume for a specific market
$Bidsize_{min}^{(m)}$	Minimum bid size for a specific market
$Bidsize_{max}^{(m)}$	Maximum bid size for a specific market
θ_h^{FCR-Dd}	Committed capacity for FCR-D down-regulation
θ_h^{FCR-Du}	Committed capacity for FCR-D up-regulation
n_{day}	Maximum amount of cycles per day
C_{imb_share}	Capacity share reserved for imbalance management
C_{market_share}	Capacity share reserved for market participation
p_h^{imb}	Imbalance price for hour h
fee_{imb}	Imbalance fee
$T.fee_{in,h}$	Transmission fee for grid input for hour h
$p_h^{(m)}$	Price for a specific market for hour h
$T.fee_{out,h}$	Transmission fee for grid output for hour h
NPV	Net Present Value
C_a	Net cash flow for year a
r	Discount rate
a	Year
$CAPEX$	Capital Expenditure
PBT	Payback time

Operators

\sum_i^N	Summation over cycles, from $i = 1$ to N
\sum_m	Summation over markets and imbalance management; m
$\sum_{h=1}^{24}$	Summation over 24 hours
$\sum_{a=1}^{PBT}$	Summation over years, from $a = 1$ to the year of payback, PBT

Abbreviations

AC	Alternating Current
aFRR	Automatic Frequency Restoration Reserve
BESS	Battery Energy Storage System
BMS	Battery Management System
BoL	Beginning of Life
BRP	Balance Responsible Party
CAPEX	Capital Expenditures
CET	Central European Time
CM	Capacity Market
DA	Day-Ahead
DC	Direct Current
DoD	Depth of Discharge
DSO	Distribution System Operator
EAM	Energy Activation Market
EBGL	Electricity Balancing Guideline
EFR	Enhanced Frequency Response
EoL	End of Life
EV	Electric Vehicle
FCR	Frequency Containment Reserve
FCR-D	Frequency Containment Reserve for Disturbances
FCR-N	Frequency Containment Reserve for Normal operation
FFR	Fast Frequency Reserve
FRR	Frequency Restoration Reserve
GCT	Gate Closure Time
HVAC	High-Voltage Alternating Current
ID	Intraday
ISP	Imbalance Settlement Period
LCO	Lithium Cobalt Oxide
LER	Limited Energy Reservoir
LFP	Lithium Iron Phosphate
Li-Ion	Lithium Ion
LMO	Lithium Manganese Oxide
LTO	Lithium Titanate

mFRR	Manual Frequency Restoration Reserve
MGA	Metering Grid Area
MTU	Market Time Unit
NBM	Nordic Balancing Model
NCA	Lithium Nickel Cobalt Aluminium Oxide
NMC	Lithium Nickel Manganese Cobalt Oxide
NPV	Net Present Value
O&M	Operation and Maintenance
OPEX	Operating Expenditures
PBT	Payback Time
PCR	Price Coupling of Regions
PCS	Power Conversion System
PPA	Power Purchase Agreement
RoCoF	Rate of Change of Frequency
RTE	Round-Trip Efficiency
SDAC	Single Day-Ahead Coupling
SEI	Solid Electrolyte Interphase
SIDC	Single Intraday Coupling
SOA	System Operation Agreement
SoC	State of Charge
SOGL	System Operations Guideline
SoH	State of Health
TSO	Transmission System Operator
VWA	Volume-Weighted Average
WPP	Wind Power Plant

1 Introduction

Cheap, emission-free electricity is a significant competitive advantage for attracting new green investments and industries to the Nordic countries (Energiategallisuus 2025). Recently, there has been broad discussion about new large-scale electricity-consuming facilities planned in the Nordics, including data centres, green hydrogen production, and the electrification of heavy industry, enabled by favourable conditions and circumstances. Among these, the availability of low-cost, emission free electricity is a key factor. The lowest electricity prices in Europe are found in Norway, Sweden, and Finland (Energiategallisuus 2024). In Finland, electricity consumption is expected to grow by 80% between 2025 and 2035, primarily driven by industrial demand and data centres (Pantzar 2024). In Sweden, the projections are similar, with an expected 72% increase (SKGS 2024, p. 6).

To support these electricity-intensive industries, power generation must increase, while remaining emission-free generation to meet carbon neutrality targets. Both Finland and Sweden forecast significant growth in renewable generation. Sweden forecasts that wind and solar power will account for 50% of its electricity mix by 2035, while Finland forecasts a 50% share from wind power alone by 2035 (Energiforsk 2025, p. 8; Pantzar 2024). Achieving these targets will require substantial new investments in renewable energy within the next decade, particularly in wind power.

However, wind and solar power have a major drawback; their intermittent and unpredictable nature, which challenges power system stability. A higher share of wind power increases uncertainty in generation, affecting system reliability. This drives greater demand for real-time balancing mechanisms, including reserve and balancing markets. (Miettinen & Holttinen 2019, p. 227.) Additionally, deviations between forecasted and actual wind power output introduce imbalance-related costs to Wind Power Plant (WPP) operators. While these pose challenges, they also create opportunities for technologies that can enhance real-time balancing and reduce imbalance-related costs.

One promising technology is energy storages, in particular Battery Energy Storage Systems (BESS), as they have attracted attention due to their favourable properties and capabilities. Additionally, recent experience shows that operating batteries in reserve markets is the most profitable application (He et al. 2017, p. 3560). However, there is a risk of saturation in specific markets, as BESS investments have grown rapidly. Globally, installed BESS capacity rose from 20 GW in 2020 to 160 GW in 2024, a 700% increase, largely driven by technological cost reductions (Volta Foundation 2025, p. 138). This risk can be mitigated by diversifying value streams, making it essential to consider other applications.

Integrating BESS with wind power can reduce generation curtailment, diversify value generation, and mitigate saturation risk. In a co-location setup with wind power, BESS can charge during periods with higher wind power generation than expected, and discharge at periods with less generation than expected, so-called imbalance management. (Li et al. 2023, p. 1.) Evaluating BESS investments alongside intermittent power production requires assessing this application, as it can reduce imbalance-related costs. BESS offers multiple value opportunities, including market participation, imbalance management, and other services that enhance system flexibility, which is an increasingly critical requirement in current power systems and markets. Although the potential for BESS to provide both imbalance management and market participation simultaneously, there is little or no research regarding this in Nordic market environments. This gap is the focus of this thesis.

The aim of this thesis is to research the potential of co-locating BESS with wind power, where the BESS is optimised to operate simultaneously in imbalance management and market participation. The primary objective is to determine the optimal capacity allocation for these two applications, and to evaluate how imbalance management affects the profitability of BESS investments. Secondary objectives include identifying the most value-generating markets in multi-market optimisation, and assessing whether imbalance management alone can support economically viable investments. The study is conducted as a quantitative mathematical simulation model for the Finnish, Swedish, and Norwegian market environments, using a BESS rated at 10 MW, with both 20 MWh and 40 MWh energy capacities. This research fills the gap in Nordic market studies, by providing insights into the value of imbalance management. Furthermore, this study supports BESS project evaluations at Fortum Oyj, for whom this thesis was written as an assignment.

After this introduction, *Chapter 2* reviews prior literature on BESS operating in electricity and reserve markets, as well as in imbalance correction, identifying more precisely the research gap for this study. *Chapter 3* provides an overview of the Nordic power system, electricity markets, reserve markets, and imbalance management. *Chapter 4* presents energy storage technologies, focusing on lithium-ion batteries and their technical, operational, and economical characteristics. The literature review ends at *Chapter 5*, which examines wind power operation, its role in the power system, and its integration with BESS. The empirical section begins in *Chapter 6*, which presents the scope, objectives, methodology, and setup of the study. It defines more precisely the research problem, and describes the simulation model and its input data. *Chapter 7* presents and discusses the results, including operational performance, economic evaluation, and the impact on imbalance correction for WPPs. Finally, *Chapter 8* summarises the research, presents the main conclusions, and suggest topics for future work.

2 Review on Previous Studies

The overall utilisation of BESS is a widely studied topic due to its growing importance alongside renewable energy. However, specific project needs and market environments vary, resulting in various research scopes. This chapter reviews seven studies on the operation and profitability of BESS, either as standalone systems or co-located with WPPs. These studies examine BESS operations in reserve and balancing markets, energy arbitrage, and imbalance correction, primarily focusing on Lithium-Ion (Li-Ion) batteries. The reviewed studies utilise modelling of BESS in real market environments, such as the British, Irish, and Nordic markets. *Table 1* illustrates the focus area of each study. The chapter concludes with a summary of the key findings and justification for the scope of this thesis.

Table 1, Focus areas of previous studies

Source	Co-located BESS	Imbalance settlement	Reserve markets	Energy Arbitrage	Nordic markets
Pusceddu et al. (2021)	-	-	✓	✓	-
Hukkinen (2024)	✓	-	✓	-	✓
Sheridan & Conlon (2021)	✓	-	✓	-	-
Fan et al. (2021)	✓	-	✓	-	-
Laine-Ylijoki (2024)	✓	✓	✓	-	✓
Zhu et al. (2023)	✓	✓	✓	✓	✓
Jaakamo (2020)	✓	✓	✓	-	✓

A techno-economic study conducted by Pusceddu et al. (2021) explored standalone BESS operation in the British markets with two distinct revenue streams: arbitrage operation in wholesale electricity markets and participation in fast frequency response. The study identified two main synergies. First, majority of the revenues from arbitrage operation focus on peak hours, which did not interfere with revenues from providing capacity to the fast frequency response market. Second, BESS could be charged at low or no cost outside the deadband of the frequency response market through State of Charge (SoC) management, generating additional revenue streams. The study concluded that simultaneous arbitrage management and fast frequency response participation increased profits by 25% compared to participating solely in the fast frequency response market. The Payback Time (PBT) was calculated to be less than 10 years, with the most optimal battery system size being 1.5–2 hours.

Hukkinen (2024), analysed the profitability of a co-located BESS with a WPP in Finland, using the same grid connection. The analysis focused on revenue streams from Finnish hourly and annual Frequency Containment Reserve (FCR) markets. The study revealed that co-located BESS using the same grid connection was more profitable than standalone BESS due to lower costs, with the hourly market generating higher revenues compared to the annual market. The study also highlighted that grid capacity limitations resulted in less available hours for co-located BESS. However, the loss in revenues was compensated with decreased grid connection costs. The most profitable FCR market was found to be FCR for Normal operation (FCR-N) and the optimal battery size was determined to be 30–40% of the WPP production capacity. Additionally, reserve market saturation posed a significant risk to future revenues for BESS in reserve markets.

Sheridan and Conlon (2021) conducted a case study on the economic and technical aspects of co-located BESS integrated with a WPP in Ireland, focusing on the impact of battery sizing and degradation on economic feasibility. The study examined three scenarios: the base case of a WPP participating in the Day-Ahead (DA) market without a BESS, which proved to be the most profitable; a co-located BESS participating in balancing markets, which created savings, however resulting in negative Net Present Value (NPV) due to high capital costs; and BESS participation in reserve markets, which resulted in positive NPV, making the investment decision profitable with an optimal battery size of 0.5–1 hours. The study concluded that considering battery sizing and degradation are crucial for profitability calculations.

Operational strategies of co-located BESS with a WPP in the United Kingdom was studied by Fan et al. (2021), focusing on Enhanced Frequency Response (EFR) services and production time-shifting. The research addressed battery SoC management, degradation, and sizing to optimise NPV over a four-year period across four scenarios. The first scenario involved a standalone BESS participating in the EFR market, resulting in the lowest NPV due to high grid connection costs. In the second scenario, a co-located BESS participated in the EFR market without energy exchange with a WPP, resulting in a similar NPV to the third scenario, which included furtherly WPP participation in the EFR market. The fourth scenario, involving a co-located BESS participating in the EFR market and exchanging energy with the WPP to manage curtailment, was identified as the most profitable, achieving almost double the NPV of the second and third scenario due to economic benefits from energy exchange with the WPP.

A techno-economic study of BESS optimisation was conducted by Laine-Ylijoki (2024) in WPP imbalance management and participation in Finnish reserve markets in two distinct scenarios. The first scenario included a co-located BESS managing only imbalance errors of a WPP, and the second scenario included a standalone BESS participating solely in FCR-N and Fast Frequency Reserve (FFR) markets. The findings revealed that while co-located BESS reduces costs associated with imbalance errors, the high investment costs made it unprofitable, with a PBT exceeding 20 years. In contrast, the standalone BESS participating in the FCR-N and FFR markets proved to be profitable, with a PBT of less than five years. Revenues generated from the FCR-N market were dominant, accounting for 80% of the annual revenue. The analysis was based on market data from 2023.

Zhu et al. (2023) researched the optimisation of a co-located BESS with a WPP within the Danish market environment, evaluating the profitability of various scenarios, including combinations of DA market, balancing markets, and wind power imbalance correction, taking into account battery degradation and grid constraints. The analysis focused on a 120 MW WPP with a 20 MW, 3-hour battery system. The research concluded that the most profitable scenario was the combination of participation in the DA market, balancing markets, and imbalance correction. Additionally, participating both in the balancing market and DA market generated 33% more revenues compared to solely participating in the DA market. No imbalance errors exceeding 10 MW occurred while managing imbalance correction with BESS, further enhancing profitability. Despite increased battery degradation costs due to BESS utilisation in multiple purposes, the revenues compensated for these costs.

A study by Jaakamo (2020) investigated the impact of electricity market transition to a 15-minute Imbalance Settlement Period (ISP), and the profitability of a co-located BESS with a WPP in the Finnish market environment. The economic feasibility of a 3MW, 1-hour battery system in the FCR-N market was studied based on 2018 and 2019 market data. The study concluded that co-located BESS in the FCR-N market was not profitable. However, if excess wind power from forecast errors were utilised for charging the battery, the case became profitable. Additionally, Jaakamo proposed that increasing wind power capacity in the power system and shifting to a 15-minute ISP would likely increase the balancing costs for WPPs, thereby improving the economic feasibility of BESS.

The reviewed studies show that co-locating BESS with WPPs is generally profitable, depending on their application. While some studies found participation in reserve markets to be profitable, others concluded that it was not economically viable on its own. However, when combined with additional revenue streams, profitability improved. Similarly, managing imbalance errors alone was unprofitable, but integrating reserve market participation enhanced economic feasibility. Moreover, implementing arbitrage strategies further increased revenues. Overall, the profitability of BESS improved as the number of revenue streams increased. Key factors influencing economic outcomes included battery degradation, battery size, and market-specific conditions.

A research gap was identified regarding the simultaneous utilisation of BESS in reserve markets, energy arbitrage, and imbalance management within the Finnish, Swedish, and Norwegian market environments. Additionally, given the risk of reserve market saturation and declining revenues, using BESS for imbalance settlement could mitigate this risk and enhance profitability. Therefore, there is an opportunity to research the simultaneous use of BESS in reserve markets, energy arbitrage, and imbalance settlement for WPPs—so-called revenue stacking—including multi-market optimisation, and to assess how this would impact profitability in the current markets. This analysis is crucial for understanding the potential of BESS in the future.

3 Nordic Electricity Markets

This chapter examines the electricity markets in Finland, Sweden, and Norway. It begins with an introduction to the operational framework of the Nordic power system, followed by a description of the wholesale electricity markets—including the DA and Intraday (ID) markets—the reserve markets—such as FCR and FFR markets—and the balancing Frequency Restoration Reserve (FRR) markets, including Automatic FRR (aFRR) and Manual FRR (mFRR). The technical aspects and market processes are examined, including how capacity is procured in each market, and how pricing is determined. Finally, the chapter concludes with an analysis of imbalance settlement mechanisms in the Nordics.

3.1 Nordic Power System

Nordic countries primarily generate electricity from nuclear, hydro, and wind power, with the highest share of renewable energy in Europe. The region's reliable power system, suitable energy mix, and competitive electricity prices have attracted energy demanding industries. (NordREG 2019.) As the share of weather dependent renewable sources increases and conventional sources decrease, power system stability is impacted. Additionally, wind power development is shifting production further north, away from demand areas, disrupting system balance. In response, market timeframes are being shortened, and Transmission System Operators (TSO) are investing in enhanced system inertia, improved balancing solutions, and grid stability. (Statnett et al. 2019, p. 3-4)

The Nordic synchronous area is a unified electricity grid shared by Finland, Sweden, Norway, and eastern Denmark, where power systems operate in sync. The national grids are connected through interconnectors, enabling power exchange across borders. (Fingrid 2025a.) The Nordic power system operates with High-Voltage Alternating Current (HVAC). The network is divided into national grids and local distribution grids, with national grids operating at voltages between 110 kV and 420 kV. For instance, Finland's national grid operates at 110 kV, 220 kV, and 400 kV, while Norway operates at 132 kV, 300 kV, and 420 kV. (Määttänen 2023; Norwegian Ministry of Energy 2024a.) The capacity of interconnections define how much power can be exchanged between regions. *Figure 1* shows the transmission system network of the Nordic synchronous area.



Figure 1, Nordic transmission system network (ENTSO-E 2025a)

Frequency stability is crucial for secure power system operation. The Nordic power system operates with a standard frequency range of 49.9 Hz to 50.1 Hz, which depends on system imbalances. Large imbalances can deviate the frequency even to 49 Hz and 51 Hz. Significant deviations may disconnect units from the grid, increasing the risk of blackout. The Nordic target is to keep frequency deviations outside the standard range to less than 1.9% of the year. Frequency imbalances are driven by the balance between production, power exchange and consumption. When production exceeds consumptions, frequency increases; when consumption exceeds production, frequency decreases. The larger the imbalances, the greater the frequency deviation. Small deviations are acceptable, but large deviations must be corrected. Major deviations occur, for instance, when a large production unit drops out, or an interconnector is disconnected. (Modig et al. 2022, p. 4-8)

Inertia is another factor affecting frequency. It refers to the grid's ability to resist frequency changes, created by kinetic energy in rotating masses, typically from conventional sources. Higher system inertia makes it harder for frequency to deviate, improving stability. (Leinonen 2018.) Rate of Change of Frequency (RoCoF) is an indicator of inertia, referring to how quickly frequency deviates, measured in hertz per second. Higher system inertia slows down the RoCoF. (Weaver 2022.) Since renewable sources increase in the Nordic countries, system inertia decreases due to the absence of large rotating masses. If a sudden power imbalance occurs with low inertia, frequency can deviate significantly. Conversely, higher inertia results in smaller frequency deviations during imbalances. (Leinonen 2018.) *Figure 2* illustrates how system inertia affects frequency deviation.

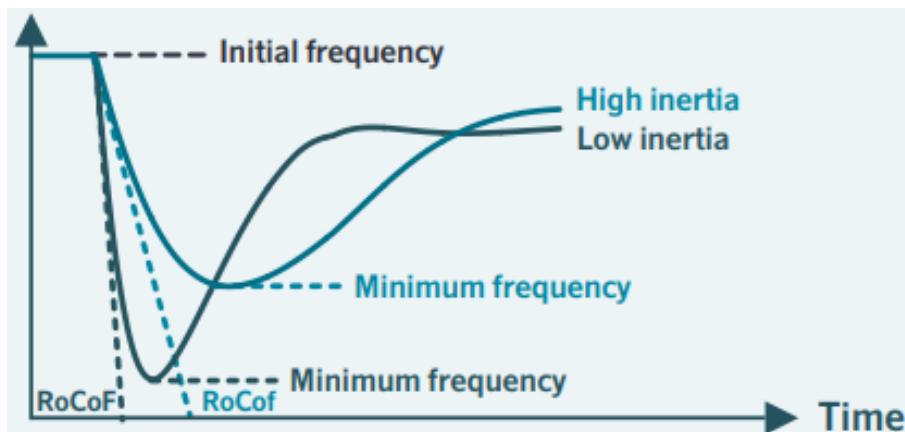


Figure 2, Inertia affecting frequency deviation (Fingrid 2025b)

The Nordic TSOs are Fingrid in Finland, Svenska Kraftnät in Sweden, Statnett in Norway, and Energinet in Denmark. According to Statnett (2018), the TSOs responsibility are maintaining a stable, balanced power system with high power quality. TSOs manage the national electricity grid and hold a natural monopoly over transmission, making their activity highly regulated. (Statnett 2018.) TSOs must comply with European legislation, including the System Operations Guideline (SOGL) and the Electricity Balancing Guideline (EBGL), which regulate system frequency, reserves, TSO collaboration, and sets reserve product requirements. The Nordic System Operation Agreement (SOA) builds on these guidelines to ensure stability and reliability within the Nordic power system. (Modig et al. 2022, p. 5.) Additionally, Distribution System Operators (DSO) manage local networks, transmitting electricity from the national grid to end users via low- and medium-voltage grids (Nord Pool 2025a).

Nordic TSOs manage reserve and balancing markets to balance the power system, utilising both fast and slow responding reserves. The Nordic power system relies on three reserve types for system frequency control; FCR, FRR and FFR. FCR is an automatic, fast reacting reserve, which monitors system frequency and it is the first reserve to act to maintain the standard range. It consists of two separate products: FCR-N and FCR for disturbances (FCR-D), which are activated at different frequency deviations. FRR restores frequency to 50 Hz after a deviation has occurred, and frees FCR for future activation. FRR consist also of two separate products: mFRR and aFRR. FFR is a very fast responsive reserve, which compensates the decreasing inertia in the system. It is activated when frequency deviates, system inertia is low, and when FCR is insufficient for containing the frequency. (Modig et al. 2022, p. 4-9.) *Figure 3* demonstrates how different reserves are activated during frequency deviations. These reserve and balancing products are discussed further in *Chapters 3.4, 3.5, and 3.6*.

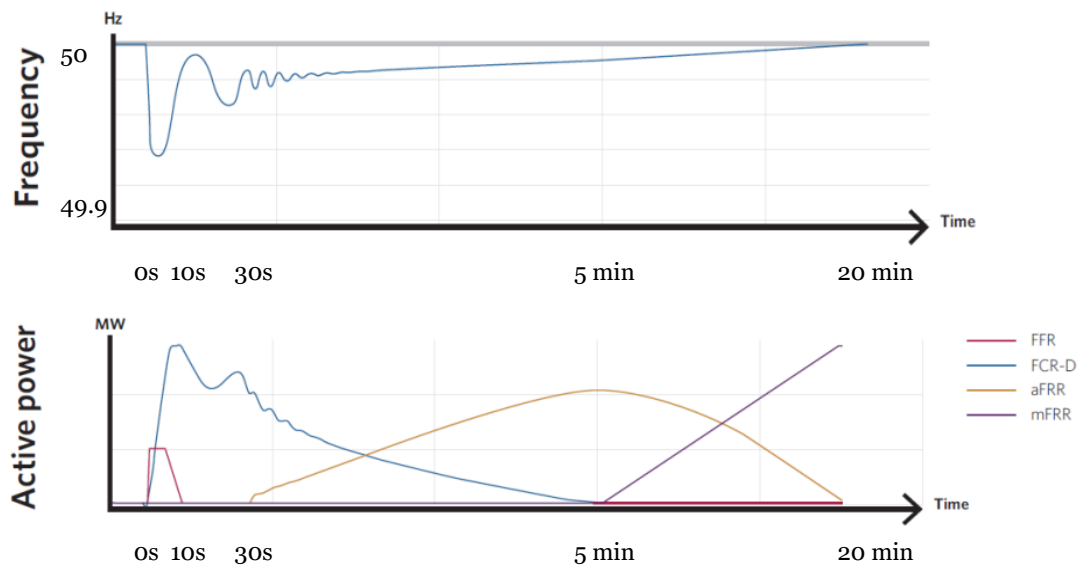


Figure 3, Reserve activations (Modig et al. 2022, p. 5)

Electricity markets enable trading of electricity and consist of different segments; financial markets, physical electricity markets – including DA-, ID-, reserve- and balancing markets – and imbalance settlement. Financial markets enable companies to hedge against electricity price risks through future electricity output trading, involving financial transactions focused on upcoming months or years, without physical trading (Fortum 2025a). Physical electricity is primarily traded in the DA market, where electricity is traded for the following day. The ID market allows traders to place bids closer to the delivery, allowing them to adjust their plans made in the DA market as forecasts change. Since all bids are forecasts, actual outcomes may differ, leading to imbalances. Reserve markets, managed by TSOs, address imbalances by providing reserves to correct differences that arise from forecast errors in the DA and ID markets during the operation period. (Fingrid 2025c)

After the delivery period, the imbalance between the offered and actual traded volumes are settled for each trading period for the Balance Responsible Party (BRP) participating in the electricity markets. Forecast errors lead to these imbalances, for which the BRP carries financial responsibility. (Fingrid 2025c.) Additionally, electricity can be traded with Power Purchase Agreements (PPA), where suppliers and consumers make long-term contracts for up to 10 to 20 years. PPAs allow pre-selling of electricity, which provides price stability. (Ilyukhin & Sainio 2024.) This thesis will focus on physical electricity markets and imbalance settlement.

Power markets are divided into bidding zones, with limited power exchange capacity between them creating price differences. In the Nordic countries, Finland has one bidding zone (FI), Sweden has four (SE1 to SE4), Norway five (NO1 to NO5), and Denmark two (DK1 and DK2), making a total of 12 bidding zones. (Nord Pool 2025b.) *Figure 4* shows the bidding zones, their DA market price, and the transmission capacities of interconnectors, for a specific delivery period.

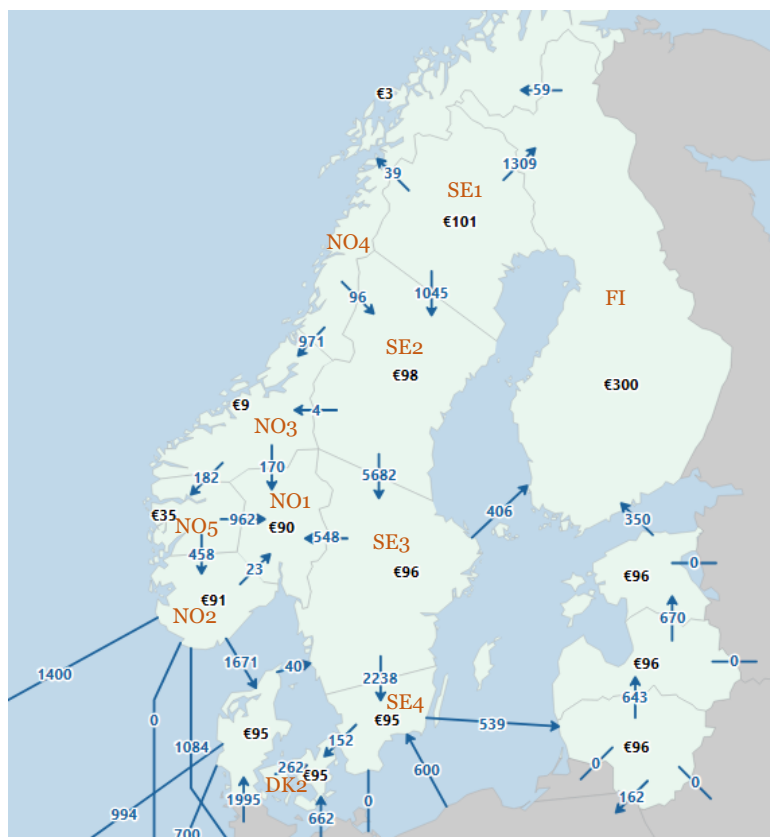


Figure 4, Bidding zones, prices, and transmission capacities (Modified from Svenska Kraftnät 2025a)

Units connected to the national electricity transmission grid are required to pay fees to the TSO for the use of the grid. These fees are based on tariffs and are designed to finance the operation of the TSO. Energy-based fees are charged according to the volume of electricity transmitted and primarily cover grid losses, and they apply to both electricity fed into the grid and electricity withdrawn from it. In addition, a capacity-based fee is charged to cover the operational and maintenance costs, and are based on the power capacity of the unit. (Svenska Kraftnät 2025b)

3.2 Day-ahead market

Majority of electricity is traded in the Day-Ahead (DA) market, which serves as the primary marketplace for electricity trading. The DA market operates as a closed auction where participants buy and sell electricity for the following day. Price is determined for each delivery period on the next day based on the purchase and sell bids submitted by participants, which rely on production and consumption forecasts. Each bid includes the exchange volume and the price at which the participant wants to trade at each delivery period. Bids for the DA market must be submitted on the previous day of delivery before the Gate Closure Time (GCT) at 12:00 Central European Time (CET). (Norwegian Ministry of Energy 2024b)

Nordic countries are part of the European electricity markets, where bids are matched with orders across Europe through a process known as Single Day-Ahead Coupling (SDAC) (Nord Pool 2025d). Market coupling is a method of uniting different markets through an implicit auction system, where multiple power exchange entities, such as Nord Pool and EPEX Spot, shares their order books into a centralised platform, while managing the trading system and collecting bids from market participants. Market coupling enables coupling of supply and demand across different bidding zones, allowing the markets to operate beyond regional boundaries. European Price Coupling of Regions (PCR) includes several power exchanges that collaborate to unify and calculate prices and electricity flows in European regions. The Euphemia algorithm is utilised in the PCR. Market participants can submit bids to any power exchange operating within the region which collects the bids, but these bids are submitted to Euphemia at the same time after GCT of the DA market. (Solovian 2019, p. 7-8.) Euphemia then calculates the prices of each bidding zone, considering the orders and grid constraints across Europe (Nord Pool 2025e).

To ensure balance between electricity supply and demand, the market-clearing price—also known as the equilibrium price—is set at the point where supply matches demand (Norwegian Ministry of Energy 2024b). A supply and demand curve is illustrated in *Figure 5*. The equilibrium price is determined through marginal price setting, which depends on the cost of producing electricity from the most expensive source required to balance supply and demand, and the price consumers are willing to pay (Nord Pool 2025c). The pricing mechanism is depicted in *Figure 6*.

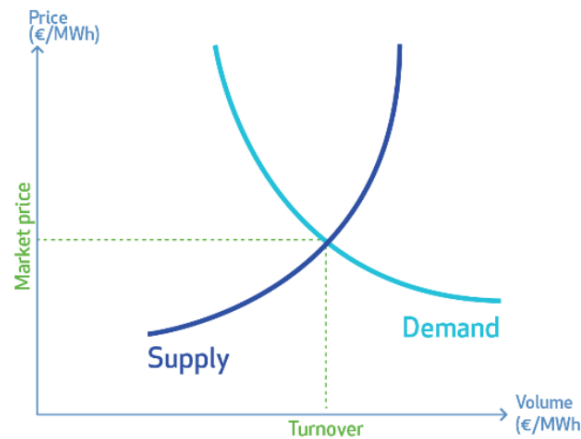


Figure 5, Supply and demand curve of the DA market (Saulny 2017, p. 12)

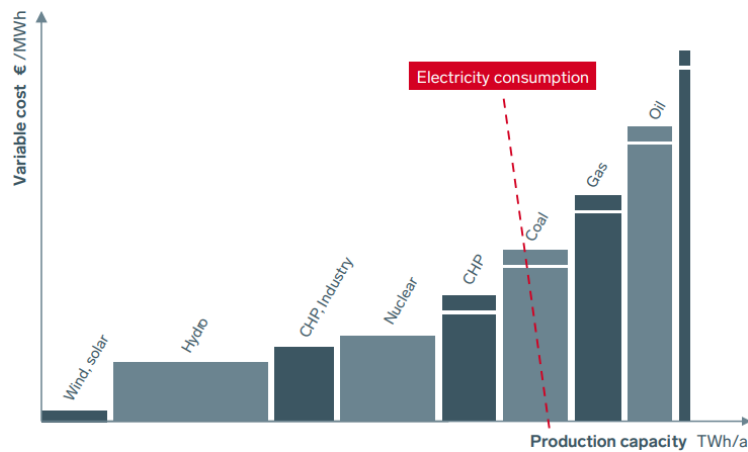


Figure 6, DA market pricing mechanism (Fingrid 2016, p. 6)

A theoretical system price is calculated for each delivery period, which assumes no congestion in the transmission grid, resulting in a uniform price across all bidding zones. Such a scenario would be ideal, and the DA market price would be identical across all regions. In reality, transmission constraints exist due to limited capacity, and production surpluses or deficits within different bidding zones. These constraints create higher prices in areas experiencing production deficits, and lower prices in surplus areas. Electricity flows from lower-price areas to higher-price areas to balance the system. (Norwegian Ministry of Energy 2024b.) At approximately 12:45 CET, the market prices are announced, and accepted bids are reported to participants (Nord Pool 2025d). Within each bidding zone, all producers with accepted bids receive the same price, whereas all consumers with accepted bids pay that price (Norwegian Ministry of Energy 2024b). Market participants are then obligated to deliver or consume electricity accordingly to the accepted bids (Nord Pool 2025d).

DA prices in the Nordic countries are the lowest in Europe. In 2024, Finland's average price was 46 EUR/MWh, while Swedish bidding zones ranged from 25 to 50 EUR/MWh. *Figure 7* shows an overview of DA prices across Europe. (Fortum 2025b, p. 4.) Starting from September 2025, DA market bids across Europe, including Nordic countries, will be settled on a 15-minute basis, meaning that the delivery period, or the Market Time Unit (MTU), is 15 minutes (EPEX Spot 2025a). In prior to that, the MTU settles at one hour, making this shift a significant change in European electricity markets.

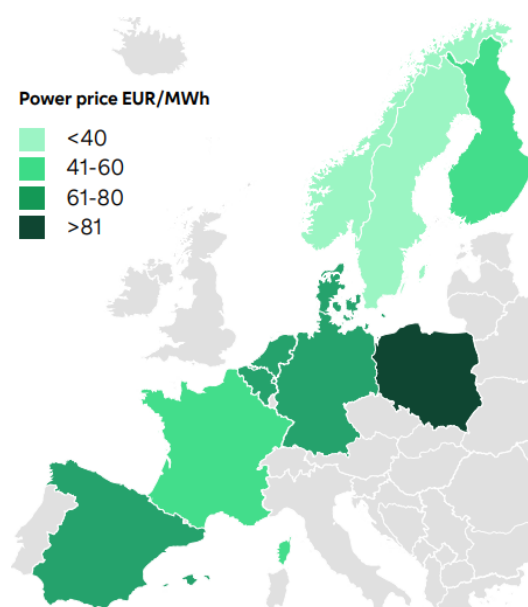


Figure 7, Average DA prices in European countries in 2024 (Fortum 2025b, p. 4)

3.3 Intraday market

Forecasted production and consumption may change after bidding to the DA market due to factors such as inaccurate weather forecasts, timetable changes, or technical problems. In particular, weather dependent renewable sources are challenging to predict accurately in advance, making closer real-time trading necessary for balancing supply and demand. Unlike DA market, the Intraday (ID) market allows trading closer to the delivery period. ID markets are typically used to adjust imbalances arising from DA market forecasts, but can be utilised to generate additional revenue through energy arbitrage or by bidding unused capacity. (Gasum 2025.) For example, if 100 MWh production is bid to the DA market based on forecasts, but as the delivery period approaches, the forecast increases to 130 MWh, the additional 30 MWh can be traded in the ID market to balance production and reduce imbalance costs. Conversely, if the forecast drops to 70 MWh, the missing 30 MWh can be purchased from the ID market to correct the forecast error and minimise imbalance costs.

Similar to the SDAC, Single Intraday Coupling (SIDC) has been established to operate an integrated market across European countries, enabling continuous electricity trading across regions. SIDC became operational in 2018, and by 2022 it included 25 coupled countries. (ENTSO-E 2025b.) ID market consists of two separate trading mechanisms: continuous ID trading and ID auctions (Nord Pool 2024, p. 2). Continuous ID trading normally starts at 14:00 CET on the previous day of delivery, a few hours after GCT of the DA market. In Nordic countries, the GCT for continuous ID trading is one hour before the delivery period, except in Finland, where trading remains open until delivery. (Nord Pool 2025e, p. 5.) ID auctions in the Nordics were introduced in June 2024 and consist of three separate auctions—IDA1, IDA2 and IDA3—each with different GCT and delivery periods, shown in *Table 2*. The MTU for ID auctions is 15 minutes in Finland and Sweden, as well as in Norway since March 2025. (Nord Pool 2025f)

Table 2, GCT and delivery periods of ID auctions (Nord Pool 2025f)

Auction	GCT (CET)	Trading period (CET)
IDA1	15:00 previous day	00:00–24:00
IDA2	22:00 previous day	00:00–24:00
IDA3	10:00 day of delivery	12:00–24:00

In continuous ID trading, prices are determined with a pay-as-bid process, meaning each transaction sets its own price, and therefore there are no fixed prices for the same products (Next Kraftwerke 2025). As a result, market prices can fluctuate within a single trading period, creating volatility. ID market participants submit both purchase and sell orders to the power exchange. A trade takes place when a buy order price exceeds a matching sell order price, with the transaction executed at the seller’s price. A purchase order may be fulfilled with multiple sell orders, with the final price determined as a volume-weighted average of the bids. (Bush 2023.) Orders are cleared based on price priority, with the highest purchase prices and lowest sell prices matched first (ENTSO-E 2025b). Bids and orders are collected in a shared order book, accessible to all market participants. This order book is shared across all coupled countries, allowing orders from different bidding zones to be matched when sufficient transmission capacity is available between regions. (Bush 2023.) *Figure 8* illustrates how the shared order book functions and how trades are executed.

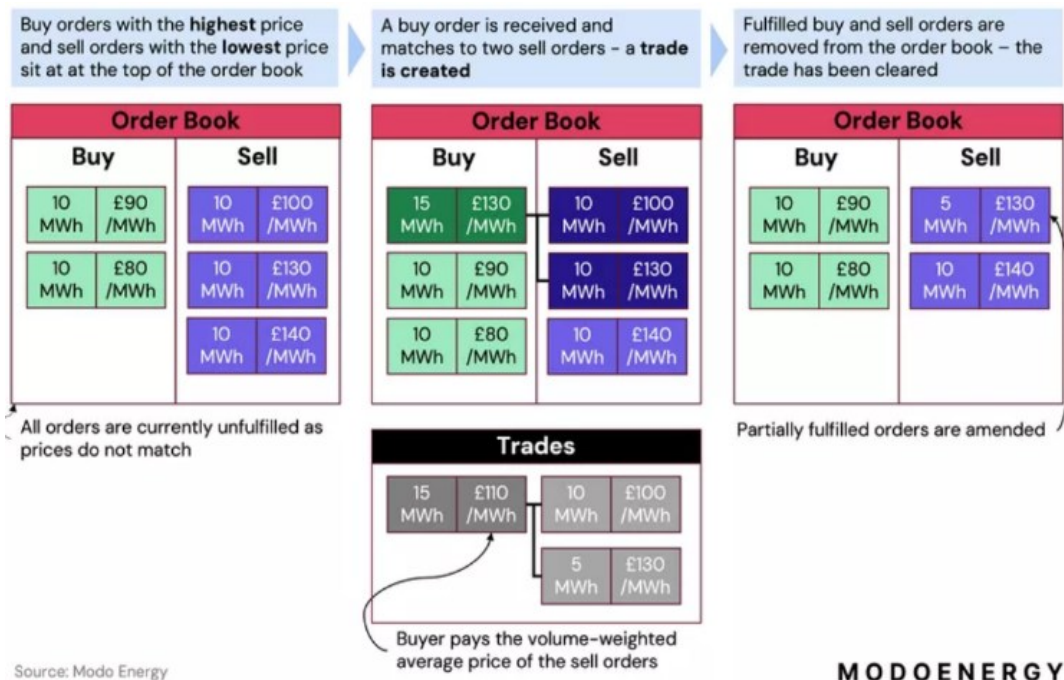


Figure 8, Shared order book and execution of trades in ID market (Bush 2023)

ID auctions, on other hand, are implicit auctions where orders and bids are matched simultaneously across bidding zones, considering all bids, orders, and available transmission capacities (NEMO Committee 2024, p. 8). In ID auctions, bids and orders are pooled into a single auction event for each delivery period and plotted on supply and demand curves, where the intersection sets the auction price. This results in fixed prices for the ID auctions, unlike continuous ID market, where prices depend on each transaction. (Nord Pool 2024, p. 9.) Price calculation for ID auctions is performed using the Euphemia algorithm, following the same process as for SDAC. Market participants submit their bids and orders to the power exchange, which collects them to the Euphemia algorithm. The algorithm then determines the clearing price for each bidding zone. (NEMO Committee 2024, p. 5-6)

In ID markets, bids can range from 0.1 MW up to 999 MW, with price range from -9999 EUR/MWh to 9999 EUR/MWh. SIDC supports delivery intervals of 15-minute, 30-minute and 60-minutes, but availability of these products varies by country. (ENTSO-E 2025b.) In the Nordic countries, Nord Pool and EPEX Spot maintain the ID marketplaces, offering different products, including 15-minute and 60-minute periods. (Nord Pool 2025e, p. 5; EPEX Spot 2025b)

3.4 Frequency Containment Reserve (FCR)

Frequency Containment Reserves (FCR) consist of three distinct reserve products: FCR for Normal Operation (FCR-N), and FCR for Disturbances (FCR-D) with up- and down-regulation. Up-regulation involves increasing power production to the grid or decreasing consumption, while down-regulation involves reducing power production or increasing consumption from the grid. The objective of all three products is to continuously maintain the frequency range, though each is activated within different frequency bands. (ENTSO-E 2023a, p. 11.) FCR-N operates within 49.9–50.1 Hz, and is a symmetrical product requiring both up- and down-regulation. FCR-D up-regulation is activated between 49.5–49.9 Hz, and FCR-D down-regulation between 50.1–50.5 Hz, making both products asymmetrical, as only one direction of regulation is required. (Fingrid 2025d.) Participating simultaneously in both FCR-D up- and down-regulation markets requires symmetrical reserve characteristics.

Entities providing reserves can either be static or dynamic. A dynamic entity can be continuously adjusted, whereas a static entity requires recovery time after activation. FCR-N participation requires dynamic properties, while FCR-D participation allows both dynamic and static entities. (ENTSO-E 2023a, p. 23 & 30.) All FCR products must be activated in a linear manner or as approximation of a linear function in respect to frequency deviation. The steady-state response must be in proximity to the theoretical steady-state response, meaning a deviation of up to 5% under-delivery and 20% over-delivery are allowed for all FCR products. The products remain active for as long as the frequency deviation continues. (ENTSO-E 2023a, p. 6 & 14.) The linearity and steady-state response range for FCR-N is shown in *Figure 9*, and for FCR-D in *Figure 10*.

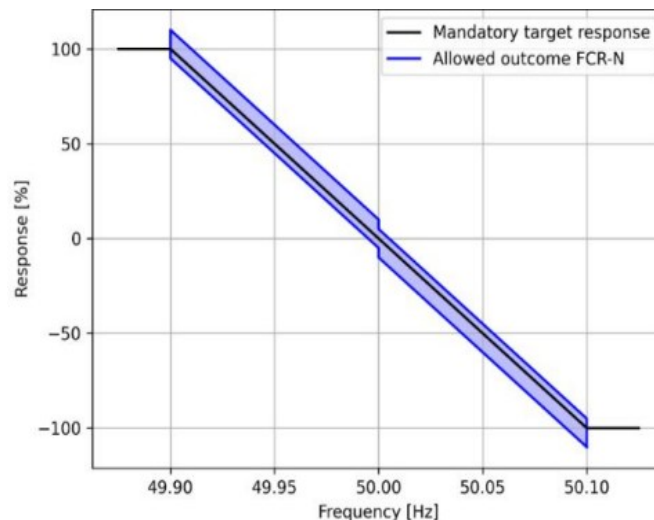
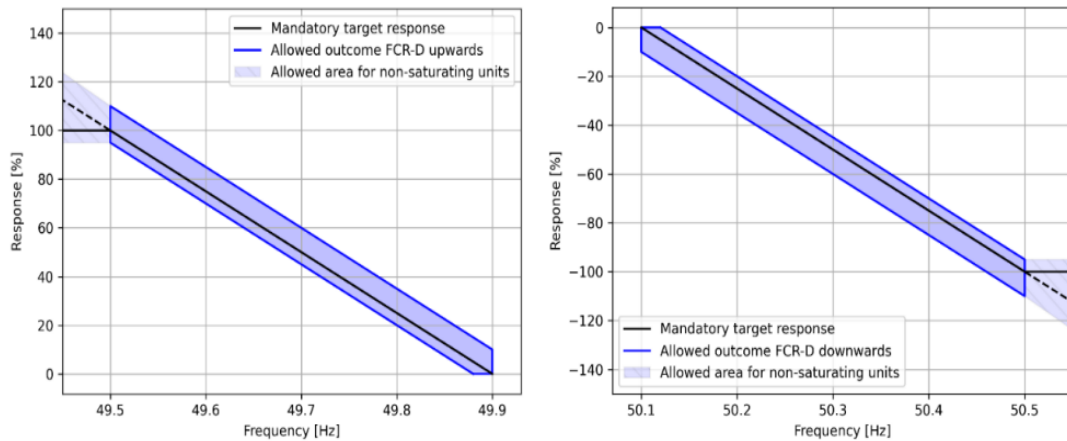


Figure 9, Activation of FCR-N in response to grid frequency (ENTSO-E 2023a, p. 32)



*Figure 10, Activation of FCR-D in response to grid frequency
(ENTSO-E 2023a, p. 34)*

Activation times are different for FCR products. Participation in the FCR-N market requires activating approximately 63% of full capacity within 60 seconds, and reaching 95% within three minutes. Both FCR-D up- and down-regulation markets obligate activating 86% of full capacity within 7.5 seconds. (ENTSO-E 2024a, p. 10.) Participation in FCR-N market has an energy duration requirement of two hours of full power activation, with one hour for both up- and down-regulation. For FCR-D products, the energy duration requirement is 20 minutes. (ENTSO-E 2023a, p. 38)

Requirements for FCR products are specifically defined for Limited Energy Reservoirs (LER). LER refers to an entity with limited activation endurance, meaning reservoirs with energy storage capacity insufficient to sustain full reserve activation for two consecutive hours. The requirements exist because the FCR response must remain active as long as the frequency deviation remains. LER entities must spare capacity for both up- and down-regulation to ensure a reliable reserve. In the FCR-N market, a LER must manage its SoC by reserving an added 34% of its power capacity from the bid. For instance, bidding 1 MW of LER to FCR-N necessitates a total power capacity of 1.34 MW. In FCR-D markets an additional 20% power capacity must be reserved in the other direction of the regulation. This spared capacity is used to restore the SoC to its target level for future activations, and cannot be used for any other purpose. The target SoC for FCR-N is set at 50% to maintain symmetry, and for FCR-D up-regulation it is 100%, and for FCR-D down-regulation 0%. If an entity participates in both FCR-D up- and down-regulation, SoC target is 50%, as the product is considered symmetrical. (ENTSO-E 2023a, p. 37-40)

An unit participating in any FCR market must be prequalified with testing. The requirements are the same across the Nordic synchronous area and must be met by all participating entities. (ENTSO-E 2023a, p. 7.) FCR products activate automatically based on system frequency, removing the need for TSOs to send separate activation signals. Participating units must be equipped with a controller that adjusts the power according to system frequency. (Fingrid 2025d.) Performance characteristics for different FCR products are listed in *Table 3*.

Table 3, FCR performance characteristics (ENTSO-E 2023a)

	FCR-N	FCR-D up	FCR-D down
Frequency band gap	49.9–50.1 Hz	49.5–49.9 Hz	50.1–50.5 Hz
Response time	63% in 60s 95% in 3min	86% in 7.5s	86% in 7.5s
Energy duration	1 hour up 1 hour down	20min	20min
Symmetry	Symmetric	Asymmetric	Asymmetric
Type	Dynamic	Dynamic or Static	Dynamic or Static
Target SoC	50%	100%	0%
Additional capacity, LER	34%	20% down	20% up

Nordic TSOs determine the necessary FCR volumes for the entire Nordic synchronous area in advance for each year. Procurement of the required volumes are then divided among the different Nordic TSOs based on the shares of generation and production within each TSOs responsible bidding zone. FCR-D volumes are determined from the risk of major disturbances, such as the tripping of a large power generator, a significant demand facility, or an interconnector. (ENTSO-E 2024a, p. 12.) For instance, in 2025, the required FCR-D down-regulation volume for the Nordic region is 1400 MW, with Svenska Kraftnät responsible for the procurement of 37.40%, Energinet for 3.2%, Fingrid for 20.90%, and Statnett 38.5%. (Svenska Kraftnät 2024a)

There is no unified Nordic market for FCR procurement, allowing each TSO to procure reserves based on their specific needs. However, reserves can be exchanged between countries, with maximum allowable exchange limit of one third of the total required volume. (ENTSO-E 2024a, p. 15.) In Finland, Fingrid procures FCR-N and FCR-D through both yearly and hourly markets. The yearly market auction is held once a year in autumn, procuring capacity for the following year, while the hourly market procures capacity for each hour of the following day. (Fingrid 2025d.) The capacity procured from hourly markets depends on the volume secured from the annual market

contracts and exchange from other TSOs, leading to varying volumes. In Finland, both FCR-N and FCR-D markets are operated in the same manner. (ENTSO-E 2024a, p. 14-15.) The minimum and maximum bid sizes for FCR-N market are 0.1 MW, and 5 MW, respectively, while for FCR-D market, they are 1 MW and 10 MW, respectively, for both up- and down-regulation. The maximum and minimum bid volumes are the same for both annual and hourly markets. (Fingrid 2024a, p. 4)

In Sweden, both FCR-N and FCR-D is procured through an hourly market (ENTSO-E 2024a, p. 15-16). The markets are split into two auctions, with different GCTs. The minimum bid size is 0.1 MW, and bids can be incremented in steps of 0.1 MW. (Svenska Kraftnät n.d., p. 7-8.) Also in Norway, there are two separate auctions for hourly FCR-N and FCR-D markets, where hourly bids are submitted separately for each bidding zone (ENTSO-E 2024a, p. 15-16). The minimum bid size is 0.1 MW (Statnett 2024a). In an email response from Statnett, Andersen (2025) clarified that, due to Norway's energy mix consisting 90% of hydro power, and the country's excessive reserve capabilities for frequency control, historically only FCR-N has been procured, with no need for FCR-D regulation. However, FCR-D up-regulation was procured during the summer seasons of 2023 and 2024, while FCR-D down-regulation has not yet been procured. (Andersen 2025.) In Nordic FCR markets, each bidding zone has its own price. Currently, in the Nordic region, no entity can provide more than 70 MW of FCR (ENTSO-E 2023a, p. 55).

Participants with accepted bids in the FCR-N and FCR-D markets receive a capacity payment. In the Nordic countries, this payment is determined through marginal pricing (ENTSO-E 2024a, p. 15-16). Under this pricing, the most expensive bid accepted sets the price. However, the actual capacity payment is based on the measured and verified reserve capacity, with the payment never exceeding the capacity bid accepted to the market. If the reserve capacity is not provided as planned, penalties are applied. The capacity payment is calculated by multiplying the verified reserved capacity by the market price, and subtracting the penalty fee. In Finland, the penalty fee is calculated as three times the unprovided capacity, multiplied by the market price. (Fingrid 2025e, p. 14-15.) In addition to the capacity payment, FCR-N energy activations are compensated with an energy payment. The energy payment is based on the activated energy, and the imbalance settlement price in the mFRR market. For up-regulation, the energy is compensated at the mFRR up-regulation price, with the TSOs paying for the energy. Conversely, for down-regulation, the energy is compensated at the mFRR down-regulation price, with the TSOs charging for the energy. Since FCR-N is a symmetric product that covers both up- and down-regulation, the payment is determined by the net activated energy during the delivery hour. (Energinet et al. 2023, p. 17; Fingrid 2025e, p. 13-14)

In Finland, by 2025, various reserve technologies were certified for the FCR markets. For FCR-N, capacity certified primarily came from hydro and thermal power, as well as energy storages. For FCR-D up-regulation, the certified reserves were similar, with the addition to consumption facilities. For FCR-D down-regulation, certified reserves included hydro, thermal, and nuclear power, energy storages, and consumption facilities. *Figure 11* illustrates the certified capacities for FCR markets. In Finland, the prices for 2024 annual FCR-N, FCR-D up-regulation, and FCR-D down-regulation markets were 25.39 EUR/MW, 4.00 EUR/MW and 9.50 EUR/MW, respectively. For the hourly markets, the average prices were 45.83 EUR/MW, 18.54 EUR/MW and 16.58 EUR/MW, respectively. (Fingrid 2025f)

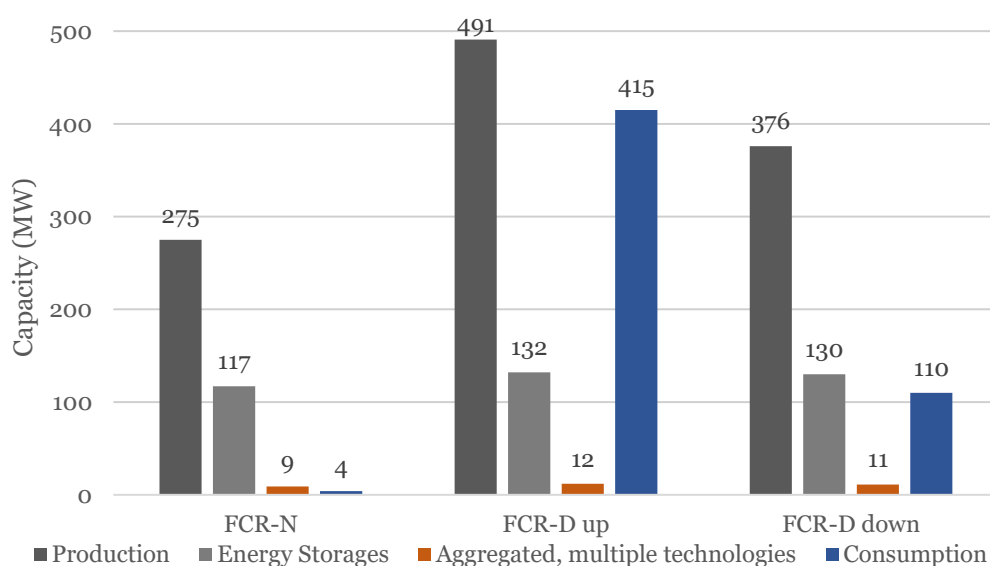


Figure 11, Certified capacity in Finnish FCR markets in 2025 (Modified from Fingrid 2025f)

3.5 Fast Frequency Reserve (FFR)

Fast frequency Reserve (FFR) was introduced in Nordic region in 2020 to mitigate fast and intense frequency deviations in situations when system inertia is low within the Nordic synchronous area, by providing artificial inertia. FFR complements FCR products, which lack the speed needed to stabilise frequency during large disturbances in low-inertia scenarios. FFR provides rapid, short-duration power to contain frequency deviation until FCR products are activated. FFR exclusively provides up-regulation, as it only mitigates disturbances when the system frequency drops. Various technologies can be utilised to provide FFR, as both disconnection of loads and increased power output are considered as up-regulation. (ENTSO-E 2024a, p. 6 & 10.) The energy volumes delivered during FFR activations are small due to the rapid nature of activations. The need for FFR is expected to increase in the future as system inertia continues to decline. (Energinet et al. 2023, p. 25)

The required FFR capacity is influenced by system inertia, causing the demand to vary daily and seasonally according to weather conditions and hydrological situation. Some years may need FFR activations for up to 1000 hours, while in others, only 100 may be enough. (ENTSO-E 2019, p. 10.) FFR demand is highest in periods of both low electricity consumption and production, particularly with high shares of wind power and imported energy. These conditions typically occurs in summer season, especially in dry hydrological years. (Statnett 2024b.) On a shorter timescale, FFR focuses primarily during nights and weekends (ENTSO-E 2019, p. 13). *Figure 12* shows simulated FFR demands from 1982 to 2012, highlighting the summer season as the period of highest need, with variations of hourly need from year to year.

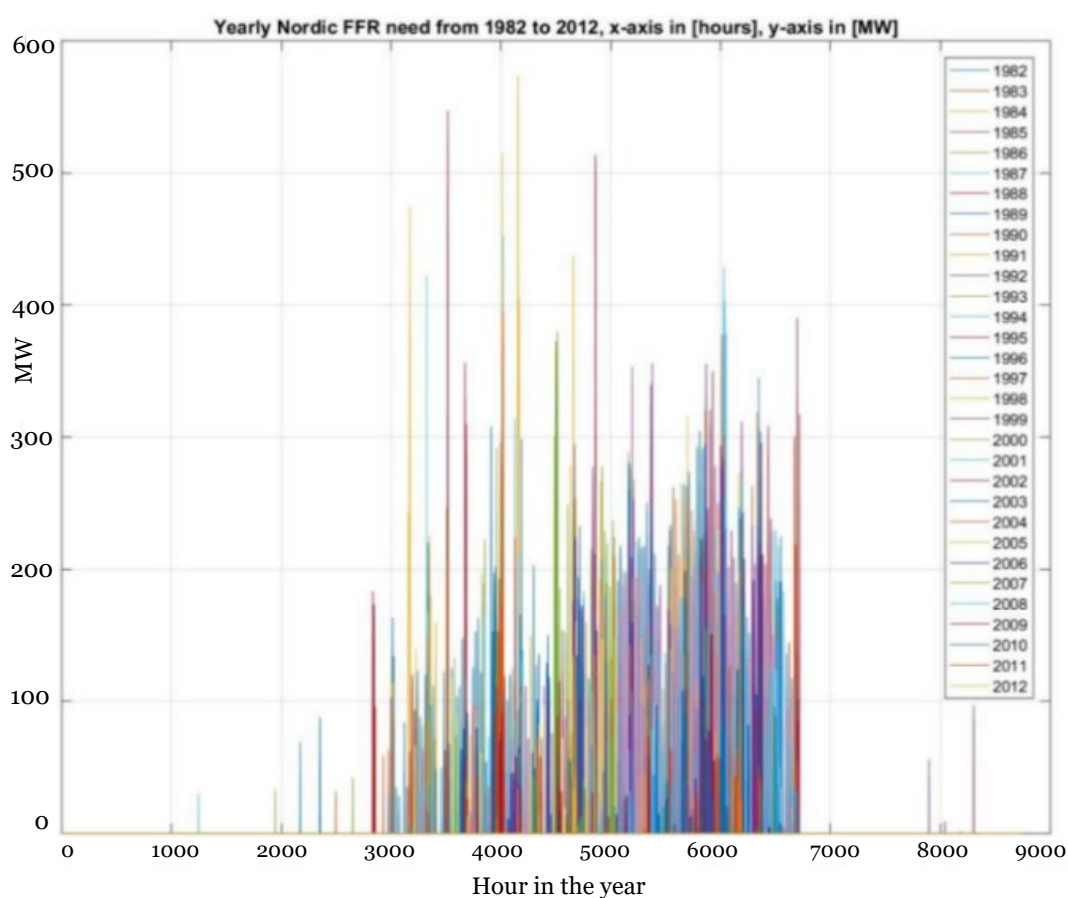


Figure 12, Yearly Nordic FFR need from 1982 to 2012 (ENTSO-E 2019, p. 11)

There are three different predefined combinations of activation time and activation level for FFR, from which the provider can choose from in advance. The frequency ranges from 49.5 to 49.7 Hz, with activation times between 0.7 to 1.3 seconds, as shown in *Table 4*. The activation frequency is the threshold at which the reserve must be activated, while activation time refers to the time from activation instant until full power delivery. Additionally, providers can choose between two FFR activation durations: long support duration and

short support duration, which are shown in *Table 5*. (ENTSO-E 2021, p. 3.) Both options have identical activation criteria but differ in deactivation requirements. The long support duration has no limitations for the deactivation rate, whereas the short support duration limits deactivation to 20% of the prequalified capacity per second. Some entities may need recovery time after activations, but all FFR providing facilities must be prepared for new activations within 15 minutes. (ENTSO-E 2021, p. 6-9)

Table 4, FFR activation frequencies and activation times (ENTSO-E 2021, p. 3)

Option	Activation frequency (Hz)	Activation time (s)
A	≤ 49.7	≤ 1.3
B	≤ 49.6	≤ 1.0
C	≤ 49.5	≤ 0.7

Table 5, FFR activation durations (ENTSO-E 2021, p. 3)

Option	Min. activation duration	Deactivation speed
I	30 s	No limitations
II	5 s	Max. 20% of reserve capacity per second

An overdelivery of 20% beyond the prequalified capacity is allowed, with some TSOs even accepting 35%, depending on the procurement process (ENTSO-E 2021, p. 7). *Figure 13* illustrates a typical activation cycle and its key parameters. Entities participating in the FFR market must be prequalified with testing to prove that technical requirements are fulfilled. Activations are triggered by automatic local frequency measurements, requiring units to have a controller that adjusts the power output or load according to the local frequency. (Fingrid 2025g). FFR is a static reserve and does not require continuous regulation. However, the development of a dynamic FFR product is being considered for the future (ENTSO-E 2024a, p. 10).

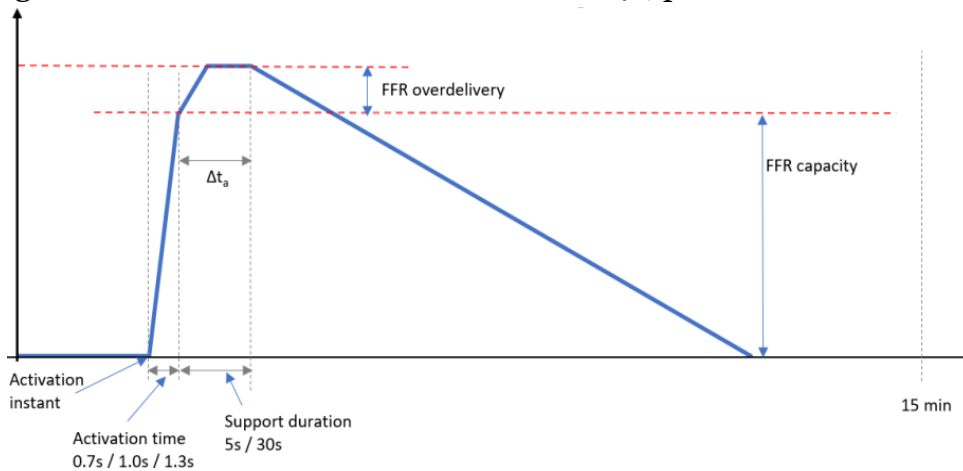


Figure 13, FFR activation cycle (ENTSO-E 2021, p. 7)

FFR capacity procurement in the Nordics is determined based on the forecasted and simulated system inertia (ENTSO-E 2024a, p. 13). Forecasts consider weather and hydrological conditions, and are made for upcoming months and seasons. However, long-term forecasts are less accurate compared to short-term, hour-to-hour predictions. (ENTSO-E 2019, p. 19.) The estimated FFR capacity needed in the Nordics is approximately 300 MW (Statnett 2024b). Similar to FCR, the required FFR reserve capacity is divided between the Nordic TSOs, with shares based on FCR allocation, and the largest possible disturbance in each country. Due to differences in procurement strategies, TSOs acquire FFR capacity with different methods. (ENTSO-E 2019, p. 19.) In 2024, capacity procurement share for Fingrid was 18%, for Svenska Kraftnät 34%, for Statnett 39% and for Energinet 8% (ENTSO-E 2024a, p. 13).

Fingrid procures FFR capacity through an hourly market for the following day, where each hour has a distinct price and varying volumes can be procured. Procurement forecasts are published on weekly periods. (Fingrid 2025g.) The minimum bid size is 1 MW, while the maximum is 10 MW. Reserve providers that can deliver both FCR-D and FFR can submit combined bids to both the FFR market and FCR-D up-regulation market. If a combined bid is not accepted to FFR market, it will automatically transfer to the FCR-D market auction. (Fingrid 2024b.) Svenska Kraftnät procures FFR with yearly contracts through a once-a-year tendering for typically the period from May to October. Svenska Kraftnät then do activation call-offs twice a week for the accepted participants in the yearly auction: on Mondays for a 4-day period, and on Fridays for a 3-day period, with reservations for specific hours. The FFR market is uniform across Sweden, with procurement and pricing unaffected by the different bidding zones. (Bjellerup 2025; ENTSO-E 2024a, p. 16.) The minimum bid size is 0.5 MW, while the maximum bid size is 5 MW (Svenska Kraftnät 2024b).

In Norway, Statnett offers two FFR products to prevent over-dimensioning of reserves: a flex product and a profile product. The seasonal FFR profile product procures capacity on a seasonal basis, specifically for nights and weekends when system inertia is low. This product provides fixed capacity throughout the needed hours of the season, which in 2025 is from May to August. The FFR flex product procures capacity only when necessary, based on demand for specific hours and short-term forecasts. The procurement period for the flex product in 2025 ranges from April to October. In 2025, the planned procurement for the profile product is 47 MW, while the flex product procures 103 MW. The minimum bid size for the FFR profile is 1 MW, and for the flex product 5 MW. The maximum bid size for both products is 50 MW. (Statnett 2024b)

Fingrid, Svenska Kraftnät and Statnett all use a marginal pricing system for their FFR products. (ENTSO-E 2024a, p. 16.) Participants with accepted bids in the FFR markets receive a capacity payment, which is based on the measured and verified available capacity, but never exceeding the bid capacity accepted into the market. If a provider fails to deliver the promised bid capacity, penalties are applied, which in Finland are calculated in the same manner as for FCR markets. (Fingrid 2024b, p. 9.) In Finland and Sweden, no energy compensation is paid for the reserve provider. However, in Norway, Statnett pays an additional energy payment for the activated energy in addition to the capacity payment. (ENTSO-E 2019, p. 20.) Additionally, in contrast to Sweden and Finland, Norway has a fixed price for FFR products throughout the year (Statnett 2024b).

3.6 Frequency Restoration Reserve (FRR)

After a frequency deviation has occurred and activated FCR or FFR products, Frequency Restoration Reserve (FRR) products are deployed to restore the system frequency to 50 Hz and release FCR and FFR for future activations. While FCR and FFR products provide an immediate response, FRR offers a slower but sustained, longer-term balancing. FRR is divided into two components: Automatic Frequency Restoration Reserve (aFRR) and Manual Frequency Restoration Reserve (mFRR). (ENTSO-E 2024a, p. 5-6)

Both aFRR and mFRR serve the same purpose of restoring system frequency, and are each divided into up- and down-regulation products. However, their technical characteristics differ. Entities providing aFRR must be fully activated within 5 minutes of receiving the activation signal, while mFRR must be fully activated in 15 minutes. Additionally, aFRR signals are sent automatically by the TSO in 10 second intervals, while mFRR activations are executed manually by the TSO. mFRR activations are primarily used for balancing purposes, managing imbalances between production and consumption. Imbalances can either be immediate or forecasted for the future. (ENTSO-E 2024a, p. 11.) The activation of mFRR releases both FCR and aFRR for further use (ENTSO-E 2024a, p. 23). This is illustrated in *Figure 14*.

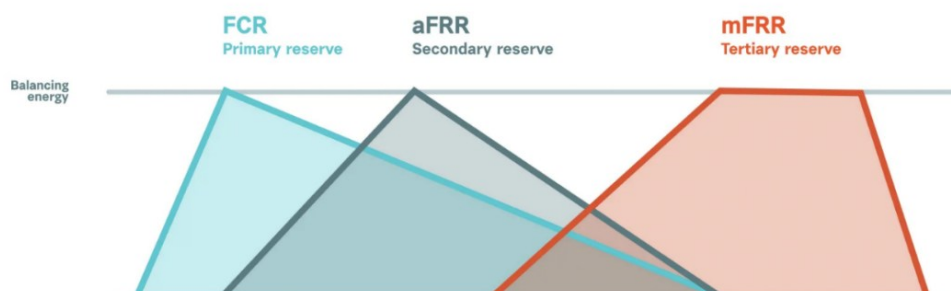


Figure 14, FCR, aFRR and mFRR activations (Nano Energies 2025)

While the FCR products stabilise the deviated frequency, aFRR restores the frequency to 50 Hz. It handles shorter-term imbalances, restoring frequency faster than mFRR, and operates as a complementary reserve for mFRR. The mFRR is necessary for the Nordic power system, as aFRR cannot provide sufficient volumes, and because of grid congestion between regions. (ENTSO-E 2024b, p. 12)

3.6.1 aFRR Markets

Dimensioning of aFRR has previously focused on the morning and evening hours, when maintaining frequency quality is challenging due to large imbalances between production and consumption. Currently, imbalances occur almost every hour, making aFRR more frequently necessary throughout the day. (ENTSO-E 2024a, p. 13.) In 2025, the Nordic procurement requirement for aFRR is 400 MW for up-regulation and 450 MW for down-regulation (Svenska Kraftnät 2025c). Similar to FCR and FFR, also aFRR procurement is divided among the Nordic TSOs, each of which procures its share of the dimensioned reserve capacity. Procured volumes are expected to increase in the future. (ENTSO-E 2024a, p. 13.) Production and consumption are unevenly distributed between bidding zones, making the exchange of balancing capacity between regions essential. Some bidding zones lack flexible reserve providing entities, such as hydro power, hence common Nordic markets are needed. (ENTSO-E 2025c)

In the Nordic countries, aFRR capacity is procured through a common Nordic capacity market (CM). Capacity reserves are procured on a daily market for each hour of the following day, with GCT set at 7:30 CET, before the GCT of the DA market. Prices are determined based on marginal pricing. If a bid is accepted in the aFRR CM, the provider must also be able to deliver the corresponding energy for the specified time unit. (ENTSO-E 2024a, p. 17.) The minimum bid size for aFRR CM is 1 MW, with increments of 1 MW. Bids can be either divisible or indivisible, depending on whether the participant allows only part of the bid to be used. The maximum bid size for an indivisible bid is 50 MW. (Nordic Balancing Model 2024a, p. 9-10.) The Nordic aFRR CM enables cross-zonal exchange between regions, and therefore interconnections must reserve capacity for aFRR exchange. (ENTSO-E 2024b, p. 12)

In addition to the CM, Finland implemented a national aFRR Energy Activation Market (EAM) in June 2024 (Fingrid 2025h). In March 2025, Finland connected the aFRR EAM to the European aFRR platform, PICASSO. In the future, all Nordic countries will join PICASSO for aFRR energy exchange. (Nordic Balancing Model 2025a.) Currently, Sweden and Norway only have aFRR CMs, but an aFRR EAM will be implemented once they join PICASSO (Svenska Kraftnät 2025d; Statnett 2025a). PICASSO enables exchange between multiple European regions, increasing the availability of balancing

energy for the TSOs. In this platform, participants submit bids to the TSO operating in the bidding zone, which in turn submits their demand, the energy bids, and cross-border capacities to PICASSO. Each TSO provides a local merit order list of the bids, which PICASSO merges to a common list. The common European aFRR platform then optimises the demand, bids, and cross-border capacities. (ENTSO-E 2024c, p.6-12)

The EAM volumes consists of procured capacity in the aFRR CM and voluntary bids submitted to the aFRR EAM (Nordic Balancing Model 2024a, p. 5). The minimum bid size for EAM is 1 MW. In Sweden and Norway, which do not have an EAM, activated energy volumes consists solely on bids accepted in the CM. (Fingrid 2024c, p. 8 & 13). Accepted bids in the CM require the participant to submit the corresponding energy to the aFRR EAM, if available in the country (Svenska Kraftnät 2024c). In Norway and Sweden, the activated aFRR capacity is compensated with the mFRR EAM price, as well as in Finland before the EAM was implemented. (Vold 2025; Muikku 2025).

3.6.2 mFRR Markets

The mFRR markets are used to balance the power system and to manage imbalances by TSOs. Dimensioning of mFRR is based on the largest expected disturbance for each region, and each TSO procures the necessary capacity according to the specific situation in their country. (ENTSO-E 2024b, p. 12.) For instance, Sweden procure up to 1180 MW of mFRR up-regulation and 1050 MW down-regulation for 2025 (Svenska Kraftnät 2025c). There are two mFRR markets: one for procurement of mFRR capacity and another for the procurement of mFRR energy activation, similar to aFRR in Finland.

Previously, mFRR capacity was procured at a national level, separately for each region. However, in November 2024, a trilateral mFRR CM was established. (Nordic Balancing Model 2025a.) This trilateral market consists of Finland, Sweden, and Denmark, excluding Norway. The goal is to extend the market to include Norway and create a common Nordic mFRR CM. Its purpose is to procure and exchange balancing capacity between regions. The market operates under the same principles and rules as the common Nordic aFRR CM. (Nordic Balancing Model 2024b, p. 3). mFRR capacity is procured on an hourly market on the previous day of delivery, with marginal pricing (ENTSO-E 2024a). The minimum bid size is 1 MW and the maximum bid size is 50 MW. Bids are submitted according to the bidding zone where the entity is located, and prices may differ between bidding zones. (Nordic Balancing Model 2024a, p. 6-7)

The trilateral CM enables mFRR capacity exchange between bidding zones. This makes the procurement of mFRR balancing capacity cost-effective for TSOs and enhances security. Connecting the three national markets enables access to a larger market. (Nordic Balancing Model 2024c.) The mFRR CM is used by the TSOs to guarantee that participants will provide bids for the mFRR EAM, and therefore accepted bids in the CM are compensated with a capacity payment for an commitment to submit corresponding bid to the EAM. (Nordic Balancing Model 2025b)

Statnett procures mFRR capacity in Norway through a national CM, which was implemented in February 2024. Before this, a market called RKOM was used, which had a different structure. (Vold 2025.) In Norway, the CM also aims to ensure sufficient bids to the EAM. mFRR capacity in Norway is procured through both hourly and a seasonal markets. The hourly market has a GCT on the day before delivery, while the seasonal market procures capacity for winter months. Each bidding zone have its distinct prices, and bids must be submitted separately for each region. (ENTSO-E 2024a, p. 18.) The minimum bid size for the mFRR CM in Norway is 5 MW (Statnett 2025b).

The mFRR energy activations are procured from a common Nordic EAM for each MTU, with a GCT 45 minutes before the delivery period (ENTSO-E 2024a, p. 17). As with aFRR, the mFRR CM volumes together with voluntary bids constitute the available mFRR EAM volumes (Nordic Balancing Model 2024a, p. 5). Finland and Sweden have a minimum bid size of 1 MW, while Norway have either 5 MW or 10 MW, depending on the bidding zone. In all countries, the maximum bid size is 50 MW. (Nordic Balancing Model 2024d.) Market participants mFRR energy bids are submitted by the TSOs to the common Nordic platform before the GCT, along with cross-border capacities and regional demands of each TSO for each MTU. The platform then matches each TSO's demand with available bids, leading to the activation of the selected bids. (ENTSO-E 2024d, p. 16-17)

In the mFRR EAM, activated energy is compensated with an energy payment, with separate prices for up- and down-regulation. Down-regulation indicates that a reserve provider purchases energy from the TSO, while up-regulation means that the provider sells energy to the TSO. In up-regulation, bids are activated starting from the cheapest, and the most expensive activated bid sets the price, but not less than the DA market price. In this case, the TSO pays the energy payment for the provider. In down-regulation, activation starts from the most expensive bid, and the cheapest activated bid sets the price, but never exceeding the DA market price. Here, the provider pays an energy payment for the TSO. (Fingrid 2025i.) Prices are published after the delivery period, once activations have been assessed. Due to grid congestion, different bidding zones may have different prices. (ENTSO-E 2024a, p. 17)

In March 2025, the Nordic mFRR EAM changed into a new automatic mFRR EAM, supporting automated balancing, and the MTU changed from one hour to 15 minutes. (eSett 2025a.) However, this is only a transition phase towards integration with the common European platform, MARI, which the Nordic countries will join in the future, similar to the common aFRR EAM platform PICASSO. This enables cross-zonal mFRR balancing exchange and increases the availability of bids across regions. (Nordic Balancing Model 2025c)

3.7 Nordic Balancing Model and Imbalance Settlement

The Nordic Balancing Model (NBM) is a program that develops and harmonises balancing processes in Nordics to accommodate the increasing share of variable renewable sources in the power system. It aims to support cross-border exchange in Nordic markets, particularly integration with European platforms, while enhancing market efficiency and cost-effectiveness. NBM drives the implementation of the common Nordic aFRR and mFRR CMs, aFRR and mFRR EAMs, and their integration into the European platforms PICASSO and MARI. It also drives the transition of markets from hourly resolution to 15-minute resolution. Additionally, NBM has developed the single price model for imbalance settlement in Nordics. All of these developments serve the primary objective of implementing the 15-minute time resolution. (Nordic Balancing Model 2019, p. 3-5.) These changes, together with increased use of automation in the system and markets, will improve TSOs capability to maintain the power system balance (Statnett 2022).

Electricity production and consumption must remain in balance at all times. A Balance Responsible Party (BRP) must plan their production and consumption in the electricity markets before every MTU and maintain balance in accordance with the plans. (eSett 2025b.) A BRP refers to a company that holds a balance agreement with a TSO and an imbalance settlement agreement with the balance provider, eSett. BRPs participate in electricity and balancing markets and are responsible for ensuring that production, consumption, and electricity trades of their units remain balanced. (eSett 2025c.) Imbalances arise when there is a difference between scheduled electricity flows, and the actual metered flows. In such cases, TSOs utilise balancing power markets, particularly mFRR market, to procure the needed balancing power. After the delivery period, and completion of physical balancing, BRPs report their imbalances to eSett, which then performs the imbalance settlement to achieve financial balancing. (eSett 2025b)

eSett operates as the balance provider in the Nordics on behalf of the four Nordic TSOs and is responsible for imbalance settlement. eSett collects, validates, and manages imbalance data while providing imbalance settlement services to BRPs, including the assessment and calculation of imbalances, monitoring activities, and invoicing. Additionally, eSett publishes data

related to imbalances. Imbalance settlement ensures economic balance between parties in the markets for each MTU. All BRP imbalances are calculated based on the scheduled traded production and consumption, and actual meter production and consumption. Each BRP is financially responsible for its own imbalances. (eSett 2024, p. 13-15)

With the Nordic Imbalance Settlement Model, imbalance settlement is performed with same principles and processes across the Nordic countries. All BRPs are treated equally under the common settlement model. (eSett 2024, p. 13.) Before November 2021, imbalances in the Nordics were managed separately for production, consumption, and trades, each calculated and settled individually with separate prices. These were merged to a single price model, utilising one calculation method and a uniform price for all imbalances within each Imbalance Settlement Period (ISP). (Nordic Balancing Model 2021.) In May 2023, the ISP changed from one hour to 15 minutes, meaning eSett began settling BRP imbalances at a 15-minute resolution. However, imbalance pricing changed from hourly to 15-minute resolution only with the introduction of the new mFRR EAM in March 2025, which enabled quarter-hourly pricing. Before this change, all quarters within an hour were priced the same. The single price model and the shift to shorter resolution supports real-time balancing. (Nordic Balancing Model 2025d)

Imbalance volumes are calculated for each BRP separately in each bidding zone. In the current model, the imbalance volume is determined based on production, consumption, fixed deliveries, imbalance adjustments, and Metering Grid Area (MGA) imbalance, as illustrated in *Figure 15*. (eSett 2024, p. 62.) Production refers to actual metered production, and consumption to actual metered consumption. Fixed deliveries represent traded electricity in the DA and ID markets, as well as agreed bilateral trades between parties. Imbalance adjustments are corrections by the BRP in the balancing markets. MGA imbalances are determined by eSett based on data reported by the metered data aggregator, representing net difference between consumption, production, and the import or export exchanges between adjacent MGAs. (eSett 2021, p. 5.) If reported values are corrected, the MGA imbalance is considered as zero (eSett 2024, p. 29). In the model, consumption and energy sales are treated as negative values, while production and energy purchases are treated as positive (eSett 2024, p. 62).

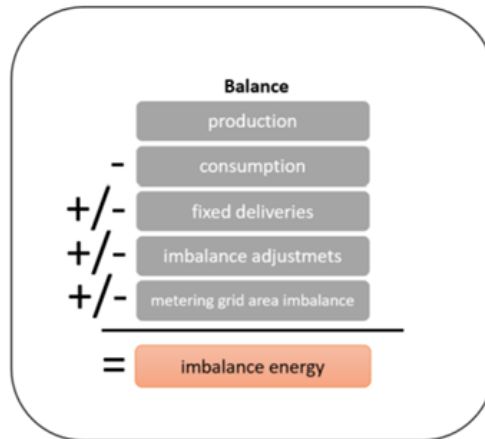


Figure 15, Imbalance volume calculation method (Fingrid 2025j)

A calculation example for a WPP is performed in Table 6. The WPP sold 100 MWh to the DA market for a specific MTU, while the actual metered production was 80 MWh. Additionally, 10 MWh were traded in balancing market for balancing purposes. As the WPP has no consumption, consumption is 0 MWh. MGA imbalances are considered as zero. This results in an imbalance volume of -10 MWh, and therefore the BRP responsible for the WPP must purchase 10 MWh balancing from eSett.

Table 6, Imbalance calculation example

Imbalance calculation (MWh)				
Production (metered)	Consumption (metered)	Fixed Deliveries (DA sales)	Imbalance Adjustments	MGA Imbalance
80	0	-100	10	0
Imbalance volume: -10 MWh				

Imbalance price is determined for each ISP based on balancing market prices. The price is set according to the dominating regulation direction, either up-regulation or down-regulation price for that ISP. As defined by the single price model, the same price is used for both positive and negative imbalance volumes. In Finland, if up-regulation is the dominating direction, the imbalance price is the higher of the aFRR and mFRR EAM up-regulation prices. In Norway and Sweden, the price is determined by the mFRR EAM up-regulation price. If down-regulation is the dominating direction, the price in Finland is the lower of the aFRR and aFRR EAM down-regulation prices, while in Norway and Sweden it is based on the mFRR EAM down-regulation price. If no balancing energy is activated, or if up- and down-regulation volumes are equal, the imbalance price is set by the DA market price. (eSett 2024, p. 67-68.) Table 7 summarises the imbalance pricing.

Table 7, Imbalance price model (Modified from eSett 2024, p. 67)

Single price model for imbalances			
Area	Up-regulation ISP	Down-regulation ISP	ISP with no direction
Sweden & Norway	mFRR EAM up-regulation price	mFRR EAM down-regulation price	DA market price
Finland	Higher up-regulation price (mFRR or aFRR)	Lower down-regulation price (mFRR or aFRR)	DA market price

When there is a positive imbalance, or a surplus in the system, a producing BRP is compensated for the overdelivered energy if the imbalance price is positive. If the imbalance price is negative, the BRP pays for the surplus energy delivered. In case of a negative imbalance, or a deficit in the system, a producing BRP must pay for underdelivered energy if the imbalance price is positive. If the imbalance price is negative, the BRP is compensated for the deficit energy it receives. (ENTSO-E 2023b)

In addition to the imbalance prices, eSett charges three types of country-specific fees: a volume fee, an imbalance fee, and a weekly fee. The volume fee is based on the total consumption and production volumes for each ISP. The imbalance fee is calculated from the BRP's imbalance volume for each ISP. The weekly fee applies for each week the BRP participates in imbalance settlement. (eSett 2024, p. 68-70.) A calculation example is performed in Table 8, using the production and imbalance volumes from Table 6. A positive value indicates that the BRP must pay eSett.

Table 8, Price calculation example (Modified from eSett 2024, p. 71)

	Volume (MWh)	Price (EUR)	Amount (EUR)
Sale of imbalance energy to eSett	0	40	0
Purchase of imbalance energy from eSett	10	40	400
Volume fee	80	0.50	40
Imbalance fee	10	1.50	15
Total amount: 445 EUR			

4 Battery Energy Storage Systems

This chapter provides a comprehensive overview of Battery Energy Storage Systems (BESS), with a focus on their technological, operational, and economic aspects. First, general energy storage systems are presented, and the justification behind selecting Lithium Ion (Li-Ion) technology for this thesis. Then, BESS components and performance characteristics are discussed. A deeper focus is placed on Li-Ion batteries, including their internal components, electrochemical principles, and material composition. Various Li-Ion chemistries are examined. Battery degradation mechanisms—both calendar and cyclic—are analysed, along with their effects on BESS lifetime modelling. Finally, the chapter addresses the economics of BESS, evaluating cost trends and presenting current data on investment costs and operational expenditures.

4.1 Energy Storage Systems and Battery Technologies

With the increasing share of renewable energy sources, the intermittent nature of their generation poses a significant challenge to maintain a reliable energy supply. In modern power systems, energy storages plays a critical role in ensuring system flexibility, security, and reliability. These systems support the integration of renewable energy through energy storage complementation, which stores excess electricity generated during periods of high production and supplying it during times of low generation. A wide range of energy storage technologies are available, which are classified into five main categories: electrochemical, electrical, thermal, chemical, and mechanical. (Apata 2023.) *Figure 16* provides an overview of these categories, with their main sub-categories.

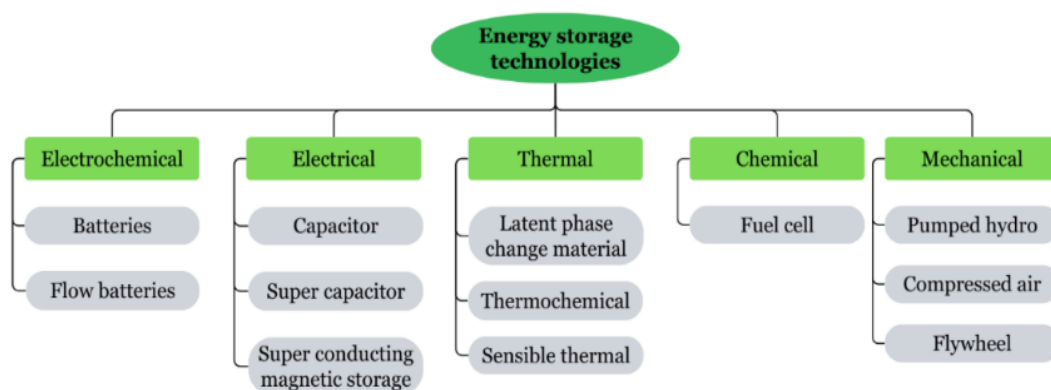


Figure 16, Main categories for energy storage technologies (Laine-Ylijoki 2024, p. 50)

All storage technologies share the common purpose of absorbing energy to store it, and releasing it when energy is needed. Storage systems are characterised by several key parameters, including cost-effectiveness, power and energy capacity, energy duration, cycle life, response time, specific energy and specific power, and efficiency. Cycle life indicates the number of charge and discharge cycles the energy storage can undergo before its performance begins to degrade noticeably. Specific energy refers to the energy storage capacity per unit weight while specific power denotes the rate at which energy can be delivered per unit weight. However, no single technology can optimise all these parameters simultaneously. This limitation has driven the development to a wide range of technologies, each offering distinct advantages and trade-offs. While certain technologies offer advantages for specific applications, they may also present limitations in other areas. The suitability of an energy storage system is highly dependent on the intended application. (Apata 2023)

BESS fall under the category of electrochemical storages, which are a widely used technology (Apata 2023). BESS are a promising solution to mitigate the generation variability of renewable energy source, due to their fast response times, modularity, and high commercial potential. They are well-suited for applications such as peak shaving, load shifting, and serving as backup systems to stabilise grid fluctuations. (Mouais & Qaisar 2023.) The five most revenue generating applications for BESS include participation in reserve markets, integration with renewable energy sources, transmission grid support, peak load management, and energy arbitrage operation. (Volta Foundation 2025, p. 147.) The installed capacity of BESS is experiencing rapid growth. In 2024 alone, 69 GW of power capacity and 169 GWh of energy storage capacity were installed globally, increasing the total cumulative capacity to 150 GW and 363 GWh. This means that the BESS capacity installed in 2024 accounted for 46% of the global total capacity. Notably, 98% of the BESS installations in 2024 represented Li-Ion batteries. (Volta Foundation 2025, p. 138.) *Figure 17* illustrates the annual installation capacities of BESS as well as the cumulative installed capacity.

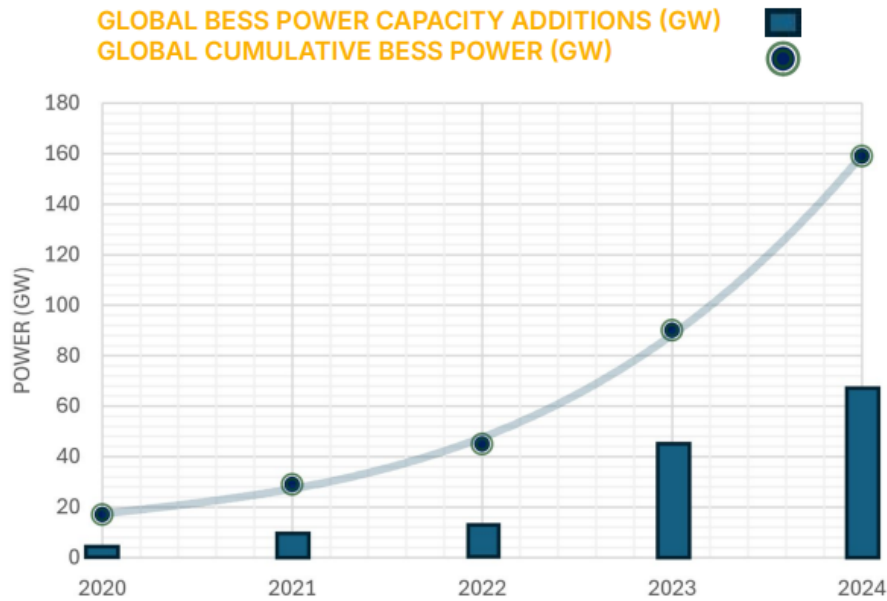


Figure 17, Yearly global installed capacity and cumulative capacity of BESS (Volta Foundation 2025, p. 138)

Battery technologies can be further categorised into sub-groups based on the battery chemistry. The main types are Li-Ion, lead-acid, sodium-sulphur, nickel-cadmium, and flow batteries (Apata 2023). Key parameters of batteries include efficiency, cycle life, specific energy, cost of battery cells and modules, maintenance requirements, overall performance, and safety (IRENA 2015, p. 9). In early years, sodium-sulphur batteries dominated the market, however Li-Ion technologies have overtaken them due to their suitability across many applications. This shift is majorly because of Li-Ion batteries high specific energy and specific power, long lifespan, lightweight design, and favourable performance-to-cost ratio compared to other technologies. Additionally, their increasing popularity and fast development have rapidly decreased the costs. (IRENA 2015, p. 26.) Furthermore, Li-Ion batteries offer high efficiency, and low self-discharge rates. (Kebede et al. 2022, p. 4-5)

Lead-acid batteries are characterised by their low cost and sufficient efficiency, however, they are significantly heavier and have lower specific energy and power compared to Li-Ion batteries. Nickel-based batteries offer long lifespan, but suffer from low specific energy and power, and relatively high self-discharge rates. Sodium-sulfur batteries have high specific energy, sufficient efficiency, and low self-discharge rate. Flow based batteries are another promising technology for stationary applications, offering long lifetime, low self-discharge rates, and fast response times. (Kebede et al. 2022, p. 4-5)

Figure 18 compares specific energy of different battery technologies, highlighting lithium-based batteries as having the highest specific energy. Figure 19 illustrates the global cumulative installation of different battery technologies, from 2011 to 2021. As the figure shows, Li-Ion batteries dominate global installations. Given the widespread preference for Li-Ion batteries in stationary applications due to their characteristics, and their dominance in global deployment statistics, this thesis will focus solely on Li-Ion batteries. Further analysis and discussion will be presented in the following sections.

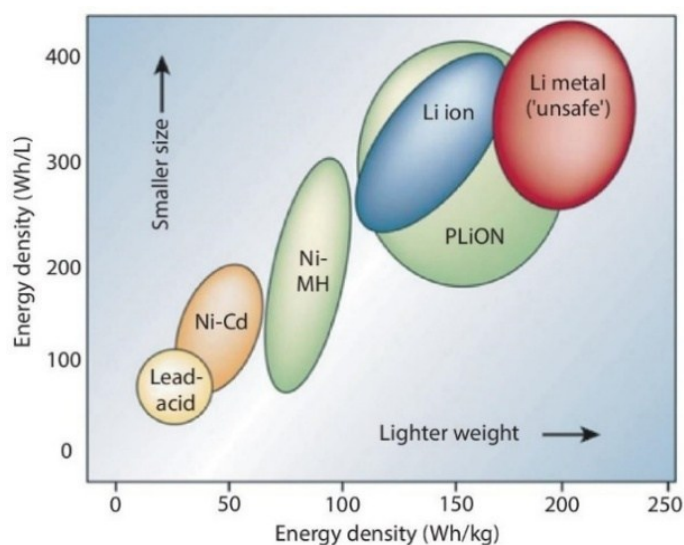


Figure 18, Specific energy of battery technologies (Mouais & Qaisar 2023)

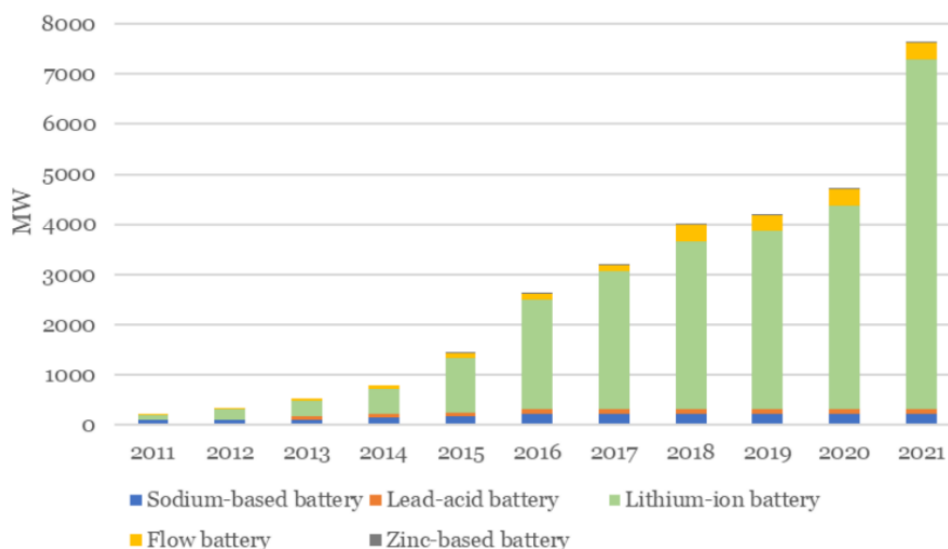


Figure 19, Cumulative installed battery capacity per technology (Laine-Ylijoki 2024, p. 51)

4.2 Overview of Battery Energy Storage Systems

A BESS comprises several key components, each performing a critical function in the operation, and integration with the electrical grid. These include the battery pack, the Battery Management System (BMS), Power Conversion System (PCS) and grid connection interface (Choi et al. 2021, p. 5). *Figure 20* illustrates the primary BESS components.

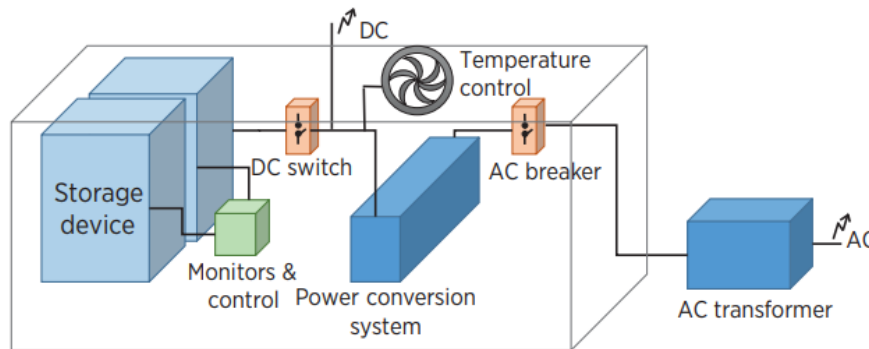


Figure 20, BESS primary components (IRENA 2015, p. 8)

The battery stores energy through electrochemical reactions, known as oxidation and reduction, by absorbing energy during charging, and releasing energy during discharging. (Choi et al. 2021, p. 7). This process is described in detail in *Chapter 4.3*. The fundamental building block of a battery is the battery cell, which do not provide sufficient capacity for large-scale applications, therefore, multiple cells are combined in series and parallel configurations to form battery modules. These configurations of cells determine the voltage and current characteristics of the battery. Battery modules are further assembled into battery packs to further increase the voltage and capacity. In BESS applications, several packs are integrated typically within a containerised unit. Battery cells can vary in physical geometry, influencing the overall performance characteristics. The most common cell geometries include cylindrical, prismatic, and pouch types, with cylindrical cells being the most widely used. (Choi et al. 2021, p. 6-10)

Each battery module is connected to a BMS, which is responsible for ensuring the proper operation and functionality of the module. The BMS maintains safe operation conditions by monitoring and managing key parameters such as temperature, cell voltage, and currents, while also optimising operation by controlling the charging and discharging cycles. Furthermore, BMS collects operational data and manages communication between different systems. Each BMS is connected with a battery control unit, which oversees the performance of the entire battery pack. (Choi et al. 2021, p. 5-6.) In Li-Ion battery systems, thermal monitoring is particularly critical to prevent the risk of overheating (IRENA 2015, p. 7-8).

As the electrical grid operates with Alternating Current (AC) and the battery operates with Direct Current (DC), power conversion is necessary during both charging and discharging processes. The PCS enables this by serving as a bidirectional converter between the battery output and the electrical grid. A PCS ensures that the battery’s power output meets grid requirements. During discharging, it converts the output DC to AC, and during charging, it converts input AC to DC. This system secures stable and controlled energy flow between the battery and the grid. The PCS relies on power electronic components, such as semiconductor devices, transistors, and transformers. (Choi et al. 2021, p. 6-7)

Technical specifications, such as power rating, energy capacity, C-rate, and Round-Trip Efficiency (RTE), of a BESS are crucial for accurately assessing performance. Power rating, typically measured in MW, refers to the maximum rate at which the battery can charge or discharge energy. Energy capacity, measured in MWh, indicates the total amount of energy the BESS can store. C-rate is the charging or discharging rate relative to its maximum capacity. For instance, a BESS with a 2 MW power rating and 4 MWh energy capacity can fully charge or discharge in two hours, corresponding to a C-rate of 0.5C. A C-rate of 1C would indicate a full charge or discharge within one hour. (Claire 2025.) RTE indicates the ratio of energy discharged by the system to the energy initially used for charging, as defined in (1) (Dhananjay et al. 2023, p. 555-556).

$$RTE = \frac{E_{output}}{E_{input}} * 100 \quad (1)$$

where E_{output} denotes the energy output during discharging and E_{input} the energy required for charging.

RTE of a battery depends on the underlying battery technology. According to IRENA (2017), the RTE for Li-ion battery technologies range from 92% to 96% as of 2017, with forecasts indicating a potential increase to between 94% and 98% by 2030. (IRENA 2017, p. 77.) Feehally et al. (2018) reported a Li-Ion cell-level RTE of 95%, while the RTE for a complete BESS—including system integration and component-level losses—was estimated at 91.1% (Feehally et al. 2018, p. 1). In another study, the research obtained a simulated BESS RTE value of 93.4% (Noyanbayev et al. 2018, p. 8). It is important to note that battery cell efficiency is higher than the total system-level efficiency of a BESS, as additional losses occur in other components. Based on current data, the RTE of modern BESS installations can be estimated to range between 91% and 95%.

4.3 Li-Ion Batteries

4.3.1 Battery Components

The properties and performance of Li-Ion batteries are determined by their internal components, the chemical composition of those components, and the interactions between them. The key components of a Li-Ion battery cell include two electrodes, known as the anode and cathode, the electrolyte, and separator. The anode is commonly composed of graphite or silicon, while the cathode consists of lithium metal oxides. The electrolyte is typically an organic solvent in liquid or gel form, containing lithium salts, which allows the transport of lithium ions between the electrodes. The separator is a membrane that allows the movement of free ions through the electrolyte while preventing electrical currents between the anode and the cathode, thereby avoiding short circuits. (Volta Foundation 2025, p. 199.) Although the separator is essential in cells using liquid electrolytes, it does not participate in the electrochemical reaction itself (Choi et al. 2021, p. 9). A schematic of a Li-Ion battery cell is shown in *Figure 21*.

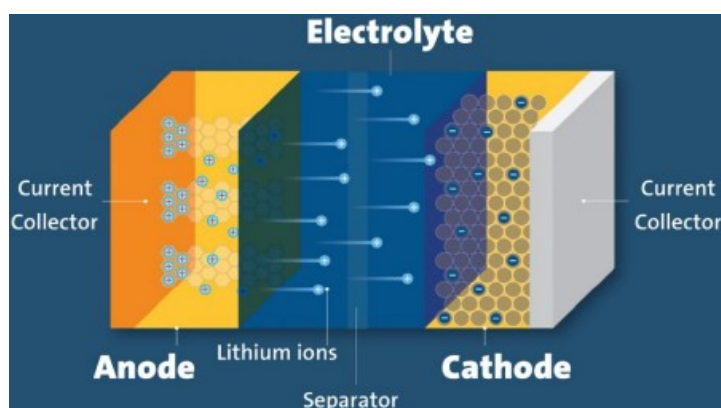


Figure 21, Li-Ion cell and its components (Volta Foundation 2025, p. 204)

The fundamental operating principle of batteries involves redox potentials—or Fermi energies—of the materials used in the anode and cathode (Choi et al. 2021, p. 7). Batteries absorb and deliver energy through electrochemical processes, in which lithium ions migrate between the electrodes, generating current flow. During discharging, lithium atoms at the anode are ionised into positive lithium ions, which then diffuse through the electrolyte from regions of higher to lower concentrations. These ions travel toward the cathode, where they are reduced by combining with electrons arriving from the external circuit, forming lithium atoms at the cathode surface. The electrons released during ionisation at the anode, flow through the external circuit to the cathode, to merge with lithium ions. During charging, this process is reversed. The chemical reactions occurring at the anode and the cathode are given in (2), (3) and (4). (Hossain et al. 2020, p. 29-30.) Both charging and discharging processes are visually illustrated in *Figure 22*.

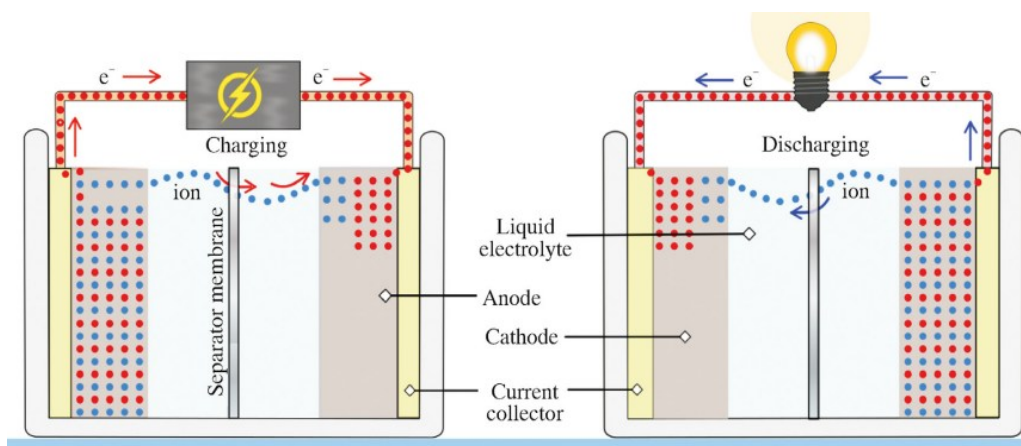
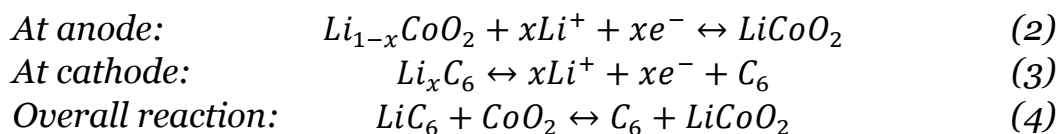


Figure 22, Charging and discharging process of a Li-Ion battery cell (Mitali et al. 2022, p. 189)

Different materials used in the battery components determines the battery performance and its characteristics, and specific material choices are made depending on the intended application. According to Volta Foundation (2025), the primary function of the lithium salt- organic solvent electrolyte is to conduct ions efficiently within the medium, which determines thermal and voltage stability. Furthermore, the electrolyte must be chemically compatible with the electrode materials. (Volta Foundation 2025, p. 251.) The separator is typically manufactured from polyolefin materials, with ceramic coating of polyethylene or polypropylene. Alternative separator materials include glass fibre and composite membranes, each with different advantages and trade-offs. (Volta Foundation 2025, p. 255)

The selection of the anode material is application specific, as it impacts the battery's cost-effectiveness, lifespan, safety, and C-rates. Graphite and silicon based materials are commonly used. Graphite has traditionally been used in Li-Ion batteries due to its good stability, reliability and cost-effectiveness, although its storage capacity is limited. In contrast, silicon offers higher specific energy but suffers from lower stability and safety as a results of volume expansion during charge-discharge cycles. Additionally, silicon is more expensive. Nevertheless, silicon is increasingly being used either to replace graphite or in blended anode materials. (Volta Foundation 2025, p. 234-236.) The cathode material is the primary factor determining battery performance, and its various chemistries will be discussed in *Chapter 4.3.2*.

4.3.2 Cathode Materials in Li-Ion Batteries

The chemistry and composition of the cathode in Li-Ion batteries vary across technologies, influencing key parameters such as specific energy, cycle life, voltage, specific power, and costs. The most widely used lithium metal oxides for cathode materials include Lithium Cobalt Oxide (LCO), Lithium Manganese Oxide (LMO), Lithium Nickel Manganese Cobalt Oxide (NMC), and Lithium Iron Phosphate (LFP) (Volta Foundation 2025, p. 204.) The six most common cathode materials are discussed and compared below.

1. *Lithium Cobalt Oxide (LCO)*

LCO have a high specific energy and high voltages output. This technology is well-established due to its long development history and reliable value chain, with LCO batteries also having high recycling value. Trade-offs include limited thermal stability and higher costs, primarily due to expensive cobalt, which's price also tend to be volatile. (Volta Foundation 2025, p. 217.) Additionally, LCO batteries have a shorter lifespan. Despite the drawbacks, the high specific energy makes LCO batteries particularly common in small electronic devices, such as mobile phones and laptops. (Battery University 2023)

2. *Lithium Manganese Oxide (LMO)*

LMO batteries are known for their thermal stability, high specific power, and efficiency, alongside relatively low manufacturing costs due to inexpensive raw materials. However, their performance is limited by a lower specific energy, high self-discharge rates, and poor performance at lower temperatures. (Volta Foundation 2025, p. 226). LMO batteries also have a relatively short cycle life. These batteries are commonly used in medical devices, power tools, and Electric Vehicles (EV), although they have become less common in recent years due to the rise of competing technologies. (Battery University 2023)

3. *Lithium Nickel Manganese Cobalt Oxide (NMC)*

NMC batteries offer a higher specific energy, high recycling value, and a strong cell voltage due to their favourable redox potential. NMC batteries face challenges related to instability, such as excessive heat generation, swelling of cells, and undesirable side reactions during cycles. Moreover, the battery constitutes of hazardous materials, and the costs are relatively high for the raw materials. (Volta Foundation 2025, p. 208-209.) NMC batteries are typically used in power tools and EVs. (Battery University 2023)

4. *Lithium Iron Phosphate (LFP)*

LFP batteries are one of the most cost-effective options available due to inexpensive materials. Their operation is considered extremely safe due to excellent thermal and chemical stability. They also have long cycle life and are durable, especially when subjected to full charge-discharge cycles. (Volta Foundation 2025, p. 220.) As disadvantages, LFP batteries have low nominal cell

potential, resulting in lower specific energy, which lead to heavier battery packs. They also have higher self-discharge rates. These batteries are widely used in stationary and portable applications requiring high load currents, such as BESS. (Battery University 2023)

5. *Lithium Nickel Cobalt Aluminium Oxide (NCA)*

NCA batteries have similar properties to NMC batteries, including very high specific energy, long lifespan, and relatively good specific power. However, NCA batteries face concerns regarding safety (Battery University 2023.) Additionally, they are costly due to expensive nickel and aluminium, which however increases the recycling value. NCA batteries are typically used in energy storage systems and EVs. (Volta Foundation 2025, p. 213)

6. *Lithium Titanate (LTO)*

LTO batteries differ from other Li-Ion batteries by replacing the graphite anode with titanate. This results in high charging and discharging currents, long lifespan, and excellent thermal stability and safety, making them among the safest battery technologies available. Additionally, they support fast charging and discharging rates. However, their high costs and low specific energy are significant limitations. (Battery University 2023)

These six Li-Ion battery chemistries and their key characteristics are summarised and compared in *Table 9*, and a visual comparison presented in *Figure 23* as a hexagonal radar chart, evaluating six parameters: specific energy, specific power, safety, performance, lifespan, and costs. Safety encompasses the overall operational safety, and performance indicates the functionality in varying temperature conditions. Lifespan includes both cycle life and calendar life, whereas cost reflects to the overall battery costs. (Bhutada 2023)

Table 9, Li-Ion battery chemistries and their key characteristics (Battery University 2023; Hossain et al. 2020, p. 31)

	LCO	LMO	NMC	LFP	NCA	LTO
Cathode	LiCoO ₂	LiMn ₂ O ₄	LiNiMn-CoO ₂	LiFePO ₄	LiNi-CoAlO ₂	LiMnO ₂
Anode	Graphite	Graphite	Graphite	Graphite	Graphite	Titanate
Nominal cell potential	3.6 V	3.7 V	3.6–3.7 V	3.2–3.3 V	3.6 V	2.4 V
Specific energy, Wh/kg	150–200	100–150	150–220	90–120	200–260	50–80
Cycle life	500–1000	300–700	1000–2000	>2000	500	3000–7000
Drawbacks	Stability, cost, life-time	Specific energy, self-discharge	Stability, cost, hazardous	Specific energy, self-discharge	Safety, cost	Specific energy, cost

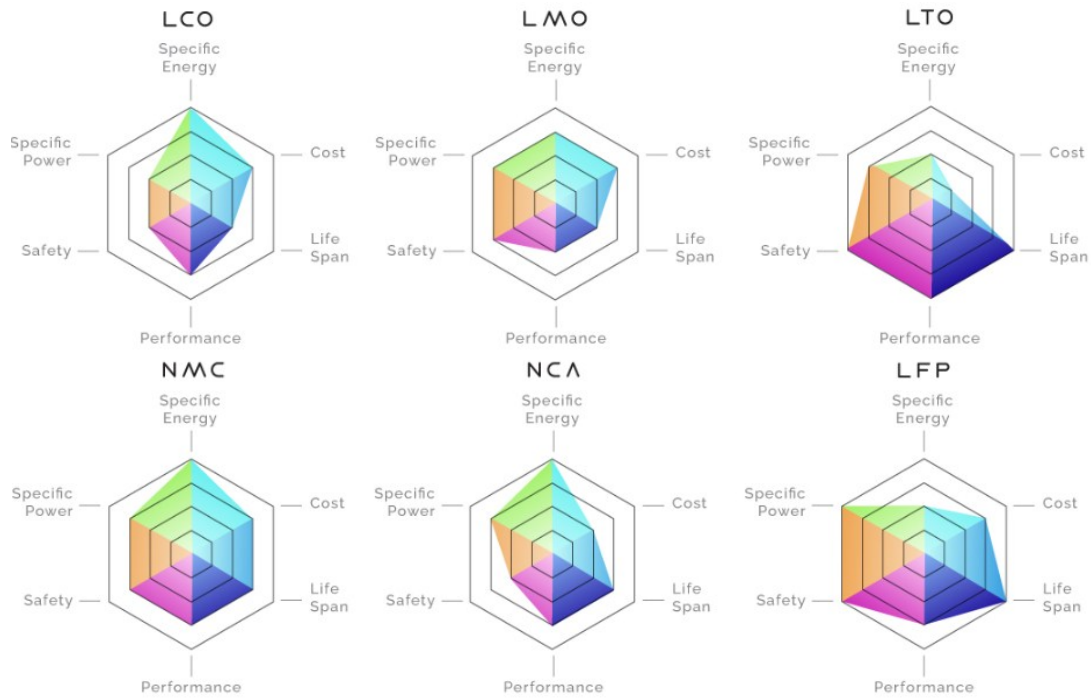


Figure 23, Comparison of Li-Ion technologies (Bhutada 2023)

4.4 Battery Degradation

Li-Ion batteries degrade over time, resulting in energy capacity reduction. Minimising this degradation enhances both battery lifetime and economic performance. According to Edge et al. (2021), the two primary mechanisms contributing to battery degradation are Solid Electrolyte Interphase (SEI) layer thickening and lithium plating. The SEI layer forms on the anode surface in Li-Ion batteries and functions as a passivation layer, preventing further reactions between the electrolyte and the anode. It is initially formed during the first cycle and it continues to thicken over time due to diffusion of solvent molecules in the existing SEI layer, exposure of new anode surface from particle cracking, and the accumulation of side reaction products. This progressive thickening reduces the permeability of the layer to lithium ions, thereby accelerating capacity fade of the battery. Operating the battery in high temperatures and with high power further accelerate SEI layer growth. (Edge et al. 2021, p. 8203-8205)

Lithium plating indicates the process where lithium ions deposit as metallic lithium on the anode surface during charging. This typically arises under high charging rates, low temperatures, or overcharging conditions. Lithium plating leads to a reduction in the battery capacity, and decreases its safety. It is more common in fast-charging applications. (Edge et al. 2021, p. 8203-8205)

Before presenting battery degradation types and models, it is essential to define the key battery parameters: State of Health (SoH), Beginning of Life (BoL) capacity, End of Life (EoL) capacity, State of Charge (SoC) and Depth of Discharge (DoD). Ovaskainen et al. (2023) defines these parameters as follows: BoL capacity refers to the battery’s capacity at the start of its life, before any degradation has occurred, when the energy capacity is at its initial value. EoL capacity denotes the capacity at the end of the battery’s useful life, typically expressed as a percentage of the BoL capacity. Although a battery may still operate beyond its EoL, its performance is no longer optimal and it is generally considered as the end of a planned investment period. Accurately determining the BoL and EoL capacities is crucial to ensure that the battery system is appropriately sized for its intended operational lifetime. For instance, if a battery system is required to maintain an energy capacity of 10 MWh until it reaches EoL, the BoL capacity must be higher, taking into account degradation and capacity losses over the operational period. (Ovaskainen et al. 2023, p. 6-7)

SoH quantifies battery degradation by measuring the available energy capacity relative to the initial BoL energy capacity, thereby indicating the remaining lifespan of the battery. At BoL, the SoH is defined as 100%, while at EoL, the SoH is determined by the battery manufacturer and typically falls within a range, such as 60–65%. (Ovaskainen et al. 2023, p. 7.) In contrast, other sources report different thresholds. Volta Foundation (2025) suggests an EoL SoH of 70–80%, while Sheridan and Conlon (2021) define it at 80% (Volta Foundation 2025, p. 325; Sheridan & Conlon 2021, p. 2).

SoC at a given moment is defined as the ratio of the battery’s energy content at that time to its maximum energy capacity. The SoC at any specific time fluctuates within the minimum and maximum possible SoC limits. SoC at a given moment is mathematically expressed in (5) and (6). (Jimenez et al. 2018, p. 3)

$$SoC_t = \frac{E_t}{E_{battery}} \quad (5)$$

$$SoC_{min} \leq SoC_t \leq SoC_{max} \quad (6)$$

where E_t refers to the energy capacity at the given moment t , $E_{battery}$ to the nominal battery energy capacity, SoC_{min} to minimum SoC possible, typically 0%, and SoC_{max} to the maximum SoC possible, typically 100%. DoD is defined as the difference between the initial SoC before discharging and the SoC after discharging (IRENA 2015, p. 6). For example, a DoD of 50% may indicate discharging from 75% SoC to 25% SoC.

Li-Ion batteries degrade due to two different processes: calendar degradation and cyclic degradation. Calendar degradation occurs even without using the battery due to passive reactions within the battery cells. It is affected by three key factors, including time, SoC and cell temperature. Elevated temperatures accelerate passive reactions within the cell, resulting in a higher degradation rate. Therefore, batteries should be stored at low temperatures to minimise degradation. SoC also plays a critical role, as it affects the terminal voltage of the cells. Higher SoC levels corresponds to a greater potential difference between the cathode and the anode, which in turn increases the rate of passive reactions and accelerates degradation. Consequently, during idle periods, the SoC should be maintained at a low level. Calendar life refers to the duration a battery remains operational solely due to calendar degradation and aging. (Ovaskainen et al. 2023, p. 6.) *Figure 24* demonstrates the impact of SoC and temperature on the expected lifespan of a Li-Ion battery, considering only calendar degradation. As shown, at normal temperatures, battery lifetime clearly extend up to 20 years.

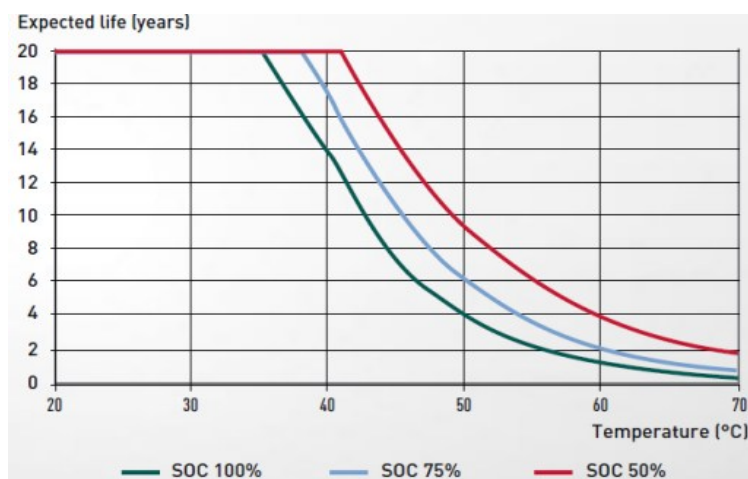


Figure 24, Expected calendar life of Li-Ion batteries (Saulny 2017, p. 40)

Calendar degradation plays a less dominant role in determining battery lifespan, with cyclic degradation being the primary factor influencing overall battery lifetime. Cyclic degradation is more complex and is influenced by several factors, including the C-rate, DoD of the individual cycles, and the heat generated during operation. The primary cause of cyclic degradation is the energy flow associated with charge-discharge cycles. Cyclic degradation defines the cycle life of the battery, referring to the number of cycles the battery can undergo before reaching its EoL capacity. (Ovaskainen et al. 2023, p. 6)

Cycle life is determined based on a specific DoD and operating temperature. Batteries operated with a low DoD can complete more charge–discharge cycles compared to those operated at a high DoD. High DoD levels and elevated temperatures reduce the expected lifetime of the battery by increasing the

degradation rate. (IRENA 2015, p. 6-7.) Determining cycle life is challenging, since the DoD typically varies for each cycle, whereas cycle life is based on a constant DoD. Additionally, to maximise battery lifespan, SoC should be kept within safe limits and should not reach 0% or 100% (Saulny 2017, p. 40). *Figure 25* illustrates the relationship between the number of cycles and the SoH of the battery, and the impact of DoD on cycle life.

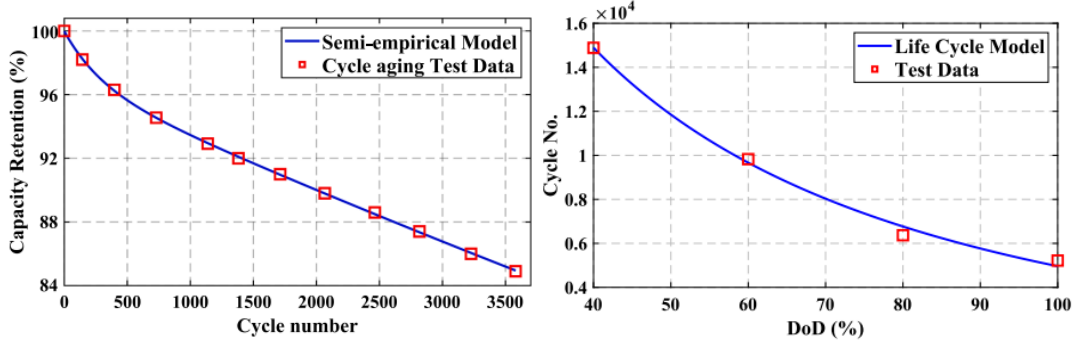


Figure 25, Cycle number affecting battery SoH, and DoD affecting cycle life, Li-Ion battery (Chen et al. 2023, p. 2-3)

Capacity degradation modelling is essential for evaluating the profitability of BESS applications, with particular significance on cyclic degradation, which is often neglected in many studies. Various models are utilised to assess the effects of degradation, including both theoretical and empirical models. (Chen et al. 2023, p. 1-2.) Xu et al. (2023) apply a semi-empirical model that incorporates both calendar and cyclic degradation, where each charge–discharge cycle contributes to the reduction of the battery life. Calendar life is defined in (7).

$$L_{cal} = f_t(t_{el}, \overline{SoC}, \overline{T}_c) \quad (7)$$

where f_t is a degradation model function, \overline{SoC} the average SoC during the elapsed time t_{el} , and \overline{T}_c is the average cell temperature during the elapsed time t_{el} . (Xu et al. 2023, p. 1131-1132)

Cyclic aging accounts for the loss of battery life associated with each individual cycle, with total degradation represented as the cumulative sum of contributions from each cycle. Cycle life is defined in (8).

$$L_{cyc} = \sum_i^N n_i f_c(DoD_i, SoC_i, T_{c,i}) \quad (8)$$

where f_c is a degradation model function, n_i indicates whether cycle i is a full or partial cycle, DoD_i is the DoD for cycle i , SoC_i the SoC during cycle i , and $T_{c,i}$ the cell temperature at cycle i . The function is summed for each cycle from $i = 1$ to N . (Xu et al. 2023, p. 1132)

Calendar degradation and cyclic degradation can be combined to form a total degradation model, described in (9). (Xu et al. 2023, p. 1132)

$$f_d(t_{el}, DoD_i, SoC, T_c) = f_t(t_{el}, \overline{SoC}, \overline{T_c}) + \sum_i^N n_i f_c(DoD_i, SoC_i, T_{c,i}) \quad (9)$$

Ali et al. (2023) presents a calendar degradation model in which different parameters are applied depending on the specific Li-Ion technology used. Calendar degradation is defined in (10).

$$D_{cal} = a_1 e^{a_2 \overline{SoC}} * b_1 e^{\frac{b_2}{\overline{T_c}}} * t_{el}^{c_1} \quad (10)$$

where a_1, a_2, b_1, b_2, c_1 are fitting parameters for different Li-Ion battery technologies, which are presented in *Table 10*. (Ali et al. 2023)

Table 10, Fitting parameters of Li-Ion batteries (Ali et al. 2023)

	a_1	a_2	b_1	b_2	c_1
NMC	0.03304	0.5036	385.3	-2708	0.51
LFP	0.00157	1.317	142300	-3492	0.48
LMO	0.3737	1.066	1410	-4421	0.8
NCA	0.0132	0.3442	10571	-2900	0.4
LCO	0.01329	0.9	4550	-3290	0.7
LTO	0.6129	0.5274	2191	-3970	0.5988

Modelling the cyclic degradation accurately is generally more complex than calendar degradation, as each cycle typically involves a different DoD. Nevertheless, many scientific studies adopt a full equivalent cycle model, in which the number of cycles is calculated as the ratio of the total energy throughput of the battery to the energy throughput of a single full cycle, as described in (11). (Ovaskainen et al. 2023, p. 6; Collath et al. 2022, p. 4-5; Ke et al. 2015, p. 71)

$$n = \frac{E_{t,p}}{2 * E_{battery}} \quad (11)$$

where n is the number of equivalent full cycles and $E_{t,p}$ is the cumulative energy throughput of the battery. This model provides a more meaningful interpretation of cycle numbers when partial cycles are made equivalent to full cycles. Furthermore, it is specified that the energy capacity of the battery used in (11) must be the degraded energy capacity at the give time, rather than the initial BoL energy capacity (Ovaskainen et al. 2023, p. 6). *Table 11* presents various cycle life values for LFP based BESS. According to the cited references, the cycle life ranges from 3500 to 10600 cycles.

Table 11, Cycle life of LFP BESS

Source	Cycle life
IRENA (2020)	3500 cycles (DoD = 100%)
Vinci et al. (2024)	5500 cycles (DoD = 80%)
Mahesh et al. (2021)	6500 cycles (DoD = 100%)
Erdozia & Ferraris (2017)	7000 cycles (DoD > 95%)
Naumann et al. (2020)	10600 cycles (DoD = 100%)

In conclusion, battery lifespan is extended when cycles are reduced, and temperatures, idling SoC, and cycle DoD levels are minimised. However, these conditions may not align when the battery operates within multi-market optimisation, where market activity is high. Therefore, a balance must be maintained between minimising degradation and optimising market activity.

4.5 Economics of BESS

The costs of a BESS must be evaluated separately for each investment case to balance the expected revenues and the associated expenditures. Unbalanced project economics pose a significant risk to investors and the overall profitability of the case. Key costs to be considered prior to an investment decision include Capital Expenditures (CAPEX), Operating Expenditures (OPEX), and end-of-life costs. (Charles River Associates 2023, p. 2-3)

BESS prices have been steadily decreasing in recent years, enabling increased investment in BESS projects. The downward cost trend is expected to continue, primarily due to ongoing technological advancements. (Charles River Associates 2023, p. 12.) Additionally, scaling up of manufacturing capacity, improved production processes, and increased market competition have further accelerated cost reductions. *Figure 26* illustrates the declining cost trend of fully installed and commissioned BESS, along with the gross installed energy capacity, showing an 89% decrease in BESS costs from 2010 to 2023. (IRENA 2024, p. 145.) Furthermore, according to Volta Foundation (2025), BESS costs dropped by 40% from 2023 to 2024, reaching an all-time low of 165 USD/kWh. (Volta Foundation 2025, p. 143). BESS costs are largely driven by Li-Ion technologies, which account for 98% of the current market. Within this, LFP chemistries hold over 80% market share, with NMC chemistries comprising the remaining share. (Volta Foundation 2025, p. 151-152.) Consequently, the CAPEX and OPEX are heavily influenced by LFP and NMC based BESS.

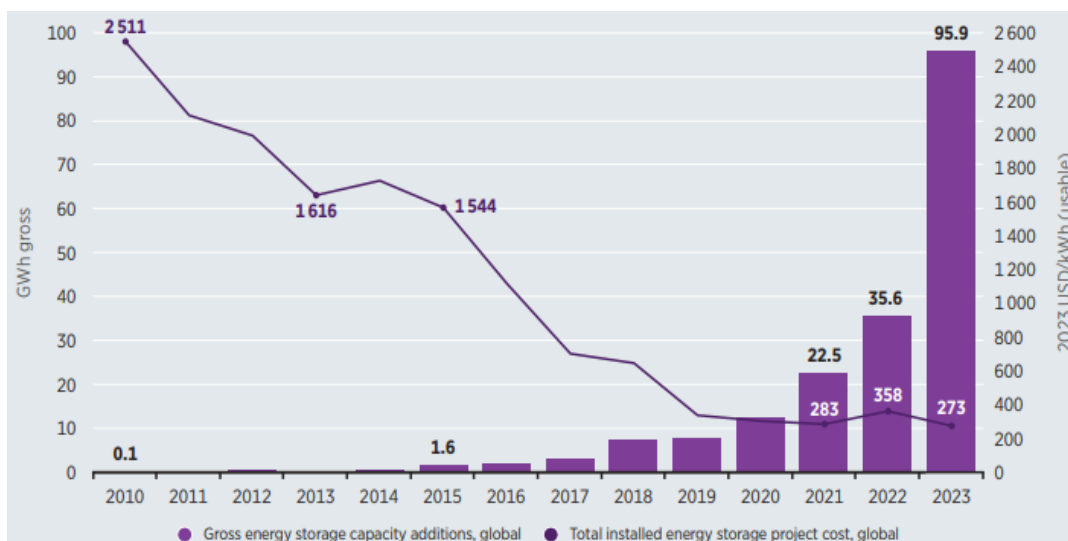


Figure 26, Price trend and gross installed energy capacity of BESS (IRENA 2024, p. 145)

4.5.1 CAPEX analysis of BESS

Determining a general CAPEX value for BESS is challenging, as it strongly depends on the system’s power rating and energy capacity. To gain a clearer understanding of the investment costs, a breakdown of CAPEX can be conducted. The components of CAPEX are presented in *Table 12*.

Table 12, Components of CAPEX (Charles River Associates 2023, p. 13)

Category	Description
System	Battery packs
	Balance of system and BMS components
Connection	Grid connection fee
	Required equipment (inverters, transformers)
Construction	Development and engineering
	Labour
Land	Land acquisition
Other	Permits and taxes

System costs—comprising battery packs, balance of system components, and BMS components—represents the most significant share of CAPEX. Battery costs are particularly dependent to the chosen battery chemistry and the system’s power and energy specifications. Long-duration batteries with low C-rates tend to have lower costs per kWh but higher costs per kW compared to systems with higher C-rates. (Charles River Associates 2023, p. 12-15.) This is illustrated in *Figure 27*. Typically, while a larger energy storage capacity reduces the cost per kWh, it results in higher total system costs.

Connection costs include of grid connection fees and equipment necessary for connection, such as inverters and transformers. Construction costs consists of development, engineering and labour expenses. Land costs refer to expenses related to land acquisition, which can significantly impact overall CAPEX depending on the location. Other costs encompass costs related to permits and taxes. (Charles River Associates 2023, p. 12-15)

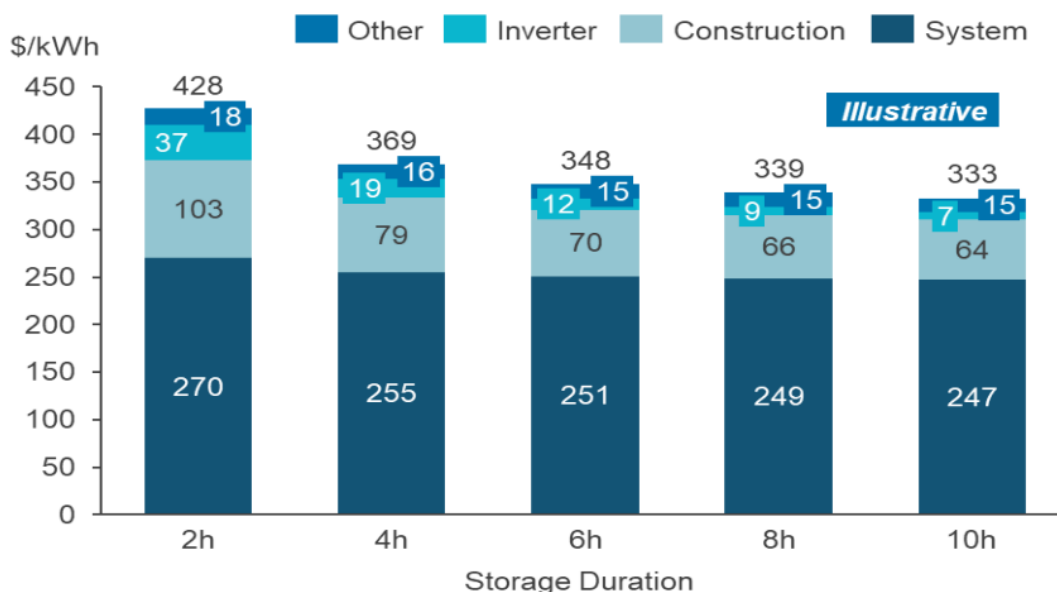


Figure 27, Effect of BESS duration on CAPEX, 60 MW system (Charles River Associates 2023, p. 14)

Accurately defining CAPEX is challenging due to the variation in values reported by different sources. Calculation models and factors included may differ significantly. A critical factor is the reference year of the data, as cost trend evolve rapidly. As noted, BESS costs were estimated to decline by 40% between 2023 and 2024, making outdated data misleading. Selected CAPEX values are presented in Table 13, with USD figures converted to EUR, using the conversion rate published by European Central Bank on 9 May 2025 (ECB 2025).

Table 13, CAPEX (EUR/kWh) estimates from different sources
(1 EUR = 1.1297 USD), n.s = Not Specified

Source	Data reference year	Technology	Power rating	C-rate	CAPEX
Rystad Energy (2023)	2022	LFP	10 MW	0.5C	388
Rystad Energy (2023)	2022	LFP	10 MW	0.25C	336
Charles River Associates (2023)	2023	n.s	60 MW	0.5C	379
Charles River Associates (2023)	2023	n.s	60 MW	0.25C	327
IRENA (2024)	2023	n.s	n.s	0.5C	226
IRENA (2024)	2023	n.s	n.s	0.25C	243
NREL (2024)	2022-2023 estimation for 2025	LFP & NMC	60 MW	0.5C	473
NREL (2024)	2022-2023 estimation for 2025	LFP & NMC	60 MW	0.25C	379
IRENA (2017)	2017 estimation for 2025	LFP	5 MW	0.7C	278
Volta Foundation (2025)	2024	n.s	n.s	n.s	146

4.5.2 OPEX analysis of BESS

Similar to CAPEX, OPEX can be divided into categories, including variable and fixed costs. The components of OPEX are presented in *Table 14*. Variable costs, particularly Operation and Maintenance (O&M) costs, account for the majority of OPEX. O&M costs are influenced by how frequently and intensively the BESS is operated. Variable costs also include grid fees, which vary by region, the cost of electricity used for charging, and component replacement costs. Fixed costs consist of expenses related to labour, land use, insurance, and management, and typically represent a minor share of the total OPEX. (Charles River Associates 2023, p. 15-17.) In this thesis, grid fees and electricity costs will be modelled separately from OPEX. Therefore, O&M represent the primary factor influencing OPEX in this study.

Table 14, Components of OPEX
(Charles River Associates 2023, p. 15)

Category	Description
Variable costs	O&M Grid fees and electricity costs Component replacement
Fixed costs	Labour and land lease Management and insurance

As with CAPEX, defining general O&M costs is challenging due to variations across sources, technologies, data reference years, regions, and the intended use of the BESS. O&M expenditures are typically expressed as a percentage of CAPEX. *Table 15* presents values from various sources, with USD figures converted to EUR, using the conversion rate published by European Central Bank on 9 May 2025 (ECB 2025).

*Table 15, O&M estimates from different sources
(1 EUR = 1.1297 USD), n.s = Not Specified*

Source	Data reference year	Technology	Power rating	C-rate	O&M per year
Cristea et al. (2022)	2022	Li-Ion	< 1 MW	n.s	0.25% of CAPEX
Pinto et al. (2024)	2021	NMC	0.1 MW	0.7C	0.5% of CAPEX
IRENA (2017)	2017 estimation for 2025	LFP	5 MW	0.7C	1.5% of CAPEX
NREL (2024)	2022-2023 estimation for 2025	LFP & NMC	60 MW	n.s	2.5% of CAPEX
Kebede et al. (2022)	2015	Li-Ion	> 1MW	n.s	8.9 EUR/kW
Hemmati et al. (2024)	2015	LFP	n.s	n.s	6.9 EUR/kW
Othman (2022)	2022	n.s	65 MW	2C	7.1 EUR/kWh
IRENA (2020)	2020	LFP	n.s	0.25C to 2C	7.1 EUR/kWh

In addition to CAPEX and OPEX, there are costs associated with end-of-life decommissioning. However, these costs vary by region due to differing regulatory requirements. Moreover, components and battery packs have recycling value, which can offsets part of the decommissioning expenses. (Charles River Associates 2023, p. 17) This thesis will not account for BESS end-of-life costs.

5 BESS Integration and Wind Power Operation

This chapter begins by discussing the operating principles of wind power and the key components of a wind turbine. It then provides an overview of the historical development of wind power, the key driving factors behind its current growth, and how the increasing share of wind power impacts the power system and electricity markets due to its intermittent and unpredictable nature. Finally, the chapter explores the integration of BESS with Wind Power Plants (WPP) and the various applications in which BESS can participate to enhance both operational efficiency and economic performance.

5.1 Wind Power

5.1.1 Operating principles

Wind power generates electricity utilising the kinetic energy of moving air. According to Kalmikov (2017), the kinetic energy of air is determined by the mass of the air in motion—which depends on air density—and the velocity of the moving air. The kinetic energy is defined by the classical mechanics equation in (12).

$$E_{kin} = \frac{1}{2}mU^2 \quad (12)$$

where m is the mass and U the velocity. By applying this definition to a moving volume of air, the fundamental equation for wind power can be derived, in (13).

$$P = \frac{1}{2}\rho AU^3 \quad (13)$$

where ρ is the air density, and A the area swept by the turbine blades. (Kalmikov 2017, p. 19-20.) Wind creates a lift force on the blades of a turbine, causing the rotor to rotate. The magnitude of the lift force depends on the angle at which the wind hits the blade, known as the angle of attack. Consequently, both the angle of attack, and the resulting lift force affects the rate at which energy is captured. Furthermore, as defined in (13), the generated power is highly dependent on wind speed and the swept area of the rotor. An increase in the sweep area leads to higher potential power output. As wind passes through a turbine, it becomes turbulent, forming a wake that reduces wind speed and creates wake losses, thereby decreasing the efficiency of energy capture. These losses can be minimised by locating wind turbines further away from each other. In a typical WPP, turbines are spaced five to nine rotor diameters apart. (Andrew 2019, p. 36-37)

The power coefficient of a wind turbine defines the efficiency, representing the proportion of kinetic energy in the wind that can be extracted to usable electrical energy. By considering this coefficient C_p , the fundamental equation becomes as (14).

$$P = \frac{1}{2} \rho C_p A U^3 \quad (14)$$

There exists a theoretical maximum to the efficiency with which energy can be extracted from the wind, known as the Betz limit. According to Betz theory, 59% of the kinetic energy in wind is the limit that can be captured by wind turbines, due to physical constraints. Another important parameter in evaluating wind turbine performance is the capacity factor, defined as the ratio of actual production over a given time period to the energy that would be produced if the turbine operated at full rated power continuously under ideal conditions. Typical capacity factor of a modern wind turbine ranges between 30% to 50%. (Kalmikov 2017, p. 21-24)

Wind turbines operate within the cut-in and cut-out wind speed range. The cut-in wind speed refers to the minimum speed at which the turbine can generate electricity, while cut-out wind speed is the threshold at which the production is ceased to prevent mechanical damage. Furthermore, wind turbines have a rated output wind speed, at which the turbine reaches its maximum power output. (Kalmikov 2017, p. 37.) The operational characteristics are illustrated in a power curve, as shown in *Figure 28*.

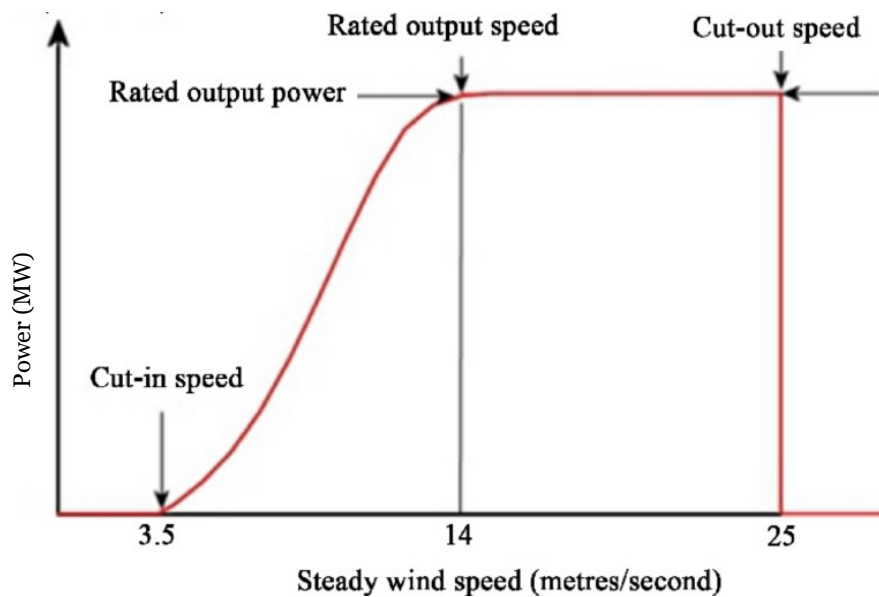


Figure 28, Power curve of a wind turbine (Joshi et al. 2022, p. 12)

A wind turbine consists of several main components, including the blades, a hub, yaw system, pitch system, gearbox, generator and brakes. The blades are connected to the hub, forming the rotor. (U.S Department of Energy 2025.) The turbine drivetrain comprise a gearbox and a generator. The rotor drives a shaft, which is connected to the gearbox to increase the rotational speed before reaching the generator. The generator converts the rotational kinetic energy into electricity. The pitch system is used to optimise the blades angle, so that at wind speeds below the rated output, it maximises energy capture, while at wind speeds above the rated output, it limits mechanical loads on the turbine. A drivetrain is housed within the nacelle, which also serves as the outer casing of the turbine. The yaw system rotates the whole nacelle to optimise the rotor with the wind direction. (Andrew 2019, p. 36-38.) Wind turbines are equipped with brakes to prevent rotor movement when the turbine is not operational, such as during maintenance periods (U.S Department of Energy 2025). Onshore and offshore wind turbines differ in technical aspects. Majority of the installed turbines are however land-based. (Andrew 2019, p. 38.) *Figure 29* illustrates the components of a wind turbine.

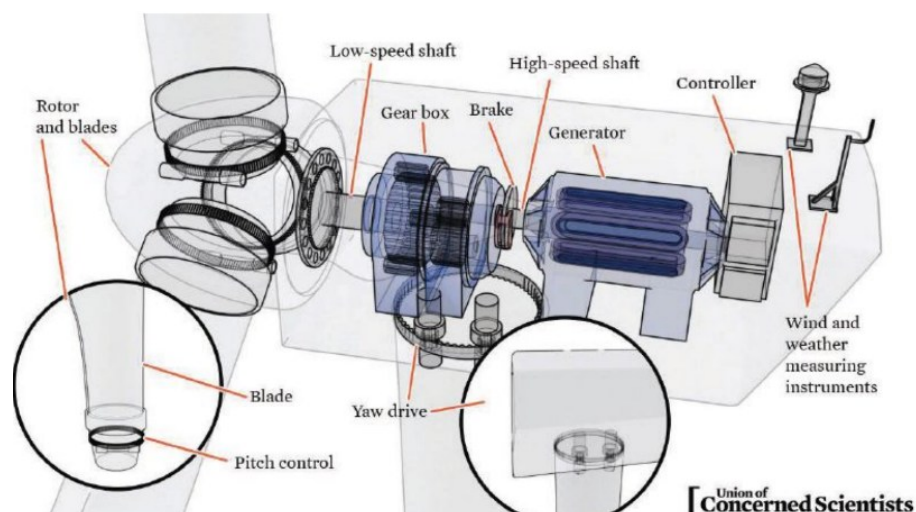


Figure 29, Wind turbine components (Andrew 2019, p. 38)

Modern wind turbines typically have rated power ranging from 2.4 MW to 5.7 MW, with majority in the range of 4.3 MW to 5.7 MW (IEA Wind TCP 2022). Offshore wind turbines, however, have reached larger scales, with the largest turbines achieving capacities up to 20 MW, and rotor diameters of 300 meters (Lundström 2024). In Finland, the average rated power of installed turbines in 2024 was 6 MW, three times higher than in 2011. As the rated power has increased, so has the physical dimensions. Hub height increased from 100 meters in 2011 to 150 meters in 2024, and rotor diameter from 90 meters to 160 meters. (Renewables Finland 2025, p. 7-9.) The current trend continues toward larger turbines, which enable higher rated power output.

5.1.2 Impact on Power System

The share of wind power is increasing across the Nordic countries. In 2024, wind energy accounted for 8.4 GW of installed capacity in Finland, representing 24% of the Finnish total electricity mix (Renewables Finland 2025, p. 2). Sweden reached approximately 16.9 GW of wind capacity in 2024, also comprising 24% of its electricity mix (Hepworth 2025). Norway had an installed wind capacity of 5.1 GW in 2024, which has remained unchanged since 2022 (NVE 2025). This contributed only to 9% of the national electricity mix in 2023 (IEA 2025). *Figure 30* illustrates the cumulative growth of Finnish wind power capacity. As depicted, unlike Norway, Finland has experienced rapid growth in wind energy over the past decade. *Figure 31* further presents the forecasted increase for the future development of wind power in both Finland and Sweden.

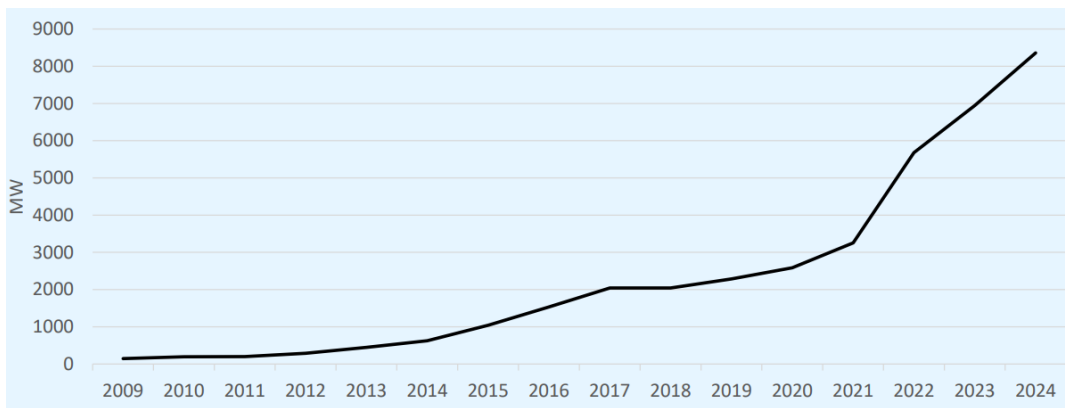
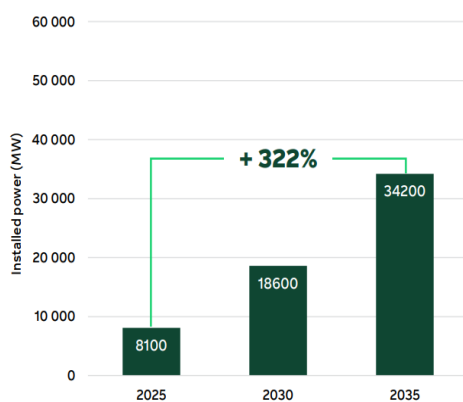


Figure 30, Cumulative capacity of Finnish wind power (Renewables Finland 2025, p. 5)

Estimate of possible wind power development in Finland



Estimate of possible wind power development in Sweden

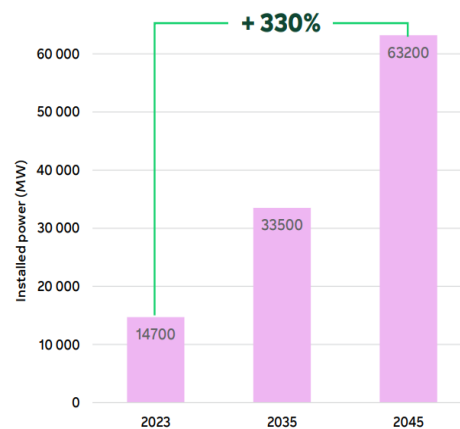


Figure 31, Estimated increase of Finnish and Swedish wind power (Fortum 2025b, p. 4)

Several factors have contributed to the rapid growth of wind turbine installations in the Nordic region, particularly Finland and Sweden. A key driver is the European ambitious climate policies, which seeks to accelerate the clean energy transition and to reduce the dependency on fossil-based fuels. One central aspect of the transition is adopting increasing amounts of renewable energy sources, such as wind power. Europe is a global leader in implementing wind energy, and the share of renewables is expected to grow. The Nordic countries have ambitious climate targets, aimed at achieving carbon neutrality well before 2050. Finland aims for carbon neutrality by 2035 while Sweden aims to reach it by 2045. (Fortum 2025b, p. 2.) These commitments are a key reason for the growing installation of wind power in the regions. In addition to policy-driven motivations, economic considerations play a crucial role. Onshore wind is currently the most cost-effective technology for large-scale electricity generation when examining the production costs of electricity (Ilyukhin & Sainio 2024). This cost advantage makes wind power an attractive option for investors seeking commercially viable renewable energy projects.

Currently, wind power producers often want to pre-sell electricity through a PPA to secure a stable price, helping to manage risks in today's volatile market (Ilyukhin & Sainio 2024). Wind power can also participate in reserve markets, if the turbines meet the technical requirements. These requirements are achievable, as modern wind turbines are capable of responding within seconds. During periods of high wind power production, down-regulation can be managed by reducing production of the WPP, and up-regulation can be managed only if a portion of capacity has been reserved for this purpose. Nevertheless, despite these capabilities, participation of wind power in reserve markets has been minimal in the Nordic countries. (Fingrid 2022)

An increased share of wind power in specific regions and across the power system has both positive and negative impacts on various sectors and systems, including industry, electricity markets, and power system stability. For instance, a positive impact is the growing share of renewable generation, which attracts green industrial investments in power-intensive industries, with Finland and Sweden identified as particularly promising locations for hydrogen production and electrification of industries (Fortum 2025b, p. 2). A major negative impact, however, is the increased unpredictability and volatility of electricity prices. The growing share of wind power contributes directly to price volatility, including more frequent occurrences of both extremely low and high electricity prices. In 2023, Nordic countries, including Finland and Sweden, experienced the most volatile prices across Europe. (Fortum 2025b, p. 5.) During periods of high wind power production, prices have dropped significantly due to the high share of wind power in the electricity mix (Ilyukhin & Sainio 2024).

The variable nature of wind power generation poses a risk to the power system. As the share of wind power increases, so does the uncertainty of electricity generation, which affects the reliability of the power system. Greater uncertainty in generation increases the need for improved real-time balancing of supply and demand, thereby raising the demand for reserve and balancing markets, as well as real-time balancing mechanisms. Geographically distributing wind power more evenly across regions can help smooth production variability and mitigate the most extreme fluctuations in generation. Additionally, more accurate forecasting reduces the risk of unexpected changes in supply. (Miettinen & Holttinen 2019, p. 227)

Figure 32 illustrates the day-ahead forecast and the actual generation of wind power in Finland on 29 September 2024. The closer the forecast aligns with the actual generation, the more stable the real-time operation of the power system. Conversely, with large forecast errors, greater real-time adjustments are required. As shown in *Figure 32*, at hours 16 to 21, actual generation deviates by more than 20% from the forecasted value, whereas at other hours, the forecast matches more closely the actual output. In addition to the importance of forecast accuracy, wind power also contribute less to system inertia, thereby reducing the overall system inertia and increasing the need for frequency control (O'Malley et al. 2024). As discussed in *Chapter 3.1*, lower system inertia increases the risk of larger frequency deviations, decreasing the stability of the power system.

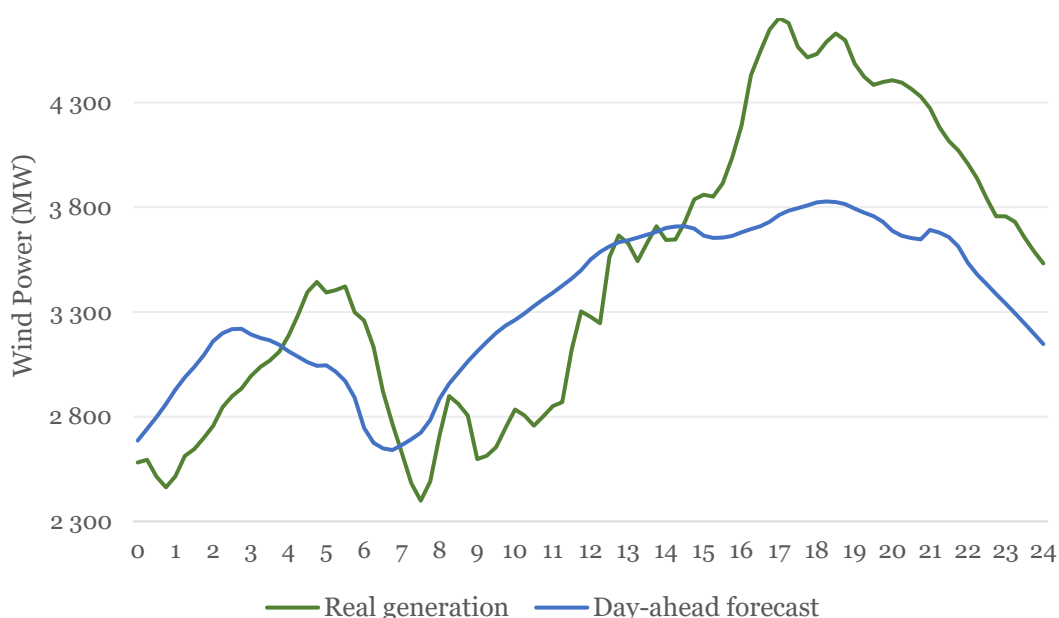


Figure 32, Day-ahead forecast and real generation of wind power in Finland 29.9.2024. (Modified from Fingrid 2025k)

5.2 BESS Applications with Wind Power

A BESS co-located with a WPP can enhance the power plants economic viability by supporting various applications. These include reserve market participation and grid services, energy arbitrage, time-shifting, peak-shaving, and imbalance management (Laukkanen 2023). In these applications, BESS serves two main functions: storing electricity and providing frequency control (Suvic 2025).

The increasing share of wind power, with its intermittent generation, reduces grid stability, however, BESS can address these challenges due to its favourable operational characteristics. Utilising a BESS alongside wind power is essential for effective frequency regulation, as it enhances system reliability and cost-efficiency while supporting the transition to renewable energy. (Ullah et al. 2024, p. 1.) In the context of grid frequency control with reserve markets, wind power and BESS complement each other; BESS offering high accuracy, while wind power contributes durability. Integrating BESS with a WPP provides flexibility, and operating both assets simultaneously enable broader participation in frequency and energy regulation. Moreover, BESS enhances the inertia response of WPPs. (He et al. 2017, p. 3560)

A WPP operator can further increase financial returns by utilising unused capacity of the BESS for energy arbitrage. As illustrated in *Figure 33*, energy arbitrage involves purchasing and storing electricity during periods of low prices and selling it later at higher prices, typically during peak demand periods. (Standard Renewables 2023)



Figure 33, Principle of energy arbitrage (ECA 2021)

In some countries, BESS revenues from energy arbitrage represent a significant share of income, such as in Great Britain accounting for 84%. Energy arbitrage can also be applied in aFRR and mFRR EAMs. In contrast, other regions gain more revenues from capacity market payments within reserve markets—for example, SE4 with a 71% share and Greece with 55% revenue share associated with reserve markets. In Nordics, most BESS revenues come from capacity payments in reserve markets. (Aurora 2025, p. 7-8.)

Historically, energy arbitrage in the Nordic ID and DA markets has not been economically viable due to limited price volatility. In Finland, reserve markets have offered better revenues compared to energy arbitrage. However, as BESS installations increases, reserve markets risk becoming saturated, leading to declining prices and reduced profitability. (Lieskoski et al. 2024, p. 8)

A co-located BESS can further enhance system stability by managing weather-dependent generation through time-shifting. Time-shifting involves storing generated electricity when wind production is high and releasing it during peak-demand periods or at times with unfavorable wind conditions. This approach optimises the use of wind resources, maximises the value of generated electricity, and enables the integration of greater shares of intermittent renewable energy into the system. (Ampowr 2025.) Time-shifting of wind power production using BESS is illustrated in *Figure 34*.

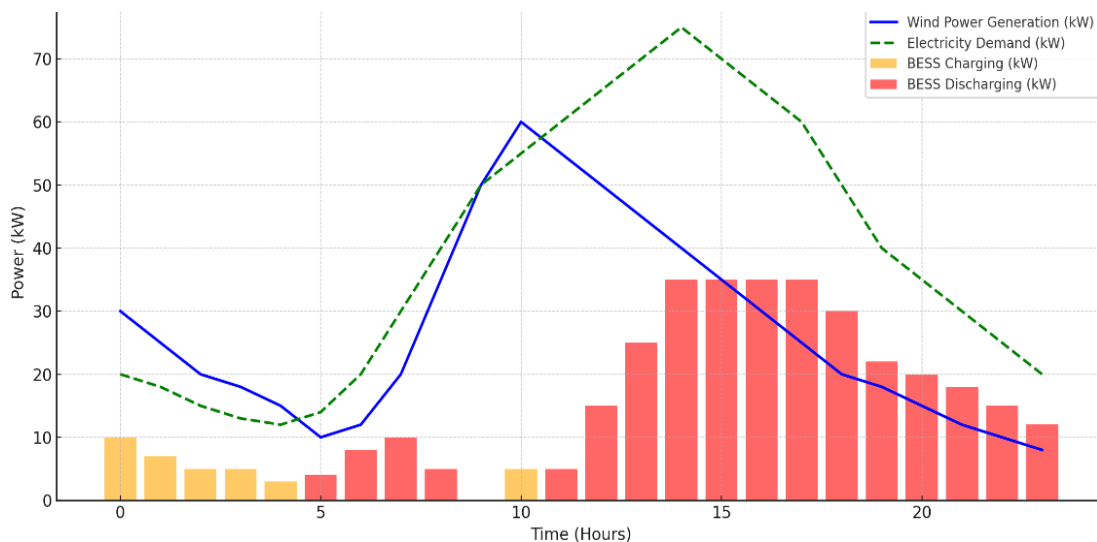


Figure 34, Time-shifting of wind power using BESS (AI-generated graph, ChatGPT)

Wind power curtailment, referring to reducing or halting wind power production despite favorable wind conditions, is necessary to ensure system security and reliability. However, this results in economic losses for WPP operators. BESS can help minimise these losses by storing the excess energy which would otherwise be curtailed. When co-located with a WPP, a BESS can participate in energy arbitrage and reserve markets, in addition to mitigating wind power curtailment. However, engaging in multiple activities—such as reserve market participation—can create operational conflicts with wind power curtailment mitigation and energy arbitrage, potentially limiting the revenues from these services. (Li et al. 2023, p. 1)

Peak-shaving with a BESS involves supplying electricity during periods of peak demand, thereby reducing reliance on peaking power plants, which are typically expensive to operate (Standard Renewables 2023). Peak-shaving benefits financially from energy arbitrage, as it involves storing energy during off-peak hours at low prices, and selling it at higher prices during peak-load hours. Therefore, energy arbitrage and peak-shaving are closely linked. (Huvilinna 2015, p. 19-20)

A key challenge associated with wind power is the unpredictability of forecast errors. Because BRPs must submit forecasted generation schedules in advance, deviations between actual output and submitted bids often occur, resulting in imbalances. Since production imbalances cannot be predicted in advance, a BESS can be used to minimise and compensate for them in real-time. This reduces imbalance risk and associated costs, potentially enhancing the economic viability of the WPP. *Figure 35* shows the initial imbalances of a WPP and the adjusted imbalances utilising a BESS, demonstrating the effect of imbalance mitigation. (Erdozia & Ferraris 2017, p. 64-65)

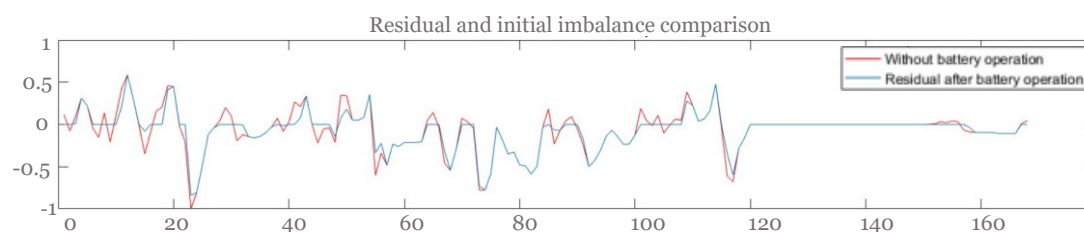
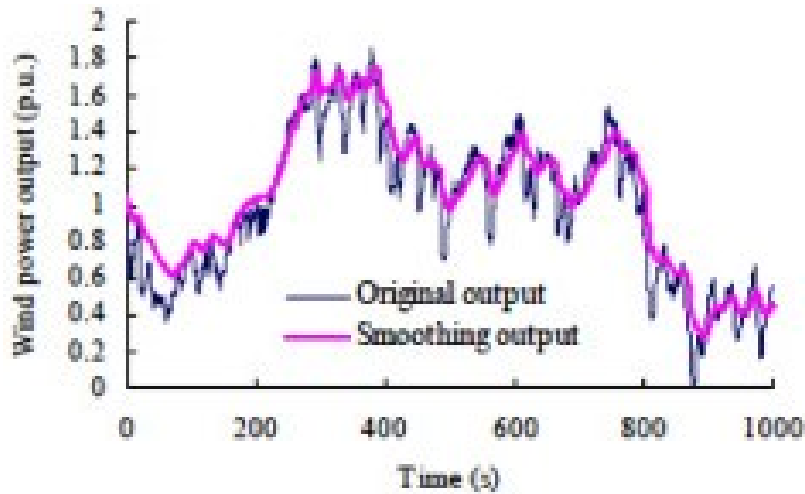


Figure 35, WPP imbalance mitigation with BESS
(Erdozia & Ferraris 2017, p. 67)

The output of a WPP exhibits small fluctuations due to random and unexpected changes in wind conditions. These fluctuations impact WPP operation, grid stability, frequency, and power quality, while a smoother power output would offer several advantages. While wind turbines can adjust their output through pitch control, this method is less efficient compared to the rapid response capabilities of a BESS. Therefore, a BESS co-located with a WPP can serve a smoothing function by reducing short-term fluctuations in generation. This is achieved through wind power filtering, where the combined output of the WPP and BESS is regulated in real-time before delivery to the grid. This approach effectively smooths power output and reduces variation, as illustrated in *Figure 36*. (de Siqueira & Peng 2021, p. 1-3)



*Figure 36, Wind power output smoothing with a BESS
(de Siqueira & Peng 2021, p. 9)*

Co-locating a BESS within a WPP reduces grid connection costs, as both assets share a single grid connection point. This also lowers expenses related to cabling, transformers, and other infrastructure, compared to a stand-alone system. However, challenges can arise regarding available grid capacity and asset sizing. For example, if the combined output of the BESS and the WPP exceeds grid’s available capacity, the two assets may compete for access. In periods of high wind generation, if the BESS is also scheduled to discharge, one of the assets may need to curtail its output, leading to reduced forecasted revenues. In such a case, the BESS may need to shift discharging to periods with lower prices, which may decrease expected revenues. (Blake Clough Consulting 2025)

In conclusion, a BESS co-located with a WPP can serve multiple functions. Several of these applications—such as time-shifting, peak-shaving, and energy arbitrage—are closely related. While operating the BESS for multiple purposes may reduce revenues from individual applications, it diversifies the revenue streams across a broader range of services, potentially enhancing the overall economic value and decreasing operational and market risks. This thesis focuses on the operation of co-located BESS participating in reserve markets, operating in energy arbitrage, and mitigating wind power imbalances. Applications such as time-shifting, peak-shaving, and output smoothing are not within the scope of this study.

6 Optimisation Setup

This chapter outlines the scope, objectives, and setup of the empirical study. It begins by defining the research problem and describing the simulation scenarios, which vary by BESS size, capacity allocation, and bidding zone. Furthermore, the included markets and relevant exclusions are detailed. Following, the input data and modelling parameters are presented, such as selected WPPs, BESS specifications, degradation models, market data, and other assumptions, along with their data sources. The chapter then explains the structure and logic of the simulation model used in the empirical study, covering the optimisation process, objective function, and operational constraints. Lastly, the capital budgeting methods used to assess the economic performance of each scenario outcome are presented.

6.1 Problem formulation and markets

This study conducts simulation-based analysis using a mathematical optimisation model to evaluate BESS participation in imbalance management and market participation. The aim is to investigate how varying the proportion of BESS capacity reserved for imbalance management impacts the profitability of a BESS investment co-located with a WPP. The analysis considers four levels of capacity reserved for imbalance management: 0%, 30%, 70% and 100%, with the remaining capacity allocated to multi-market optimisation. Two BESS configurations are studied: a 20 MWh system with a 10 MW power rating, and a 40 MWh system with a 10 MW power rating. The optimisation is performed for three different bidding zones: FI, SE2 and NO4. In total, 24 distinct simulation scenarios are evaluated, representing all combinations of imbalance management shares, BESS sizes, and bidding zones. The goal is to analyse how different allocations of imbalance capacity affect the profitability of BESS across various sizes and bidding zones, and to conduct further analysis and comparison of the scenarios.

The simulated multi-market optimisation includes participation in the DA market, continuous ID market, hourly FCR-N market, and both up- and down-regulation for the hourly FCR-D market, aFRR CM, aFRR EAM, mFRR CM, and mFRR EAM. Transmission fees for both grid input and output are accounted for whenever the BESS charges from or discharges to the grid, thereby affecting potential revenues. The optimisation excludes ID auctions, the FFR market, and in the case of Finland, the annual FCR-N and FCR-D markets, and for SE2 and NO4, the second FCR-N and FCR-D auctions. ID auctions are excluded because they are rarely used, with the majority of hours showing no traded volumes. The FFR market is similarly excluded due to its limited role and inconsistent procurement, since FFR volumes are typically procured only during specific seasons, on selected days, and during certain hours when system inertia is forecasted to be low. *Table 16* presents the share

of hours in 2024 with 0 MW trades in the ID auctions and the percentage of hours without procured volumes in the FFR market. Given their limited relevance, these markets are excluded from the optimisation model.

Table 16, Share of hours with zero traded volume in ID auctions and no procured volumes in FFR market in 2024 (Based on: Nord Pool 2025g; Fingrid 2025l; Svenska kraftnät 2025e; Statnett 2024b)

	FI	SE2	NO4
IDA1	98.0%	96.3%	99.4%
IDA2	98.6%	98.2%	99.4%
IDA3	94.0%	94.0%	100%
FFR	82.7%	85.3%	84.1%

The Finnish annual FCR-N and FCR-D markets are excluded to enable proper hourly optimisation without reserving capacity for the entire year, and to ensure comparability with the SE2 and NO4 simulations, where no annual markets exist. Furthermore, the hourly markets typically provide better hourly income than the yearly markets. For SE2 and NO4, which each consist of two hourly FCR-N and FCR-D up and down-regulation markets, only the first auction is included in the simulation, as it accounts for the majority of the procured volumes and potential revenues.

The study applies a deterministic approach, where all market prices, procured volumes, and activated volumes are known for each hour. This allows the optimisation model to allocate BESS capacity to the most valuable markets and imbalance management opportunities at every hour. Additionally, as a result for the deterministic approach, the BESS is always able to deliver the committed capacity, and no penalties or non-delivery risks need to be considered.

6.2 Simulation input data

This section presents the input data, including BESS parameters, market data, imbalance data, and transmission fees. All BESS input parameters are based on publicly available sources, with justification provided for each selected value. The market data is downloaded for the year 2024. Since some markets operated with a 15-minute MTU in 2024 while other used an hourly MTU, a simplification has been applied, including averaging the 15-minute data into hourly values to align with the optimisation models time resolution.

Wind Power Plants

The simulation will be conducted independently for three existing WPPs owned partially by Fortum, which will be compared throughout the study. The first simulation focuses on the Kalax WPP, located in the FI bidding zone. Commissioned in 2020, Kalax comprise 21 wind turbines, each with a rated capacity of 4 MW, resulting in a total installed capacity of 90 MW (Fortum 2025c). The second simulation involves the Solberg WPP, located in the SE2 bidding zone. Operational since 2017, Solberg consists of 22 turbines, each rated at 3.45 MW, yielding a total capacity of 76 MW (Fortum 2025d). The third simulation examines the Sør fjord WPP in the NO4 bidding zone. Sør fjord became operational in 2020 and includes 23 turbines, each with a capacity of 4.3 MW, totalling 99 MW (Fortum 2025e). Each scenario will include a co-located BESS simulated alongside the corresponding WPP. It is assumed that there are no grid capacity limitations, allowing both the WPP and the BESS to deliver their full power output to the grid.

BESS Parameters

The simulations consider a Li-Ion battery, with LFP chemistry, as identified in *Chapter 4.5* as the dominant technology for BESS applications. Two battery durations are evaluated: a 2-hour system and a 4-hour battery system. Both scenarios have a power rating of 10 MW, with BoL nominal capacities of 20 MWh and 40 MWh, respectively. An EoL capacity corresponding to 70% of the BoL capacity is used, as an average of given values presented in *Chapter 4.4*, implying a SoH of 70% at EoL. The SoC is simulated according to (5) and (6). Operational buffers are applied to restrict SoC between 5% and 95%, resulting in a maximum DoD of 90%. This constraint does not significantly impact system performance, but reduces intensive degradation and extends cycle life. For each simulated hour, the maximum energy capacity considered in the SoC calculation is the degraded capacity, not the BoL capacity.

Calendar degradation is calculated on a daily basis and simulated using (10), with fitting parameters for LFP chemistry from *Table 10* and an assumed operating temperature of 21°C. Each day, calendar degradation incrementally reduces the battery's energy capacity. Cyclic degradation is modelled based on the number of equivalent full cycles using (11). Each cycle contributes to the cumulative energy throughput until the EoL SoH is reached. A linear degradation model is applied between a SoH of 100% and 70%. Cyclic degradation impacts the maximum available energy capacity on a daily basis. The cycle life is assumed to be 7000 cycles, based on the values provided in *Table 11*. The RTE applied in the simulation is 91%, corresponding to the lower bound of the range specified in *Chapter 4.2* and is implemented using (1).

Different CAPEX values are used for the 2-hour and 4-hour systems, with 240 EUR/kWh used for the 2-hour system and 220 EUR/kWh for the 4-hour system. These values are derived from the data presented in *Chapter 4.5.1*, with greater emphasis on the most recent published data while also considering figures from earlier sources. In the simulation, CAPEX is treated as a one-time initial investment at the first simulated hour. O&M costs are estimated based on the values presented in *Chapter 4.5.2*, with annual costs of 6 EUR/kWh. These are allocated on an hourly basis throughout the simulation, accumulating expenses incrementally over time. BESS operation is simulated using two full equivalent cycles per day. *Table 17* provides a summary of the input data related to the BESS used in the simulation.

Table 17, Simulation input data for BESS

Battery technology	Li-Ion, LFP
Power rating	10 MW
Energy capacity (BoL)	Case 1: 20 MWh / Case 2: 40 MWh
C-rate	Case 1: 0.5C / Case 2: 0.25C
BoL SoH	100%
EoL SoH	70%
SoC min.	5%
SoC max.	95%
Cycle life	7000 cycles
RTE	91%
a_1 (LFP)	0.00157
a_2 (LFP)	1.317
b_1 (LFP)	142300
b_2 (LFP)	-3492
c_1 (LFP)	0.48
Operating temperature	21 °C
CAPEX	Case 1: 240 EUR/kWh / Case 2: 220 EUR/kWh
O&M	6 EUR/kWh/a
Max. cycles per day	2 cycles

Imbalance management

For the purpose of this simulation, Fortum provided hourly day-ahead forecasted and realised wind power generation data for the Kalax, Solberg, and Sørffjord WPPs. Since Solberg data is only available from February 2024 onward, day-ahead forecasted and realised generation data for January was sourced from publicly available SE2 data (ENTSO-E 2025d; ENTSO-E 2025e). To approximate Solberg's forecasts and generation for January, the SE2 wind generation data was scaled in proportion to Solberg's capacity relative to the total installed wind power capacity in SE2 during that month. Due to confidentiality reasons, the original data provided by Fortum has been anonymised. Specifically, a random percentage adjustment between -3% and

6% is applied to both for the forecasted and realised values, on an hourly basis, without exceeding the nominal capacity of the respective WPP. A different random adjustment is applied for each hour to preserve variability.

In calculating the WPP imbalance volumes as outlined in *Figure 15*, it is assumed that all forecasted generation is sold through DA and ID markets, with no imbalance adjustment in balancing markets. Since WPPs have no consumption and the MGA imbalances are assumed as zero, only trades and metered production are considered in the imbalance calculation. Imbalance prices for each hour were obtained from eSett open data (eSett 2025d). Imbalance volumes for the WPPs and the imbalance prices between 16.1.2024–22.1.2024 are shown in *Figure 37*, along with the yearly average values.

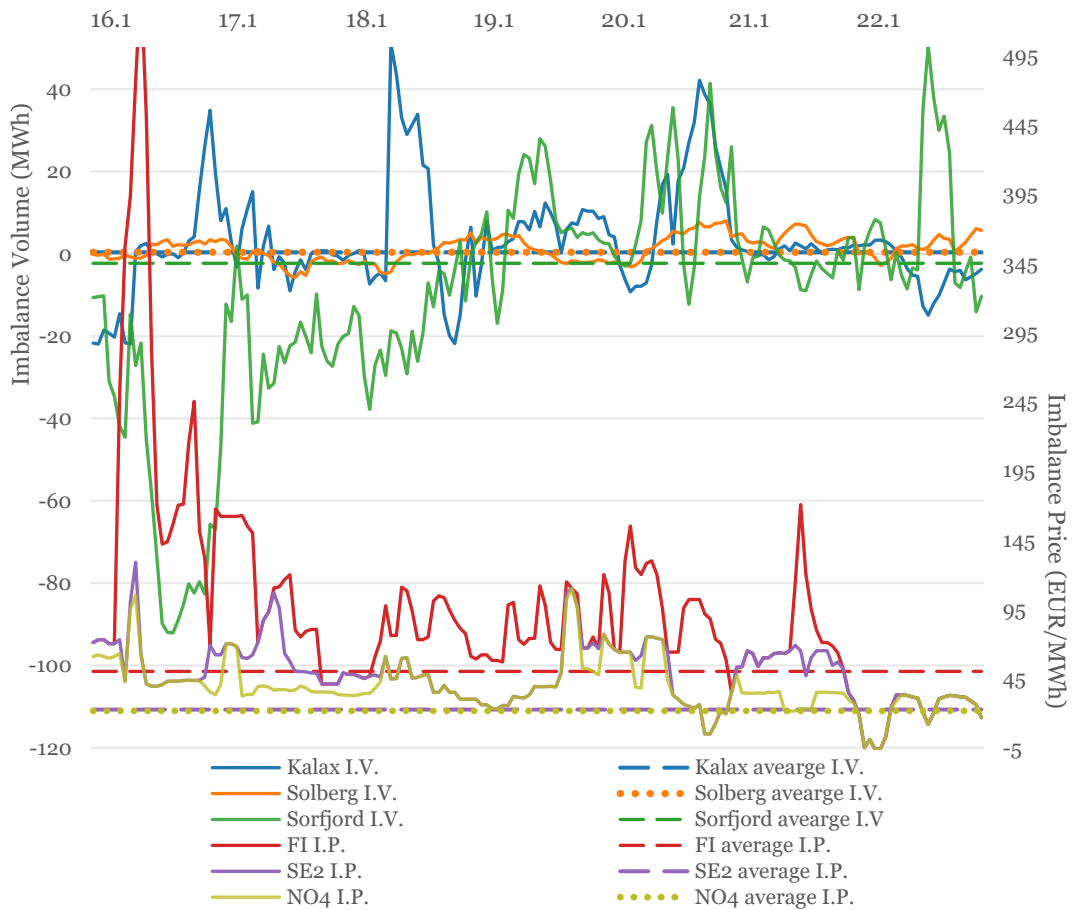


Figure 37, Anonymised imbalance volumes (I.V.) and imbalance prices (I.P.) 16.1.2024–22.1.2024 with corresponding 2024 average values

Both imbalance- and volume fees are included in the simulation, while weekly fees are excluded. The imbalance fees remained constant throughout 2024, while the volume fees are calculated as a Volume-Weighted Average (VWA) based on 2024 prices (eSett 2025e). The applicable fees for each bidding zone are summarised in *Table 18*.

Table 18, Imbalance fees 2024 (eSett 2025e)

	Volume fee (EUR/MWh)	Imbalance fee (EUR/MWh)
FI	1.36	1.15
SE2	1.6	1.15
NO4	0.21	1.15

Day-Ahead and Intraday

Data for the DA and ID market prices and volumes for 2024 are obtained from Nord Pool data portal, with a granted student license to access the data. For the continuous ID market, where multiple prices can exist for the same product within a MTU, a VWA price is calculated for each hour. Figure 38 displays the hourly DA and ID prices for the period 16.1.2024–22.1.2024, along with the corresponding 2024 average prices. It also includes hourly traded volumes in the continuous ID market, with the 2024 average volumes.

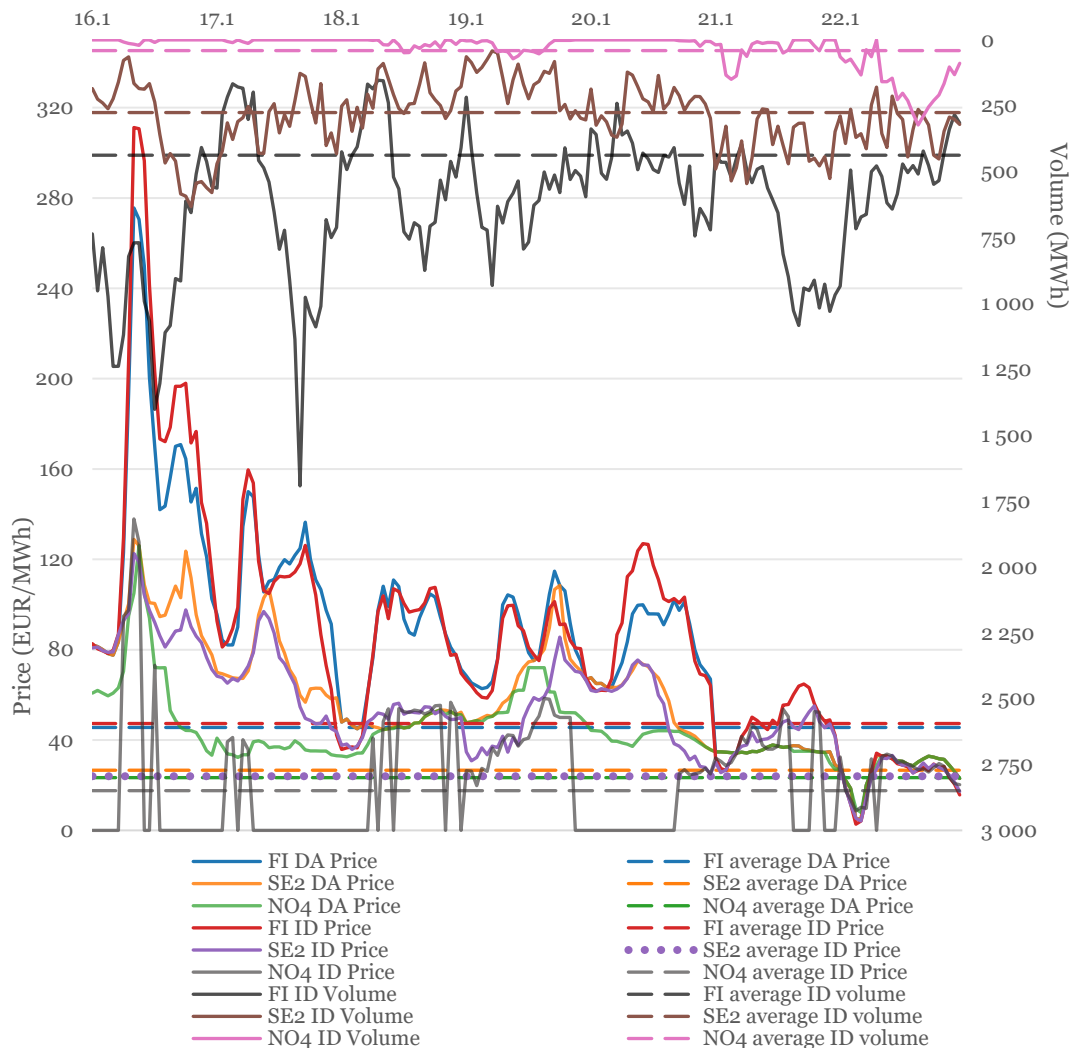


Figure 38, DA and ID prices, and ID volumes 16.1.2024–22.1.2024 with 2024 average values (Nord Pool 2025g)

FCR-N

Price and procured volume data for FI are sourced from Fingrid datasets, for SE2 from Mimer, and for NO4 from Statnett open data. (Fingrid 2025l; Mimer 2025; Statnett 2025c). *Figure 39* presents the prices and procured volumes for the period 16.1.2024–22.1.2024, along with the corresponding average values for 2024. For FCR-N markets, it is critical to simulate not only the procured capacity but also the activated energy, as this impacts the hourly battery SoC, battery degradation and generates both costs and revenues associated with energy payments and transmission fees. The activated energy is calculated on an hourly basis, derived from system frequency data in accordance with the linear activation model presented in *Figure 9*. System frequency data for the Nordic Synchronous Area, with a three-minute resolution, are obtained from Fingrid datasets for the year 2024 (Fingrid 2025l).

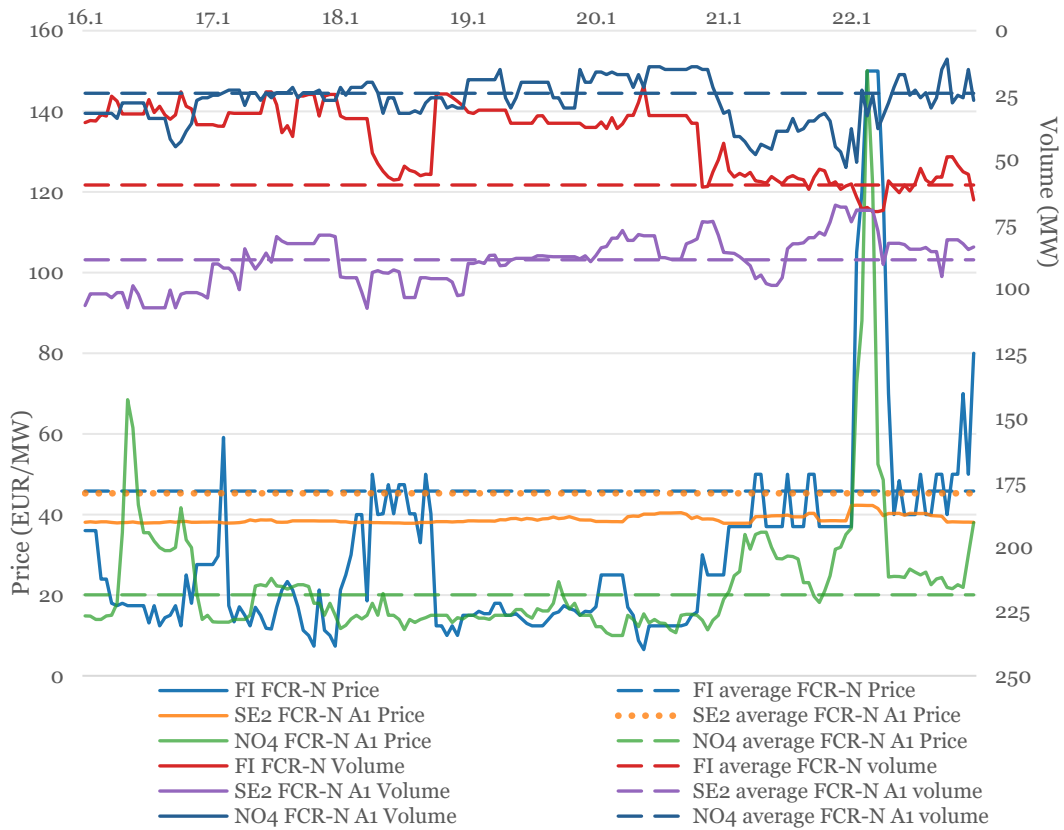


Figure 39, FCR-N prices and volumes 16.1.2024–22.1.2024 with 2024 average values (Fingrid 2025l; Mimer 2025; Statnett 2025c)

FCR-D

FI prices and procured volumes for FCR-D up- and down-regulation are obtained from Fingrid open data, while SE2 data from Mimer (Fingrid 2025l; Mimer 2025). Since FCR-D down-regulation has not been procured in Norway, only the FCR-D up market is simulated for NO4, where procured volumes occur during the summer season, which are downloaded from Statnett

(Statnett 2025c). *Figure 40* illustrates the prices and procured volumes between 16.1.2024–22.1.2024, alongside the average values for the year 2024. Simulating FCR-N market participation required accounting for activated energies, as activations occur within the 49.9–50.1 Hz range where frequency typically remains. In contrast, FCR-D activations, as show in *Figure 10*, occur only below 49.9 Hz and over 50.1 Hz. Analysis of the three-minute resolution frequency data for 2024 shows FCR-D up-regulation activations occurred only 0.57% of the time, and down-regulation 0.73% (Fingrid 2025l). Therefore, excluding activated energies in the FCR-D markets is unlikely to impact the simulation results significantly.

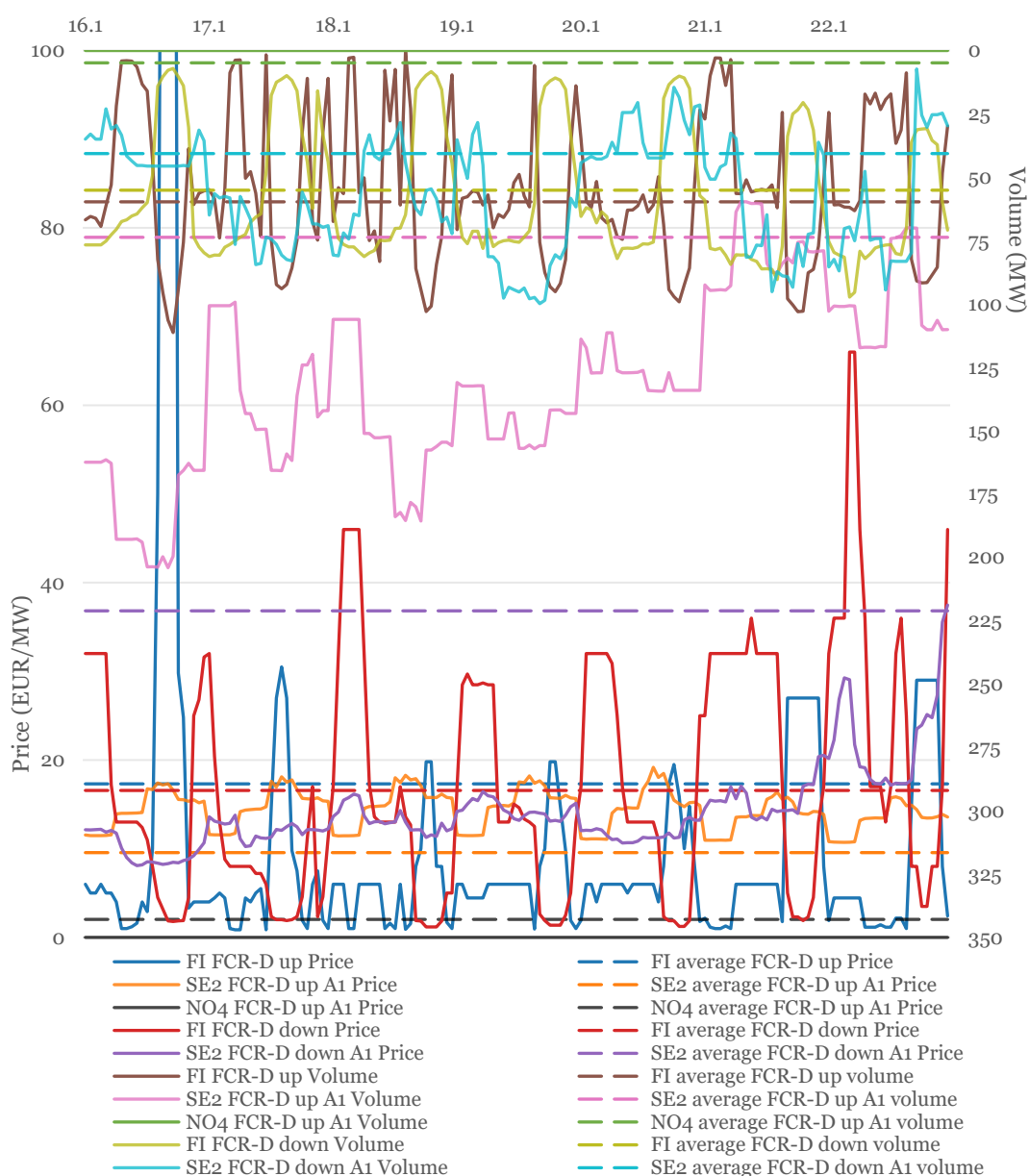


Figure 40, FCR-D prices and volumes 16.1.2024–22.1.2024 with 2024 average values (Fingrid 2025l; Mimer 2025; Statnett 2025c)

aFRR and mFRR

All aFRR CM up- and down-regulation prices and procured volumes for FI, SE2, and NO4 are obtained through an email response from a Statnett representative (Vold 2025). While the CM data are provided at an hourly resolution, for FI the activated volumes in aFRR EAM are available at a 15-minute resolution and have been aggregated to hourly values using Fingrid datasets (Fingrid 2025l). Prior to the introduction of the aFRR EAM on 12 June 2024, the activated aFRR prices for FI were defined from mFRR EAM data from eSett data portal, while after the introduction, the data was sourced from Fingrid datasets (eSett 2025d; Fingrid 2025l). For SE2 and NO4, aFRR activated volumes are sourced from ENTSO-E open data, with the corresponding activated prices, based on mFRR EAM, obtained from eSett (ENTSO-E 2025f; eSett 2025d). mFRR CM prices and procured volumes are sourced from Fingrid datasets for FI, from Mimer for SE2, and via correspondence with the Statnett representative for NO4 (Fingrid 2025l; Mimer 2025; Vold 2025). mFRR EAM prices and activated volumes for all bidding zones are obtained from Nord Pool data portal (Nord Pool 2025g). A summary of hourly market average prices, procured volumes, and activated volumes for 2024 is presented in *Table 19*.

Table 19, 2024 average hourly aFRR and mFRR prices, procured volumes and activated volumes (Vold 2025; Fingrid 2025l; eSett 2025d; ENTSO-E 2025f; Mimer 2025; Nord Pool 2025g)

	FI	SE2	NO4	FI	SE2	NO4
	aFRR price			mFRR price		
CM up (EUR/MW)	24.67	19.13	18.41	11.32	12.04	2.94
CM down (EUR/MW)	22.15	25.49	24.98	14.93	15.69	2.42
EAM up (EUR/MWh)	67.92*	28.54**	26.74**	64.21	28.54	26.74
EAM down (EUR/MWh)	14.28*	18.75**	18.32**	32.32	18.75	18.32
	aFRR volume			mFRR volume		
CM up, Procured (MW)	50.82	12.61	12.56	264.65	78.72	78.80
CM down, Procured (MW)	52.00	40.21	20.87	405.04	202.54	18.54
Activated energy up (MWh)	13.21	3.67	3.00	20.20	25.60	22.40
Activated energy down (MWh)	22.99	18.06	8.68	47.40	48.10	75.00

* aFRR EAM began on 12 June 2024; earlier energy prices are based on mFRR EAM

** No aFRR EAM operated; energy prices based on mFRR EAM

Transmission fee

The grid connection fee is typically included in the CAPEX, as is assumed in this study. The simulation considers running costs solely as the O&M costs. Therefore, transmission fees are modelled alongside BESS operation in market participation to provide a more accurate representation. The annual power capacity-based transmission fee is excluded from the analysis, as a co-located BESS does not influence the capacity-based fee of the power plant in Finland. The same assumption is applied for SE2 and NO4. Energy-based transmission fees, both for grid imports and exports, are accounted for in the optimisation whenever the BESS charges from or discharged to the grid.

In FI, energy-based fees were fixed throughout 2024. In all cases, both grid imports and exports lead to a fee payable to the TSO, reducing potential net income. (Fingrid 2025m.) In SE2 and NO4, the transmission fee varies with the DA market price. The energy-based fee is identical for grid input and output, and is calculated using (15). (Svenska Kraftnät 2024d; Statnett 2024c)

$$T_{fee} = (p_h^{DA} + r_p) * F \quad (15)$$

Where p_h^{DA} is the DA price for the specific hour, r_p a risk premium, and F a margin loss rate defined for each grid connection point. Solberg WPP is connected to Hällby station, with a loss coefficient of 6.2%. Sør fjord WPP is located nearest to Kjølsvik132 station, where the loss rate varies weekly, with separate values for night and day hours. The simulation applies a weekly average loss rate for NO4. In 2024, the SE2 risk premium was 1.19 EUR/MWh, while Norway applies no risk premium ($r_p = 0$). In SE2 and NO4, when the fee value is positive, grid input is charged and grid output earns a payment, while for negative prices, this is reversed. (Svenska Kraftnät 2024d; Statnett 2024c.) *Figure 41* shows the energy-based transmission fees for 2024.

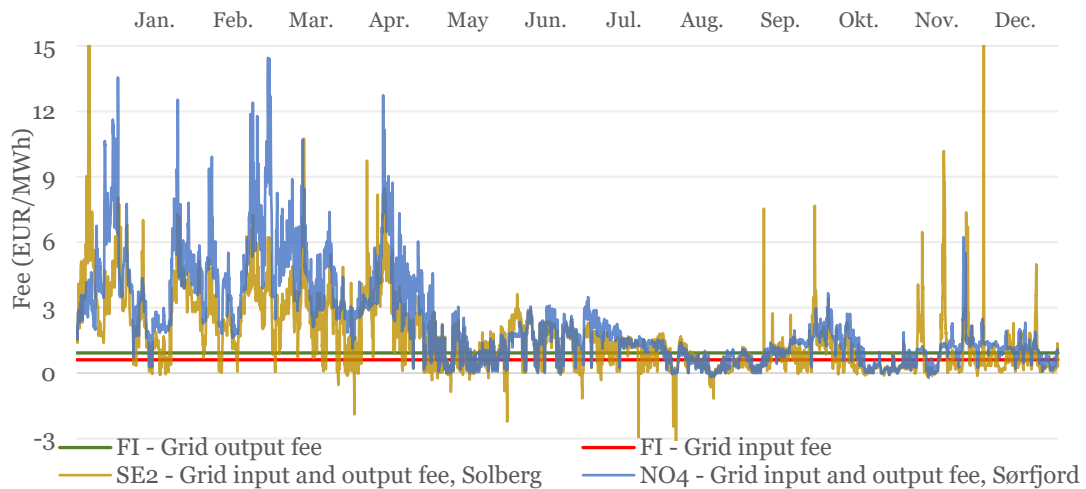


Figure 41, Energy-based transmission fees for 2024 (Fingrid 2025m; Svenska Kraftnät 2024d; Statnett 2025d)

6.3 Optimisation objective and constraints

For the simulation, a Python program was developed using the PyCharm integrated development environment. The program uses a built-in mixed-integer programming optimiser, which is designed to solve both linear programming and mixed-integer linear programming problems. This optimiser is provided by Google OR-Tools. The simulation operates with an hourly resolution and runs continuously until the EoL SoH is reached, utilising hourly data from 2024 in a repeatable manner. The optimisation is conducted on a daily basis, determining the optimal allocation of the available power and energy capacity for each hour of the day. At the start of each new day, the allocation process is repeated. The optimiser identifies the maximum possible value that the BESS can generate within each day.

Certain BESS parameters, specifically battery degradation and SoH, are simulated externally of the optimiser. The optimiser itself provides hourly SoC values, as well as the charged and discharged energy for each market within the hour. These outputs serve as inputs for calculating battery degradation and SoH. Equations (16), (17) and (18) defines parameters for BESS.

$$E_{ch,h} = \sum_m E_{ch,h}^{(m)} \quad (16)$$

$$E_{dch,h} = \sum_m E_{dch,h}^{(m)} \quad (17)$$

where $m \in \{imb., DA, ID, FCR-N, aFRR EAM, mFRR EAM\}$

$$SoH_h = \frac{E_h * (D_{cal,h} + D_{cyc,h})}{E_{BoL}} \quad (18)$$

Where $E_{ch,h}$ and $E_{dch,h}$ are the sum of charged and discharged energy for the hour h , $E_{ch,h}^{(m)}$ and $E_{dch,h}^{(m)}$ the charged and discharged energy for a specific market m , including imbalance management, for a specific hour. SoH_h , E_h , $D_{cal,h}$, and $D_{cyc,h}$ are the SoH, degraded energy capacity, calendar degradation and cyclic degradation, respectively, for a specific hour. E_{BoL} is the energy capacity at BoL. In (16) and (17), the total charged and total discharged energy for each hour is calculated, which are used to calculate battery degradation, as described in Chapter 6.2. In (18), the SoH at the end of the hour is defined.

The optimiser applies a set of predefined constraints that govern the optimisation process. These constraints include the allowable SoC range, the allowable charging and discharging values for each market, the allowable capacity reserved for market participation, compliance with BESS power rating, and the maximum allowable number of cycles per day. (19) and (20) defines the constraints related to the SoC.

$$SoC_{min} \leq SoC_h \leq SoC_{max} \quad (19)$$

$$SoC_h = SoC_{h-1} + \frac{\sum_m E_{ch,h-1}^{(m)} - \sum_m E_{dch,h-1}^{(m)}}{E_h} \quad (20)$$

where $m \in \{imb., DA, ID, FCR-N, aFRR EAM, mFRR EAM\}$

In (19), the hourly SoC, SoC_h , is constrained within specified minimum and maximum limits, which it must not exceed. (20) defines the SoC at the start of the hour as the SoC at the start of the previous hour, SoC_{h-1} , summed by the contribution of energy charged and discharged during that previous hour, $E_{ch,h-1}^{(m)}$ and $E_{dch,h-1}^{(m)}$, for each market m , including imbalance management.

There are multiple constraints for the allowable energy that the BESS can charge and discharge, as well as the capacities reserved for participation in reserve markets. Constraints (21), (22) and (23) defines hourly allowable commitments to the markets and imbalance management.

$$0 \leq \theta_h^{(m)} \leq P_{rating} * C_{share} \quad (21)$$

$$\theta_h^{(m)} \leq V_{realized,h}^{(m)} \quad (22)$$

where $m \in \{imb., DA, ID, FCR-N, FCR-D, aFRR CM, aFRR EAM, mFRR CM, mFRR EAM\}$

$$\text{If } \theta_h^{(m)} \neq 0, \text{ then } Bidsize_{min}^{(m)} \leq \theta_h^{(m)} \leq Bidsize_{max}^{(m)} \quad (23)$$

where $m \in \{DA, ID, FCR-N, FCR-D, aFRR CM, aFRR EAM, mFRR CM, mFRR EAM\}$

Where $\theta_h^{(m)}$ denotes the committed bid at hour h for a specific market m , including imbalance management, which may represent discharged or charged energy volume, or reserved capacity for capacity markets. P_{rating} is the rated power of BESS, and C_{share} the capacity share reserved for imbalance

management or market participation. $V_{realized,h}^{(m)}$ is the realised traded energy volume or procured reserve capacity for each market, based on 2024 data. $Bidsize_{min}^{(m)}$ and $Bidsize_{max}^{(m)}$ define the smallest and highest bid sizes for each market. Constraint (21) limits the market commitment to the capacity share reserved for either imbalance management or market participation, taking into account the power rating. This ensures that charging, discharging and capacity committed do not exceed the actual power limits. Constraint (22) ensures that the commitment does not exceed the actual traded energy or procured capacity for the hour in 2024, while (23) restricts the commitment to market-specific bid size limits, if the market has these.

Constraints (24) to (29) define allowable charged and discharged energy, as well as the committed capacity for each market, based on the battery's available energy at a given time, which is determined by the SoC.

$$E_{ch,h}^{(m)} \leq (SoC_{max} - SoC_h) * E_h \quad (24)$$

$$E_{ach,h}^{(m)} \leq (SoC_h - SoC_{min}) * E_h \quad (25)$$

where $m \in \{imb., DA, ID, aFRR EAM, mFRR EAM\}$

$$\theta_h^{(m)} \leq (SoC_{max} - SoC_h) * E_h \quad (26)$$

$$\theta_h^{(m)} \leq (SoC_h - SoC_{min}) * E_h \quad (27)$$

where $m \in \{FCR-N, aFRR CM, mFRR CM up\}$

$$\theta_h^{FCR-Dd} * \frac{1}{3} \leq (SoC_{max} - SoC_h) * E_h \quad (28)$$

$$\theta_h^{FCR-Du} * \frac{1}{3} \leq (SoC_h - SoC_{min}) * E_h \quad (29)$$

Constraints (24) and (25) limit the amount of energy that can be charged or discharged each hour in each market, based on the SoC at beginning of the hour and the defined SoC boundaries. Constraints (26) and (27) ensure sufficient energy availability to support the committed capacity in FCR-N, aFRR CM, and mFRR CM. Constraints (28) and (29) ensure that energy is available to support the committed capacity in the FCR-D up- and down-regulation markets, corresponding to 20 minutes of full activation.

In addition to these constraints, the optimiser enforces that within a given hour and market, the BESS cannot simultaneously charge and discharge. However, charging and discharging may still occur within the same hour across different markets. For imbalance management, the BESS participates only during hours when it can reduce imbalance-related costs. It discharges in response to negative imbalance volumes and charges in response to positive volumes, but refrains from any action if it would result in negative saving. This restriction does not apply to market participation, where the BESS may charge at a loss during low-price hours to discharge later at higher prices, namely energy arbitrage. This allows negative income in individual hours, but ensuring a positive total income over the optimised day.

Finally, constraints are defined which limit the total power capacity used or reserved within each hour, as well as the maximum allowable energy throughput for the optimised day. These constraints are presented in (30) to (33).

$$\sum_m E_{ch,h}^{(m1)} + \sum_m \theta_h^{(m2)} \leq P_{rating} \quad (30)$$

where $m1 \in \{imb., DA, ID, aFRR EAM down, mFRR EAM down\}$

where $m2 \in \{FCR-D down, FCR-N, aFRR CM down, mFRR CM down\}$

$$\sum_m E_{dch,h}^{(m1)} + \sum_m \theta_h^{(m2)} \leq P_{rating} \quad (31)$$

where $m1 \in \{imb., DA, ID, aFRR EAM up, mFRR EAM up\}$
 where $m2 \in \{FCR-D up, FCR-N, aFRR CM up, mFRR CM up\}$

$$\sum_{h=1}^{24} (E_{ch,h}^{imb} + E_{dch,h}^{imb}) \leq n_{day} * 2E_h * C_{imb_share} \quad (32)$$

$$\sum_{h=1}^{24} \sum_m (E_{ch,h}^{(m)} + E_{dch,h}^{(m)}) \leq n_{day} * 2E_h * C_{market_share} \quad (33)$$

where $m \in \{DA, ID, FCR-N, aFRR EAM, mFRR EAM\}$

Constraints (30) and (31) ensure that the total power used or reserved within an hour does not exceed the BESS power rating. Constraints (32) and (33) limit the daily energy throughput to the maximum number of allowable cycles a day, n_{day} , taking into account the capacity shares reserved for imbalance management, C_{imb_share} , and for market participation, C_{market_share} .

An important feature of the simulation is that the capacity share reserved for imbalance management can also be used for charging in the DA market. This is justified by the observation that, during extended periods with only negative imbalance volumes, the BESS energy capacity becomes the limiting factor for imbalance management. Allowing charging in DA market with the reserved capacity enables additional discharging in imbalance management, thereby enhancing flexibility and cost saving potential in imbalance management. The reason why discharging is not allowed in DA market with imbalance management capacity, is to restrict energy arbitrage in DA market, and to restrict the optimiser to focus on revenue generation in the DA market with the capacity reserved for imbalance management. By allowing discharging, the optimiser would start allocating available energy for energy arbitrage in DA market, which would limit operation in imbalance management. However, with the capacity reserved for market participation, the simulation allows energy arbitrage operation within the optimised day, if most value is generated by charging at low prices, and discharging at higher prices.

Based on the predefined constraints, the optimiser maximises the daily monetary value generated. The objective function consists of a set of equations representing the charged volumes, discharged volumes, and reserved capacities, for imbalance management and each market, multiplied by the corresponding prices and applicable fees. Efficiency is incorporated by adjusting the value of discharging through multiplication with the efficiency, and the value of charging by dividing with the efficiency. This ensures that the actual cost or revenue accurately reflects the committed energy and capacity volumes. Although imbalance management does not generate direct revenue, it reduces the imbalance costs of the WPP. These cost saving are however treated in the same manner as market revenues. The equations defining the objective function are presented in (34) to (36).

$$\sum_{h=1}^{24} (p_h^{imb} + fee_{imb}) * E_{ch,h}^{imb} + (p_h^{imb} + fee_{imb} - T.fee_{in,h}) * E_{dch,h}^{imb} \quad (34)$$

$$\sum_{h=1}^{24} (-p_h^{(m1)} \pm T.fee_{out,h}) * E_{ch,h}^{(m1)} + (p_h^{(m1)} - T.fee_{in,h}) * E_{dch,h}^{(m1)} \quad (35)$$

$$\sum_{h=1}^{24} p_h^{(m2)} * \theta_h^{(m2)} \quad (36)$$

where $m1 \in \{DA, ID, aFRR EAM, mFRR EAM, FCR-N activations\}$

where $m2 \in \{FCR-N, FCR-D, aFRR CM, mFRR CM\}$

Where p_h^{imb} denotes the hourly imbalance price, fee_{imb} the total imbalance fee, and $T.fee_{in,h}$ the hourly transmission input fee. $p_h^{(m1)}$ and $p_h^{(m2)}$ are the hourly market prices, while $T.fee_{out,h}$ is the hourly transmission output fee, which is negative for FI and positive for SE2 and NO4. (34) represents the value generated from imbalance management, consisting of imbalance prices and related fees. (35) reflects the value from market-based charging and discharging, consisting of market prices and relevant transmission fees. (36) represents the value generated from capacity reservations in the capacity markets, consisting of the market prices.

Although the optimiser operates on a daily basis, the simulation returns hourly values for each day. These optimised hourly values include the charged and discharged volumes for imbalance management and market participation, the reserved capacities for capacity markets, and the value generated for each hour from both imbalance management and market participation. The results are compiled into an Excel file containing the mentioned values for each hour over the BESS lifetime. Revenues and savings are further analysed for profitability using capital budgeting methods, which are described in detail in *Chapter 6.4*.

6.4 Economic evaluation

To properly evaluate the profitability of each scenario, capital budgeting methods are employed, include Net Present Value (NPV) and Payback Time (PBT). These methods will be applied to the hourly simulation output data generated over the operational lifetime of the BESS. All economic evaluations will be conducted using Microsoft Excel.

The NPV method evaluates the profitability of an investment by accounting for the time value of money. It considers the time at which the cash flows, costs, and revenues are generated, discounting them to their present value. This approach is crucial, as money has a greater value at the present time than in the future. A positive NPV indicates that the investment is expected to be profitable. NPV analysis is essential in evaluating profitability, as it

provides a clear measure of the projects economic viability over its lifetime. NPV calculates the net cash flow for each year and discounts it to its value today. (Dai et al. 2022.) The equation for calculating the NPV is presented in (37).

$$NPV = \sum_{a=1}^A \frac{C_a}{(1+r)^a} - CAPEX \quad (37)$$

Where C_a is the net cash flow at year a , r the discount rate, and $CAPEX$ the initial investment cost.

A PBT analysis is also essential, as it indicates the time required to recover the starting investment by the projects generated cash flows. This provides a measure of both financial risk and liquidity. The payback period corresponds to the point at which the cumulative cash flow equals the initial investment cost. This method indicates how quickly the investment begins to generate returns. Shorter PBTs are preferred, as they indicate better investments. (Ikäheimo et al. 2024, p. 188.) However, it is important to note that the PBT method does not account for the time value of money. The equation for calculating PBT is presented in (38).

$$\sum_{a=1}^{PBT} C_a - CAPEX = 0 \quad (38)$$

A company should prioritise investments in projects that generate a positive NPV, as this adds value to the company. Furthermore, the PBT should be shorter than the projects expected operational lifetime to ensure recovery of the initial investment. In this analysis, a discount rate of 7% is used for the NPV calculation, and the project lifetime is defined by the simulated operation period until the BESS reaches its EoL SoH.

7 Simulation Results

This chapter presents and discusses the results of each simulated scenario. The discussion focuses first on operational performance, including energy capacity degradation, operational lifetime, SoC profiles, and energy allocation across different markets through trading and activations. This is followed by an evaluation of economic performance, covering market-specific net cash flows, overall financial summary, NPV and PBT. The impact of imbalance correction on the WPPs is then assessed. Finally, a sensitivity analysis is conducted to examine how changes in imbalance prices and market prices influence the overall profitability of BESS investments.

7.1 Results on Operational Performance

7.1.1 FI results

The BESS was simulated to operate until its SoH reaches 70%, with the resulting lifetime varying across scenarios. *Figure 42* illustrates the degradation of energy capacity over time for the FI bidding zone scenarios, showing how each system approaches the 70% SoH. Additionally, the figure presents the cumulative cycle count throughout the lifetime. The endpoint of each line indicates the lifetime for each scenario. The percentage shown in the legend indicates the share of capacity reserved for imbalance management.

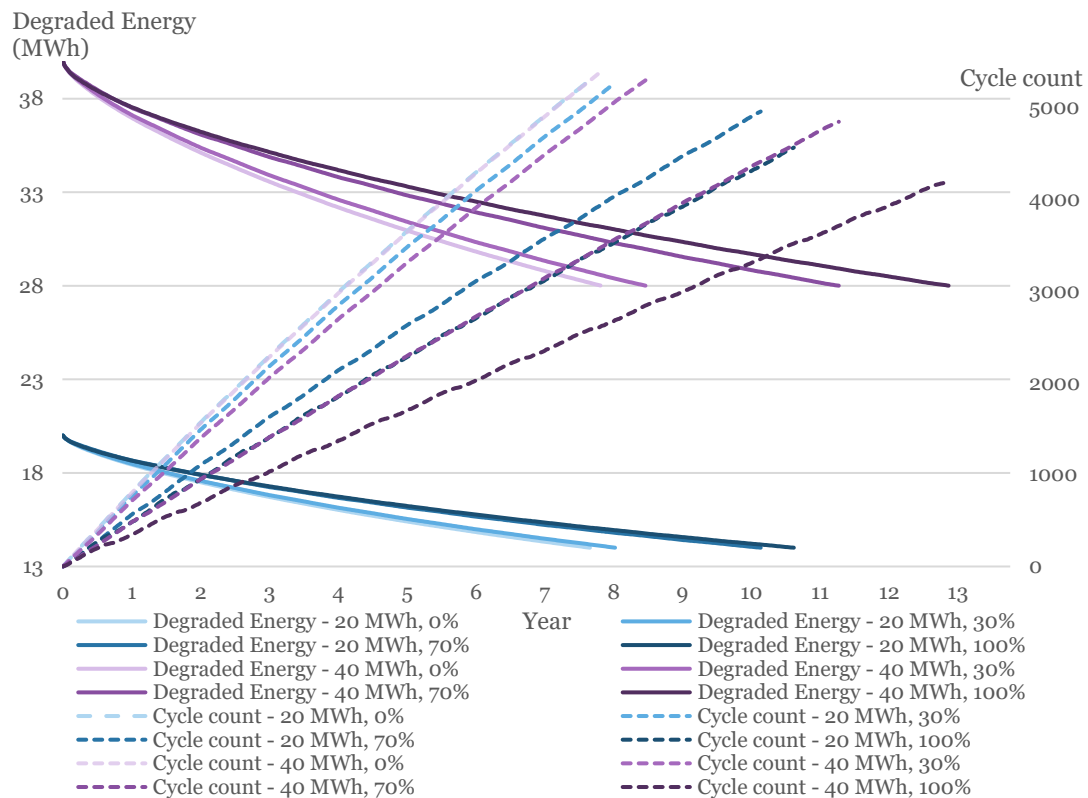


Figure 42, Energy capacity degradation, cumulative cycle count, and lifetime across scenarios in the FI bidding zone

The figure shows a correlation between the share of capacity reserved for imbalance management, number of cycles, energy capacity degradation, and operational lifetime. Lifetime is highly influenced by cycle count, as increased cycling accelerates battery degradation. For both the 20 MWh and 40 MWh systems, the results show that a higher capacity share reserved for imbalance management leads to less cycles and a longer operational lifetime. This is due to that imbalance management offers fewer hours in which the BESS can operate to generate value, compared to market participation. For instance, in the case of Kalax WPP, only 57% of the hours in 2024 offered opportunities to generate savings through imbalance management.

The simulated lifetimes range from 7.6 to 10.6 years for the 20 MWh scenarios and from 7.8 to 12.8 years for the 40 MWh scenarios. The 40 MWh systems proved to have longer lifetimes and fewer cycles than their 20 MWh counterparts. This is because the systems with less capacity reach their full equivalent cycles more quickly, resulting in accelerated degradation of energy capacity, which further decrease the lifetime.

Charging and discharging activity of the BESS can be analysed by observing its SoC profile. *Figure 43* presents the SoC profiles over a one-week period for three of the simulated scenarios in FI bidding zone: the 20 MWh system with 100% capacity share reserved for imbalance management, and the 40 MWh system with both 0% and 100% shares for imbalance management.

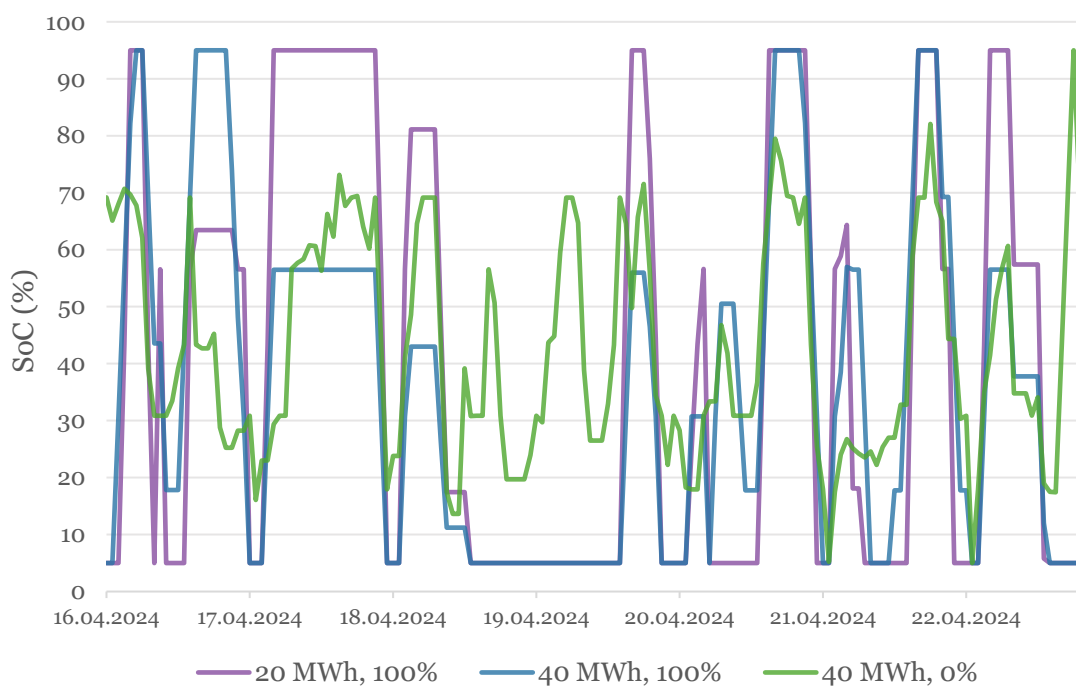


Figure 43, SoC profiles for FI bidding zone scenarios for a one week period

The figure clearly presents how charging and discharging activity differs between the scenarios with solely imbalance management and with exclusive market participation. A comparison of the two 40 MWh scenarios shows that activations occur more frequently in market participation than in imbalance management. Similar to the trends observed in the lifetime, this is due to the lower number of value-generating hours in imbalance management. Furthermore, the figure reveals that while activation volumes in market participation are generally smaller, they occur more frequently. In contrast, imbalance management tends to have larger but less frequent activations.

It is also evident that the SoC reaches its limits more frequently when the system operates exclusively in imbalance management. During the first simulated year, the 40 MWh system reached its SoC limits in 3.1% of the hours in market participation, compared to a significantly higher 40.8% in imbalance management. This is because the optimiser only allows the BESS to operate when it results in cost savings in imbalance management. If the SoC is already at a limit and the next hour offers no possible savings, the system remains at that limit. This, again, is an outcome due to limited value-generating hours in imbalance management. Lastly, the figure shows that, in imbalance management, the 20 MWh system reaches its limits more frequently than the 40 MWh system. This is due to its smaller energy capacity, which provides a narrower energy buffer. As a result, the system reaches the SoC limits more quickly, limiting its operation in imbalance management.

Charging and discharging activations of the BESS occur in different markets, depending on which market offers the highest value for each hour, and the real activations for the year 2024 for each market. *Figure 44* presents the total energy trade and capacity market activation shares, across market participation and imbalance management in the FI bidding zone, over the full simulated lifetime for each scenario.

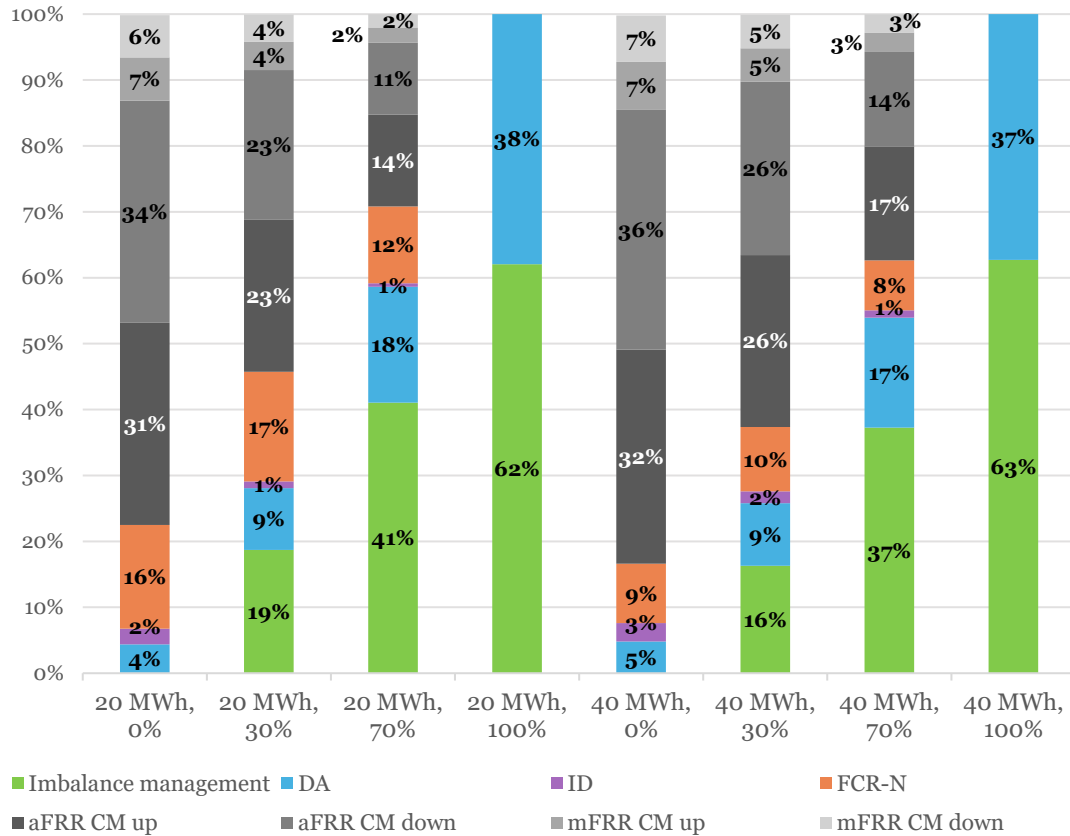


Figure 44, Energy trade and activation shares for each market across scenarios in the FI bidding zone

As shown in the figure, for market participation, the BESS primarily allocates its energy through activations in the aFRR up- and down-regulation CMs. There are no direct trades in EAM because the optimiser prioritises reserving capacity in the CM, which is then activated in EAM to maximise revenue. Trading directly in EAM without first reserving capacity would miss the opportunity to earn from CMs. The preference for energy allocated to aFRR over mFRR is explained by higher average CM payments for aFRR, and more favourable energy prices in the EAM. Specifically, aFRR in average offers better compensation for both up- and down-regulation, as shown in *Table 19*.

Furthermore, in market participation, FCR-N market also plays a notable role in energy activations, whereas the DA and ID markets contribute less. However, when the share of capacity reserved for imbalance management is increased, also the trades in DA market increases, as charging in DA market is allowed with the capacity share reserved for imbalance management. Additionally, the figure shows that the relative energy shares allocated to each market within market participation remain largely consistent across different imbalance management capacity shares.

7.1.2 SE2 results

The same analysis conducted for the FI bidding zone has been applied to SE2, resulting in similar results. *Figure 45* presents the energy capacity degradation, cumulative cycle count, and the operative lifetime for the SE2 scenarios.

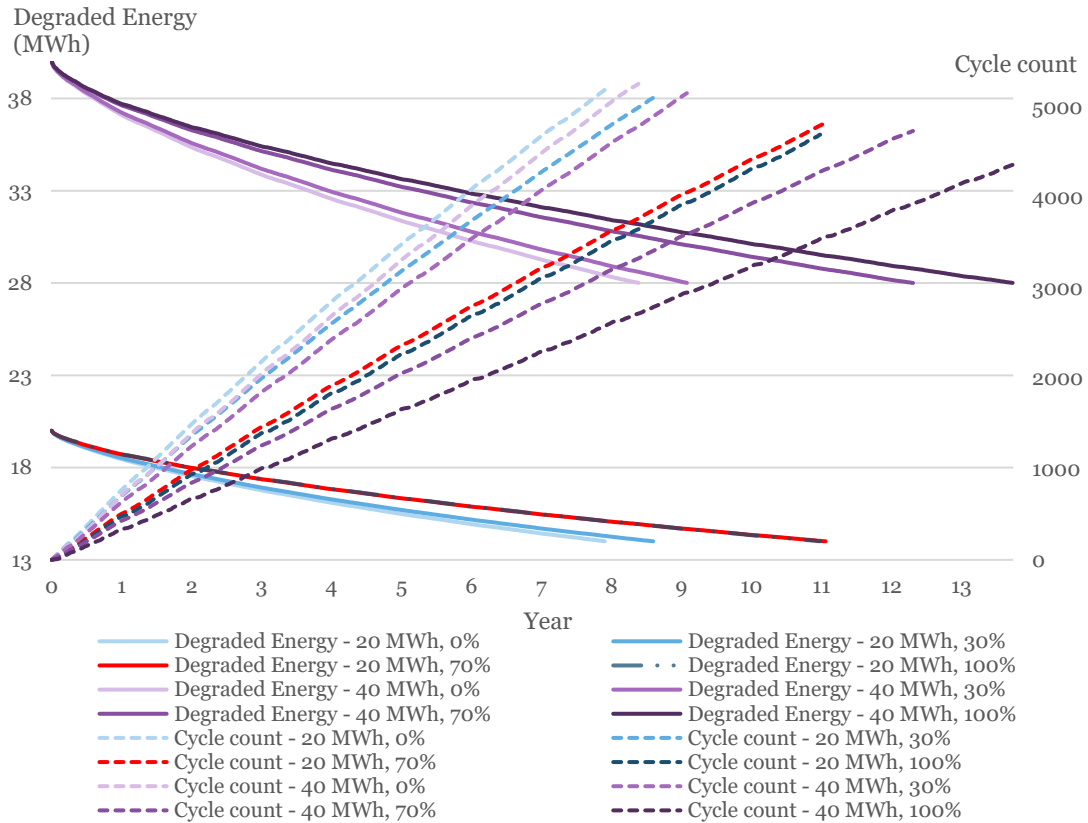


Figure 45, Energy capacity degradation, cumulative cycle count, and lifetime across scenarios in the SE2 bidding zone

The SE2 scenarios show similar correlations as for FI scenarios. In general, scenarios with fewer cycles results in lower energy capacity degradation and longer lifetimes. However, the figure shows that for the 20 MWh system, the scenarios with 70% and 100% reserved capacity share show similar levels of degradation and lifetime. A closer analysis indicates that the 70% scenario averages 1.2 cycles per day, while the 100% scenario averages 1.17 cycles per day. The 100% scenario achieves a lifetime that is one month longer, supporting the trend that a higher number of cycles accelerates degradation. It should be noted, however, that energy capacity degradation is also influenced by calendar aging, which is significantly affected by the system’s SoC levels.

In terms of value-generating potential for imbalance management, Kalax had 57% of the hours in 2024 where cost savings could be achieved, while Solberg had 52%. This again highlights that, in SE2 scenarios, the BESS operates more frequently in markets than in imbalance management due to the

limited number of value-generating hours. Simulated lifetimes for SE2 range from 7.9 to 10.9 years for the 20 MWh systems, and from 8.4 to 13.7 years for the 40 MWh systems. Compared to the corresponding FI scenarios, SE2 lifetimes are 3% to 9% longer. Similar to the FI results, the 40 MWh systems in SE2 exhibit longer lifetimes than their 20 MWh counterparts.

Figure 46 presents the SoC profiles over a one-week period for SE2 scenarios with 20 MWh system with 100% capacity share reserved for imbalance management, and the 40 MWh system with both 0% and 100% shares for imbalance management.

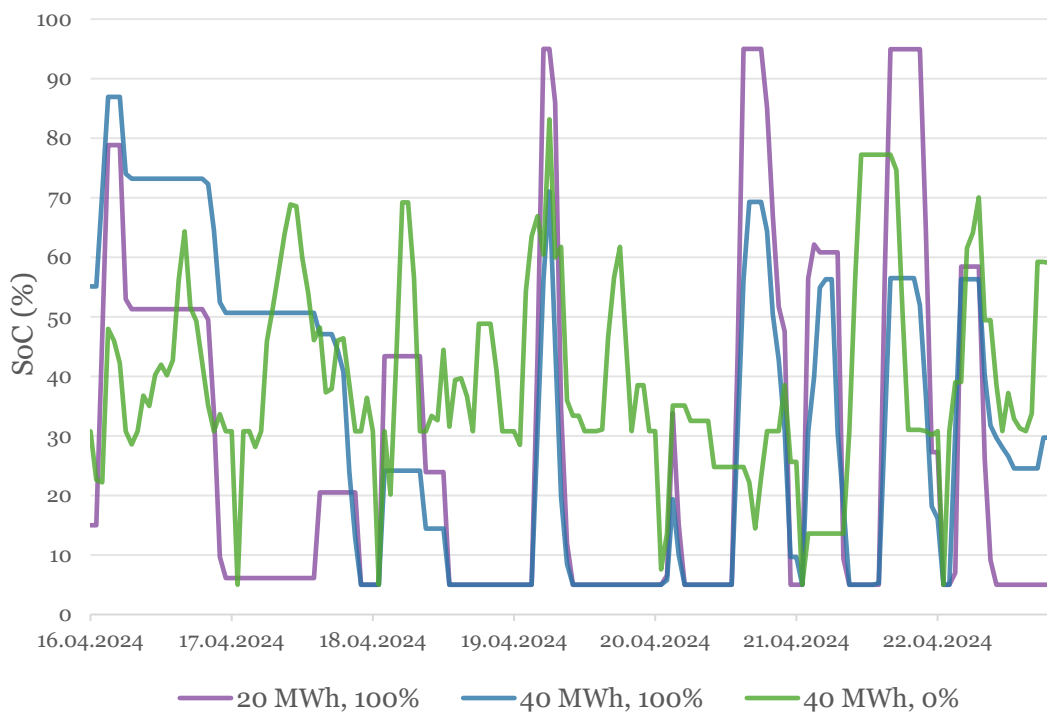


Figure 46, SoC profiles for SE2 bidding zone scenarios for one week

The figure confirms that charging and discharging activity is higher in exclusively market participation compared to solely imbalance management, which have larger but less frequent activations. For the 40 MWh system with 0% imbalance share, the SoC limits were reached 2.0% of the hours during the first simulated year in SE2, compared to 3.1% in FI. With 100% of capacity allocated to imbalance management, the value increase significantly to 50.0% for SE2, compared to 40.8% in FI. The high contrast between market participation and imbalance management is again explained by the limited number of value-generating hours available in imbalance management. Similar to the FI analysis, the 20 MWh system in SE2 reaches its SoC limits more frequently than the 40 MWh system under imbalance management.

Figure 47 illustrates the total energy trade and capacity market activation shares across market participation and imbalance management in the SE2 bidding zone, over the full simulated lifetime for all scenarios.

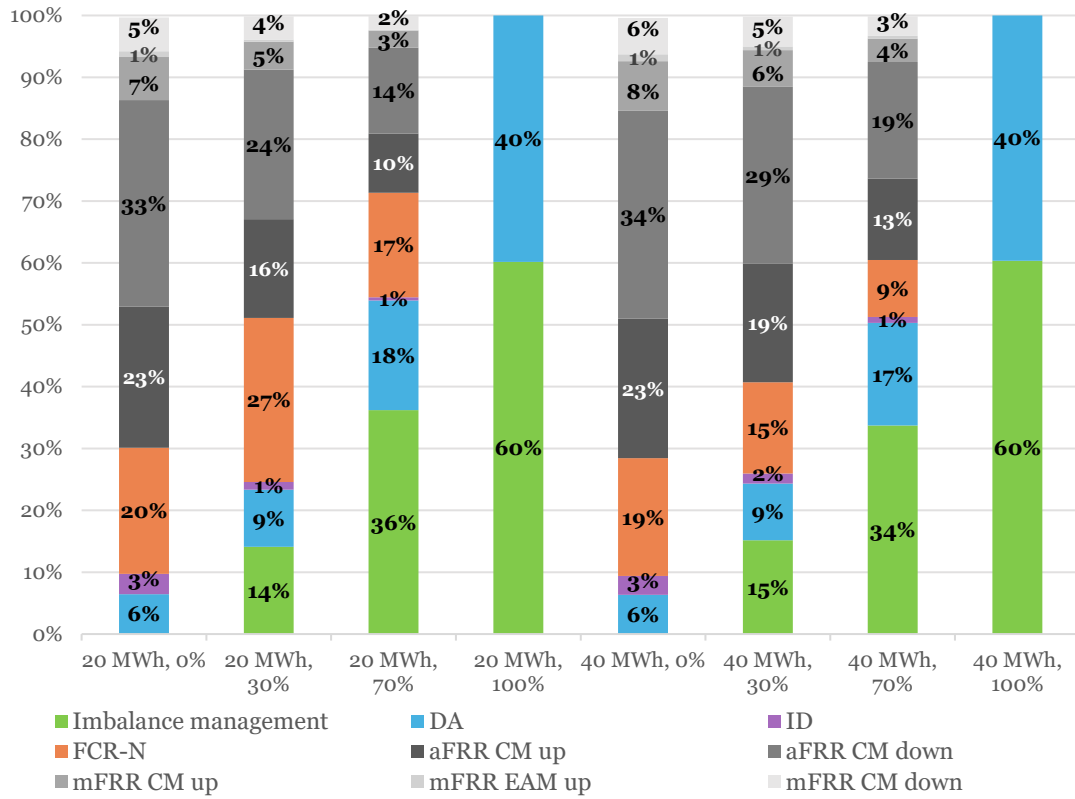


Figure 47, Energy trade and activation shares for each market across scenarios in the SE2 bidding zone

For SE2, energy activations and trades in market participation primarily focus on the FCR-N and aFRR CMs, similar to the FI bidding zone. However, a difference exists in the share of aFRR CM up-regulation energy, which is lower in SE2 scenarios. This is due to two main factors. First, the optimiser reserves less capacity in the aFRR up-regulation CM in SE2, as the average capacity and energy compensation is lower in relation to other markets. Second, in 2024, aFRR up-regulation energy was activated 70.1% of the hours in FI, while in SE2 it was activated only 48.9% of the hours, resulting in fewer opportunities for energy activation. The reduced share of aFRR CM up-activations in SE2 is partially offset by higher activations in the FCR-N market, where prices are comparable to those in FI. As in FI, aFRR is preferred over mFRR due to generally higher CM compensation, as was shown in Table 19. DA and ID markets contribute only marginally to energy allocation, though the DA market's role increases with higher imbalance management capacity shares. Finally, the figure shows that the distribution of energy across different markets in market participation remains relatively consistent regardless of the capacity share allocated to imbalance management.

7.1.3 NO4 results

Figure 48 illustrates the degradation of battery energy capacity, the cumulative cycle count, and the operative lifetime across different scenarios within NO4 bidding zone. Figure 49 presents the SoC profiles over a one-week period for NO4 scenarios, with 20 MWh system with 100% of its capacity reserved for imbalance management, and a 40 MWh system with 0% and 100% capacity shares for imbalance management.

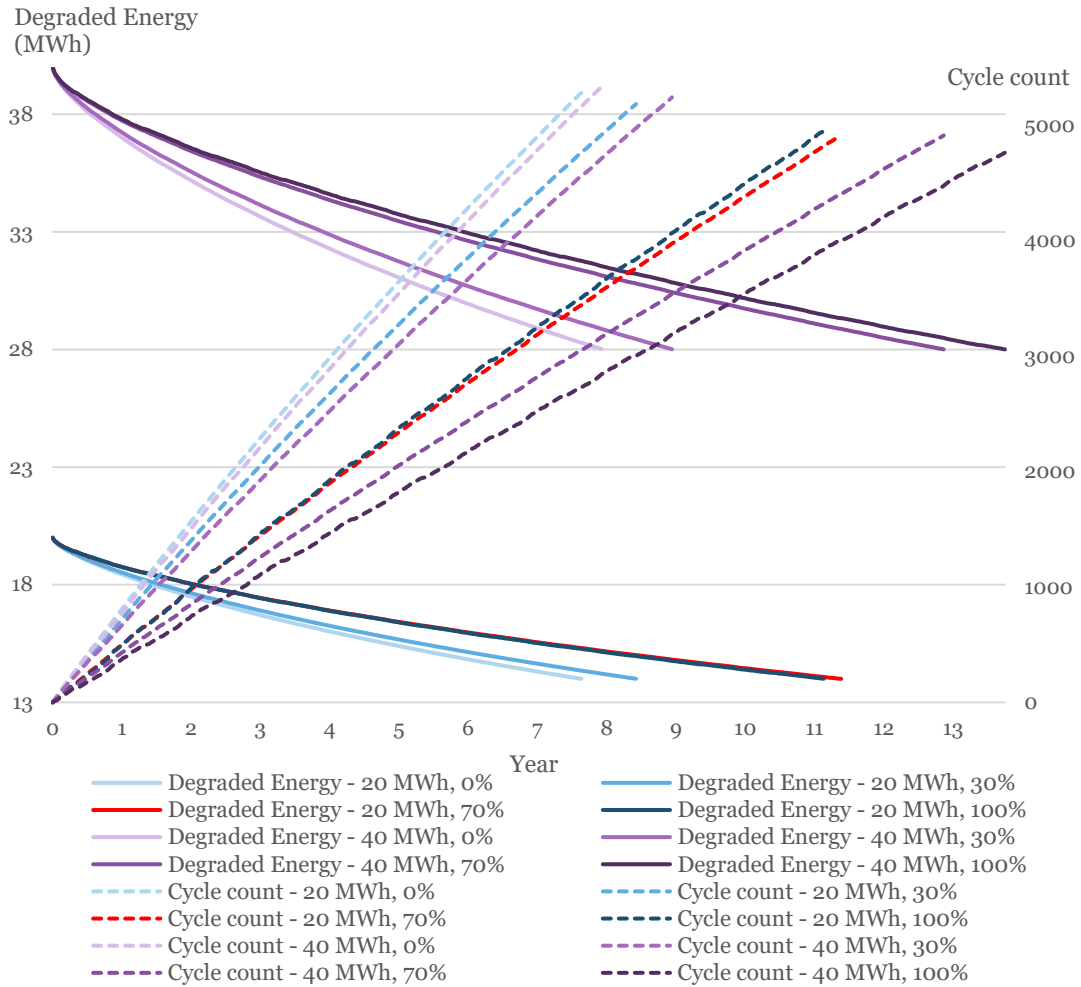


Figure 48, Energy capacity degradation, cumulative cycle count, and lifetime across scenarios in the NO4 bidding zone

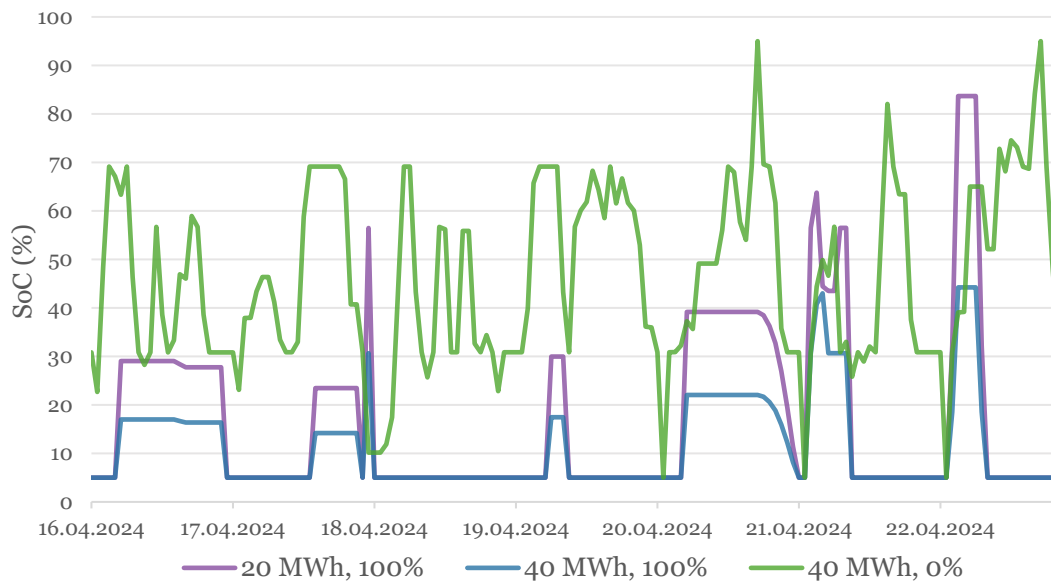


Figure 49, SoC profiles for NO4 bidding zone scenarios for one week

In the NO4 bidding zone scenarios, the same overall trends are observed in Figure 48 as in the FI and SE2 bidding zones, with one exception. The 20 MWh system with 100% imbalance share has a slightly shorter lifetime than the 70% scenario, despite the general trend of longer lifetimes as more capacity is reserved for imbalance management. As illustrated in the figure, the 100% scenario has a higher number of cycles than the 70% scenario, which contributes to its reduces lifetime. At Sørffjord WPP, only 58.1% of hours in 2024 offered the potential for cost savings through imbalance management. As in the FI and SE2 bidding zones, this results generally in lower activity and fewer cycles compared to market participation. The simulated lifetimes in the NO4 scenarios range from 7.6 to 11.3 years for the 20 MWh scenarios and from 7.9 to 13.7 years for the 40 MWh scenarios, supporting the trend that larger battery systems tend to achieve longer operational lifetimes.

Figure 49 results for the NO4 bidding zone are consistent with those observed in FI and SE2. In the first simulated year, the 40 MWh system with 0% imbalance share reached its SoC limits in 2.6% of the hours, while the 100% imbalance scenario reached these limits 41.8% of the hours. During the one-week period shown, the SoC in the 100% scenarios never reached the maximum limit, indicating that most SoC constraints occur at the lower bound. Further analysis confirm this, revealing that nearly three-quarters of the SoC limit hours correspond to the minimum SoC threshold.

Figure 50 illustrates the total energy trade and capacity market activation shares, across market participation and imbalance management in the NO4 bidding zone, over the full simulated lifetime for all scenarios.

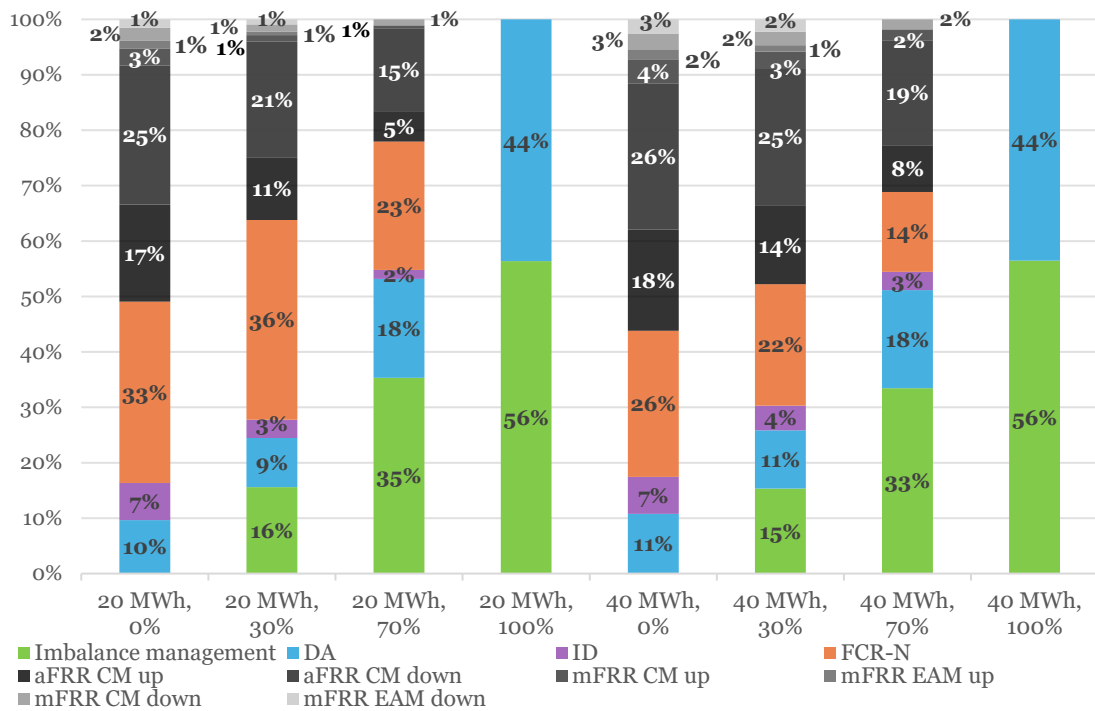


Figure 50, Energy trade and activation shares for each market across scenarios in the NO4 bidding zone

In contrast to the FI and SE2 bidding zones, energy activations in markets for NO4 scenarios are primarily concentrated in the FCR-N market, followed by the aFRR up- and down-regulation markets. This is largely due to relatively higher FCR-N prices compared to other markets. In NO4, aFRR and mFRR market activations account for only 50–60% of the energy trades and activations, whereas in FI and SE2 the corresponding shares are around 80% and 70% respectively. This difference is primarily driven by the lower frequency of aFRR activations in NO4, with 27% of the hours in 2024 for up-regulation and 44% for down-regulation, compared to 70% and 86% in FI. Although aFRR compensation in NO4 remains competitive, the reduced activity is mainly due to the limited number of activation hours in 2024 rather than price. In contrast, mFRR activations plays a minimal role due to lower compensation in capacity markets. Another notable difference in NO4 is the increased share of energy allocated to the DA and ID markets.

7.1.4 Summary on operational performance

The simulation results across all scenarios in FI, SE2 and NO4 bidding zones demonstrated that increasing the capacity share reserved for imbalance management reduces the frequency of charging and discharging activations. This, in turn, lowers the total number of cycles, thereby reducing degradation and extending the operational lifetime of the BESS. Furthermore, the results confirm that 40 MWh systems consistently achieve longer lifetimes than their 20 MWh counterparts. Analysis of the SoC profiles revealed that scenarios

involving solely market participation exhibited higher activity compared to those focused exclusively on imbalance management. While market-related activations occurred more frequently, they involved smaller energy volumes. Additionally, it was observed that SoC limits were reached significantly more often during imbalance management operation. This effect was more notable in the 20 MWh systems compared to the 40 MWh systems. In conclusion, the BESS with 40 MWh energy capacity, and a greater allocation to imbalance management is associated with improved operational lifetime.

Key differences between the bidding zones were observed in energy allocation across markets, as summarised in *Figure 51* for the 20 MWh and 40 MWh systems with 0% capacity reserved for imbalance management. In all bidding zones, the aFRR CMs and FCR-N dominated energy allocation. In the FI bidding zone, activations dominated in the aFRR CMs, followed by FCR-N, with low activity in mFRR, DA and ID markets. SE2 showed similar pattern, but with less allocation in aFRR up-regulation and more in FCR-N. NO4, had significantly higher allocation in FCR-N market, reduced aFRR activations, and greater shares in the DA and ID markets. These differences are mainly due to market-specific pricing and the frequency of real activations during 2024 for each market. Specifically, both SE2 and NO4 experienced fewer activations in the aFRR up-regulation CM compared to FI. Across all bidding zones, the relative share of markets within market participation remained stable across different imbalance management shares, except for the DA market, which share increased with higher imbalance capacity.

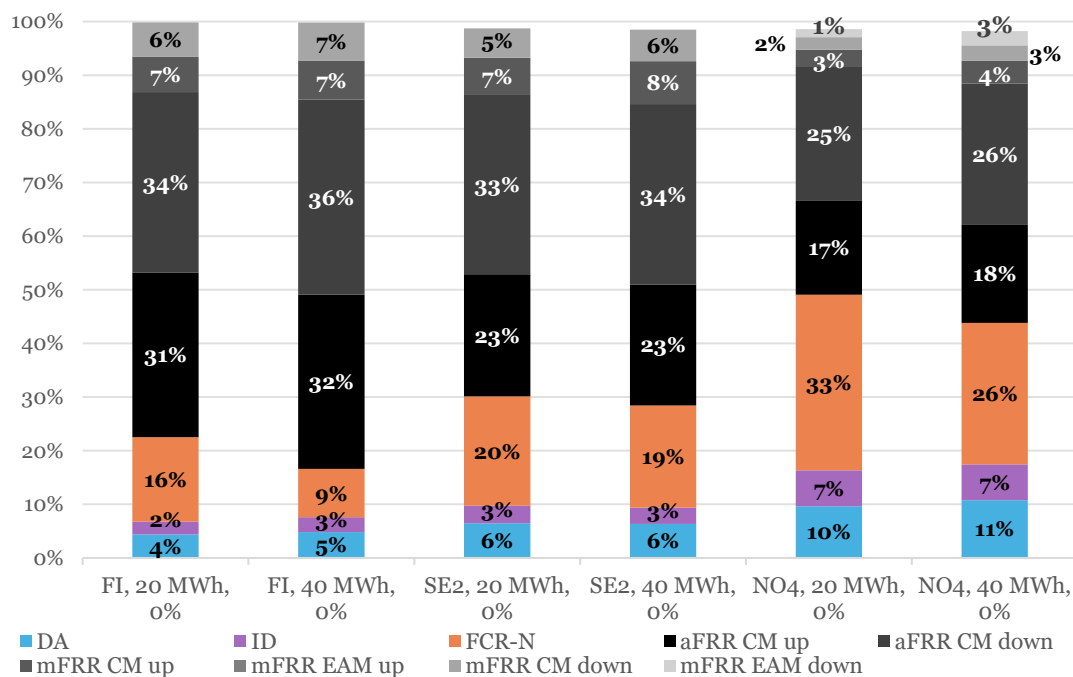


Figure 51, Energy trade and activation shares for each market across market participation in FI, SE2, and NO4

7.2 Economic Evaluation of Scenarios

7.2.1 Net cash flow analysis

Figure 52 illustrates the net cash flows across individual markets, as well as from imbalance management, for each scenario in the FI bidding zone. I.M on the horizontal axis denotes imbalance management, and the percentage shown in the legend the share of capacity reserved for imbalance management. Net cash flow includes both the transmission fees and imbalance fees.

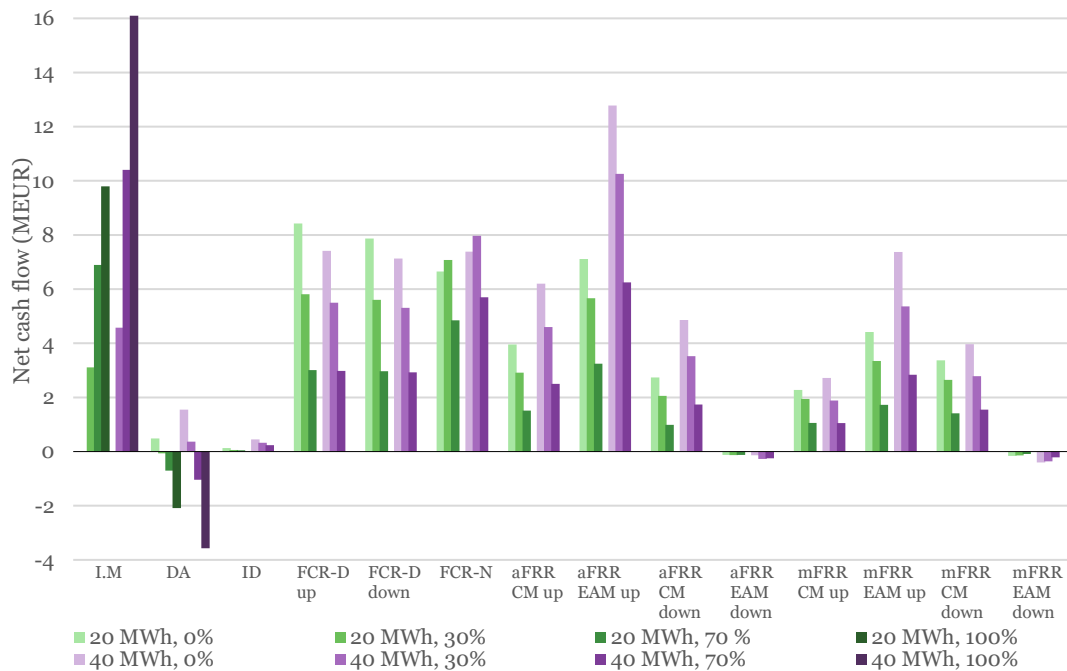


Figure 52, Net cash flows for markets and imbalance management in FI

It is evident that the DA market, aFRR and mFRR EAM down-regulations results in negative net cash flows. This is due to energy purchases that occur in these markets, along with those in the ID market and through FCR-N market activations. Net cash flow is evenly distributed across FCR-D and FCR-N markets in each scenario. Similarly, the aFRR and mFRR CMs show a fairly balanced distribution. In the 40 MWh system, aFRR EAM up-regulation becomes more important, while the ID contributes very little in all scenarios.

All markets with a positive net cash flow show a consistent reduction in profitability as the capacity share for imbalance management increases, with the exception of FCR-N market. This highlights a clear trade-off where allocating more capacity to imbalance services enhance savings in imbalance management, but reduces cash flow from markets. For FCR-N market, however, net cash flow increases when the imbalance management share rises from 0% to 30%, but then declines as the share increases further to 70%. This pattern is consistent for both the 20 MWh and 40 MWh systems.

Notably, at a 70% imbalance management share, imbalance management generates the highest net cash flow among all markets. Even at a 30% share, imbalance-related savings are comparable to the revenues from the aFRR and mFRR CMs in the 20 MWh system, accounting for approximately 7.8% of the total net cash flow. In the 40 MWh system, with the same 30% share, the contribution from imbalance management is similar to that of the FCR-D markets and aFRR CMs, comprising 8.8% of total net cash flow. The slightly higher share in the 40 MWh case reflect the increased battery energy capacity, which enhances the potential for imbalance-related activations, while having less influence on the capacity-based markets, where power rating remains the dominant constraint.

This contrast becomes more apparent when comparing how different markets respond to increased system size. Doubling the energy capacity has only a minor impact on capacity-based market revenues such as FCR-D and FCR-N. Conversely, energy-based markets, such as aFRR and mFRR EAM up-regulation benefit significantly more from larger energy capacity, especially when no capacity is reserved for imbalance. Among all market segments, aFRR EAM up-regulation shows the most notable growth in net cash flow with increased energy capacity.

Figure 53 presents net cash flow for each market, as well as for imbalance management in the SE2 bidding zone scenarios, following the same principles as for FI in Figure 52.

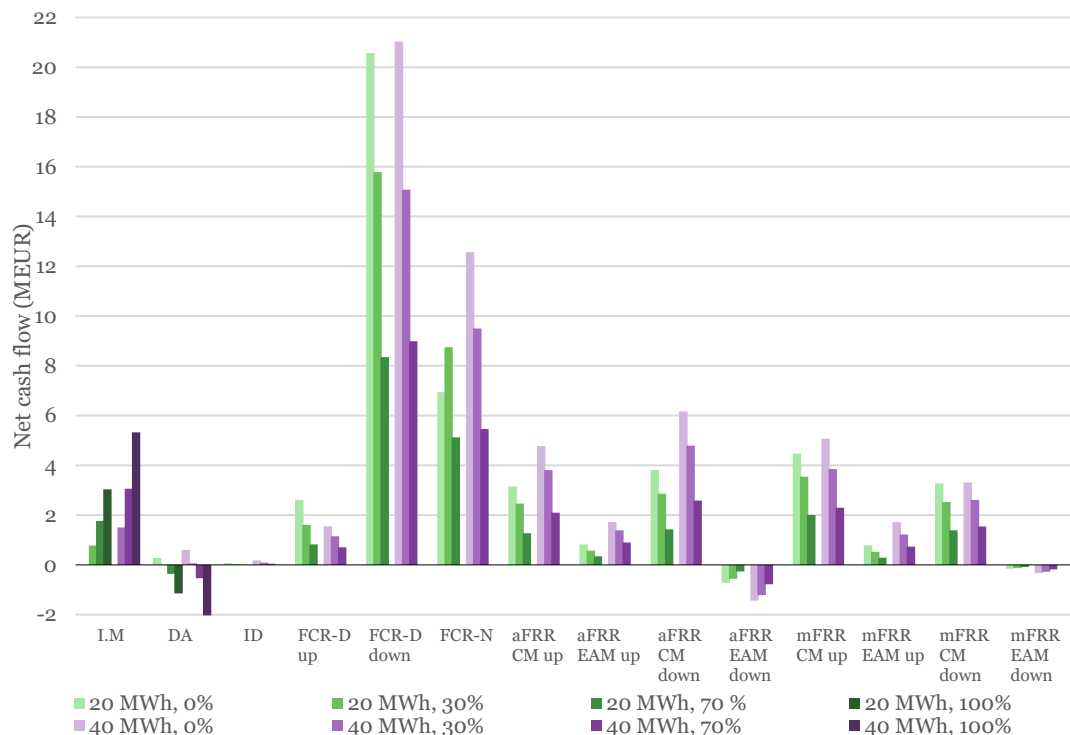


Figure 53, Net cash flows for markets and imbalance management in SE2

As in the FI bidding zone, the DA, aFRR and mFRR EAM down-regulation in SE2 result in negative net cash flows due to energy purchases. However, unlike FI, the DA market in SE2 is less negative, while aFRR EAM down-regulation is more negative, reflecting lower charging in DA market and higher charging volumes and average price in aFRR EAM down-regulation. Net cash flows in SE2 are more unevenly distributed than in FI. Revenues are heavily concentrated in the FCR-D down-regulation market, contributing 33% to 45% of the total net cash flow in all market participation scenarios. This is significantly more than in FI, making it the dominant source of market-based revenues. FCR-N follows in importance, whereas aFRR and mFRR CMs show a relatively even distribution. FCR-D up-regulation market plays a minor role to the total net cash flow, whereas the ID market remains insignificant.

Consistent with the FI results, increasing the share of capacity reserved for imbalance management leads to a general decline in net revenues across all markets. The only exception is FCR-N in the 20 MWh system, where net cash flow increases between the 0% to 30% imbalance share scenarios.

A key difference from the FI results emerges in the overall value of imbalance management. In SE2, even at a 70% imbalance management capacity share, net cash flows remain marginal. For the 20 MWh system, imbalance management cost savings reach levels comparable only to those of aFRR and mFRR CMs. For the 40 MWh system, these cost savings are only marginally higher. This contrasts with FI, where imbalance management represented the most profitable component at 70% share. At the 30% share level, imbalance management net cash flow is among the lowest contributors in SE2, roughly matching aFRR and mFRR EAM up-regulation, both of which have low contribution.

This indicates a weaker trade-off in SE2. Although allocating more capacity to imbalance management reduces market revenues, the corresponding cost savings from imbalance services are relatively small. For instance, under the 100% imbalance management share scenario, the 40 MWh system in FI achieved a reduction in imbalance costs of 16.1 MEUR, whereas SE2 achieved only 5.3 MEUR under the same conditions. This is largely driven by significantly higher imbalance prices in FI, which are approximately double those in SE2, making imbalance management considerably more valuable in the FI bidding zone.

Doubling the energy capacity has only a minor impact on the FCR-D and FCR-N markets, with the exception of the 0% imbalance management capacity share scenario, where cash flow in the FCR-N market nearly doubles. The aFRR and mFRR CMs also experience increased cash flows with higher energy capacity. In contrast, energy-based markets, such as aFRR and mFRR

EAM up-regulation, benefit considerably more from larger energy capacity. However, because these markets generate relatively low cash flows in SE2, the overall impact of increased energy capacity on net cash flow is less pronounced than in FI.

Figure 54 illustrates the market-specific net cash flows, including those from imbalance management, for the NO4 bidding zone scenarios, following the same structure as the FI and SE2 analyses.

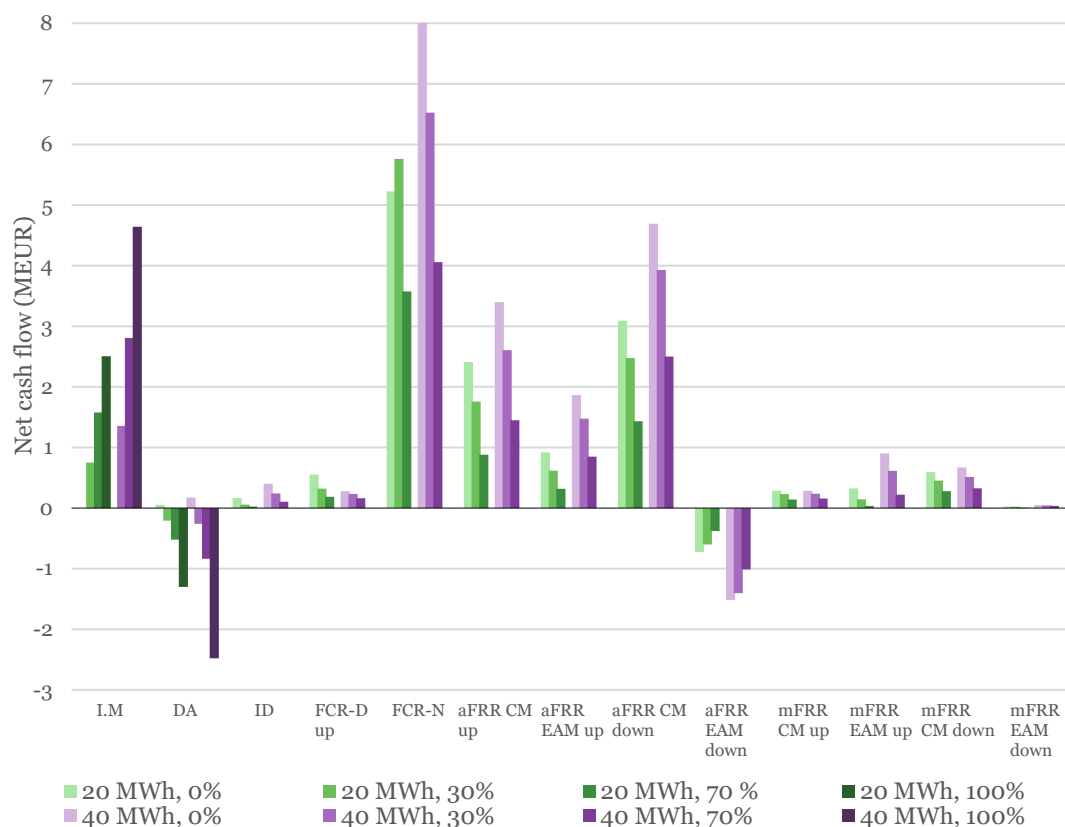


Figure 54, Net cash flows for markets and imbalance management in NO4

In the NO4 bidding zone, negative net cash flows are observed in the DA market and aFRR EAM down-regulation, indicating energy purchase. These negative cash flows are more notable than in SE2. The lower average DA market price in NO4 may have led the simulation to allocate higher charging volumes to the DA market, increasing the overall cash flow for energy purchase. In contrast to FI and SE2, a larger number of markets contribute only marginally to the total net cash flow, including the ID market, FCR-D up-regulation market, mFRR CMs, and mFRR EAMs, which all contribute less than 1 MEUR to the total net cash flow. Across all scenarios, FCR-N is the most significant revenue-generating market, followed by aFRR CM down-regulation. As observed in both FI and SE2, net cash flow from all markets decline as the share of capacity allocated to imbalance management increases, with FCR-N again being an exception.

Analysing the cost savings from imbalance management places NO4 between FI and SE2 in terms of overall significance. Imbalance management appears to be more impactful in NO4 than in SE2, but less so than in FI. At a 70% imbalance capacity share, cost savings from imbalance management represent the second largest source of net cash flow in both the 20 MWh and 40 MWh scenarios, following the FCR-N market. When the imbalance capacity share is reduced to 30%, the contribution from imbalance management declines to below that of the aFRR CMs.

When comparing the ratio of imbalance-related net cash flow to total net cash flow, NO4 shows a higher share than SE2, but a lower share than FI. However, in the 100% imbalance management scenario with the 40 MWh system, cost savings in NO4 amount to only 4.6 MEUR, which is lower than for FI with 16.1 MEUR, and SE with 5.3 MEUR. Despite this lower value, the relative contribution of imbalance management to total net cash flow is higher in NO4 than in SE2, due to generally lower market-based revenues. This is not driven by elevated imbalance prices, since average prices are approximately equal, but a result of lower average prices in other markets, which increases the relative value of imbalance-related cost savings. This indicates that increasing the share of capacity reserved for imbalance management offers a more favourable trade-off in NO4 compared to SE2.

Doubling the energy capacity increases net cash flows in imbalance management, the FCR-N market, aFRR CMs, and aFRR EAM up-regulation, while the impact on other markets on the overall cash flow is low. In this case, it is evident that increased energy capacity has a greater effect on capacity markets in NO4 compared to FI and SE2, where the benefits were more concentrated in energy-based markets.

As a summary, the net cash flow analysis across FI, SE2, and NO4, reveals clear differences in market diversification. FI shows an evenly distributed net cash flow across markets, with no single market excessively dominating. SE2 and NO4 have less diversified net cash flow distribution, with SE2 heavily reliant on FCR-D down-regulation and NO4 on FCR-N market. Additionally, several markets in NO4 contribute only marginally to the overall net cash flow. A diversification reduces the risk of profitability loss due to market saturation or price declines, making FI a lower-risk zone for BESS investment in this perspective. In contrast, as net cash flows in SE2 and NO4 are heavily dependent on specific markets, a price decrease in those markets would significantly impact the overall viability of a BESS investment.

Increasing capacity for imbalance management generally reduces market-based net cash flows, except for FCR-N, while enhancing imbalance-related cost savings. This trade-off between lower market revenues and higher

savings is further examined in *Chapter 7.2.2* to determine if the savings compensate for lost market income. Larger BESS energy capacity improves cost savings in imbalance management and net cash flow in energy-based markets. Capacity-based markets are less impacted, except for NO4, where FCR-N and aFRR CM revenues also increased. However, higher energy capacity increases CAPEX and O&M costs, a trade-off also analysed in *Chapter 7.2.2*.

Overall, the results for FI scenarios indicate that cost savings from imbalance management are already significant at 30% capacity allocation, being comparable to the net cash flows from individual markets, and becomes the largest contributor at 70%. In SE2, the value of imbalance management remains relatively low, even at 70% capacity allocation. NO4 performs better than SE2. At 70%, imbalance management is the second largest contributor, while at 30% its value is comparable with other lower-impact markets. In summary of this analysis, FI provides the highest value for imbalance management, followed by NO4, with SE2 showing the weakest performance.

7.2.2 Financial summary, NPV and PBT

Table 20 and *Table 21* present a financial summary for the 20 MWh and 40 MWh systems, respectively. Energy-based revenues and costs include imbalance management, DA and ID markets, and aFRR and mFRR EAMs. Capacity-based revenues consist of FCR-D, and FCR-N—including its activations—and aFRR and mFRR CMs. Net cash flow accounts for all these components, along with CAPEX and O&M costs over each scenarios lifetimes.

Table 20, Financial summary for the 20 MWh scenarios

	0%			30%			70%			100%		
	FI	SE2	NO4	FI	SE2	NO4	FI	SE2	NO4	FI	SE2	NO4
Energy-based revenue (MEUR)	13.5	2.3	1.8	13.4	2.3	1.8	12.5	2.6	2.0	9.8	3.1	2.5
Capacity-based revenue (MEUR)	35.3	44.8	12.2	28.1	37.5	11.0	15.8	20.4	6.5	-	-	-
Energy-based costs (MEUR)	-1.6	-1.2	-1.0	-1.5	-1.1	-1.0	-1.5	-0.9	-1.0	-2.1	-1.2	-1.3
CAPEX (MEUR)	-4.8	-4.8	-4.8	-4.8	-4.8	-4.8	-4.8	-4.8	-4.8	-4.8	-4.8	-4.8
O&M (MEUR)	-0.9	-0.9	-0.9	-1.0	-1.0	-1.0	-1.2	-1.3	-1.4	-1.3	-1.3	-1.3
Net cash flow (MEUR)	41.4	40.2	7.2	34.1	32.9	6.0	20.8	16.0	1.4	1.6	-4.2	-4.9

Table 21, Financial summary for the 40 MWh scenarios

	0%			30%			70%			100%		
	FI	SE2	NO4	FI	SE2	NO4	FI	SE2	NO4	FI	SE2	NO4
Energy-based revenue (MEUR)	24.7	4.8	4.0	23.3	5.0	4.2	21.1	5.2	4.3	16.1	5.4	4.6
Capacity-based revenue (MEUR)	39.7	54.5	17.4	31.6	40.8	14.1	18.4	23.7	8.7	-	-	-
Energy-based costs (MEUR)	-3.1	-2.4	-2.2	-3.1	-2.2	-2.2	-2.9	-1.9	-2.1	-3.6	-2.1	-2.5
CAPEX (MEUR)	-8.8	-8.8	-8.8	-8.8	-8.8	-8.8	-8.8	-8.8	-8.8	-8.8	-8.8	-8.8
O&M (MEUR)	-1.9	-2.0	-1.9	-2.0	-2.2	-2.1	-2.7	-2.9	-3.1	-3.1	-3.3	-3.3
Net cash flow (MEUR)	50.6	46.1	8.6	41.0	32.6	5.2	25.2	15.2	-1.0	0.7	-8.8	-9.9

Starting with energy-based revenues, it is evident that for FI, revenues decrease as the imbalance management capacity share increases. In contrast, revenues slightly increase for SE2 and NO4. This is primarily due to the high market prices in FI, where reducing market participation capacity lowers energy-based revenue, while increasing participation in imbalance management does not fully offset this loss, despite its relatively high prices. When the energy capacity is doubled, energy-based revenues approximately double in all scenarios, which is expected given that more capacity is available for revenue generation. These revenues are significantly higher in FI compared to SE2 and NO4, largely due to the higher imbalance prices, DA and ID market prices, as well as aFRR and mFRR EAM prices.

Capacity-based revenues decline in all scenarios as the share reserved for imbalance management increases, since less capacity is available for market participation. While the 40 MWh system yields higher capacity-based revenues than the 20 MWh system, the increase is not as substantial as for energy-based revenues. Unlike energy-based revenues, SE2 have the highest revenues in capacity markets, followed by FI and NO4. This is mainly due to the significantly higher prices in FCR-D down-regulation market, which, as shown in *Figure 53*, was also the main contributor to net cash flow in SE2.

Energy-based costs remain relatively constant as the imbalance management capacity share increases. However, the source of purchased energy shifts increasingly to the DA market, where charging is allowed with the capacity reserved for imbalance management. As with revenues, energy costs also approximately double when energy capacity is increased from 20 MWh to 40 MWh, with FI showing the highest costs. O&M costs increase slightly with higher imbalance management shares, due to the longer operational lifetimes. Furthermore, doubling the BESS size directly doubles the O&M costs.

All these factors, including a change in imbalance management capacity share and BESS size, affect revenues and costs, thereby influencing the overall net cash flow. In FI, all scenarios result in a positive net cash flow. However, the 100% imbalance management scenario yields significantly lower values, indicating that relying solely on imbalance management is less profitable than combined market participation. Scenarios with 30% and 70% imbalance management shares maintain reasonable net cash flows, but the highest is achieved with 0% reserved for imbalance management. SE2 follows a similar trend, where the 30% and 70% scenarios maintain reasonable net cash flows, but the 100% imbalance management scenario results in negative values for both 20 MWh and 40 MWh systems. Again, the highest net cash flow is seen in the scenario with full market participation. NO4 behaves similarly, although even the 70% imbalance management share with a 40 MWh system results to a negative value.

These results suggest that the trade-off of increased cost savings from imbalance management do not sufficiently compensate for the revenue losses from reduced market participation. More precisely, market revenues remain more attractive than imbalance cost savings.

By doubling the energy capacity from 20 MWh, FI scenarios show approximately a 20% increase in net cash flow across all imbalance management shares, except for 100%, where net cash flow decreases. This indicates that increasing BESS size benefits market participation more than imbalance management. A 20 MWh system may already be sufficient to cover most typical imbalance volumes for Kalax WPP, meaning that the additional capacity of a 40 MWh system adds less value. The average negative and positive imbalance volumes for Kalax WPP are -8.3 MWh and 10.2 MWh, respectively, indicating that a 40 MWh system may be oversized. At 100% imbalance management share, the lack of market revenues, combined with the higher CAPEX and O&M costs of a larger system, results in reduced profitability.

SE2 and NO4 show similar behaviour, but differs from that observed for FI. For 0% imbalance management share, doubling the energy capacity increases net cash flow. However, with higher imbalance management shares, increasing the energy capacity leads to declining net cash flow. This indicates that in the case of Solberg and Sør fjord WPPs, the more capacity is reserved for imbalance management, the less beneficial a larger BESS becomes. In SE2, the most revenues are generated from capacity markets, which are less sensitive to energy capacity than energy-based markets. Therefore, doubling the BESS size increases CAPEX and O&M costs without a corresponding increase in revenues. For both SE2 and NO4, the lower net cash flows at higher imbalance management shares for the 40 MWh system further suggest that a 20 MWh BESS may already be of sufficient size for the imbalance profiles of Solberg and Sør fjord WPPs. The average negative imbalance volumes are -7.0 MWh for Solberg and -10.5 MWh for Sør fjord, while the positive values are 8.3 MWh and 11.7 MWh, respectively. Thus, upsizing to 40 MWh may result in higher costs without significantly enhancing imbalance cost savings.

In all scenarios, a BESS located in FI consistently yields higher net cash flows compared to SE2 and NO4. At 0% imbalance management share, the cash flow for SE2 scenarios nearly matches that of FI, but the gap widens as more capacity is reserved for imbalance management, highlighting a greater value in imbalance management in FI. Furthermore, the difference in net cash flow between FI and SE2 increases with increased BESS size, reflecting that FI derives a larger share of revenues from energy-based markets. NO4 shows significantly lower net cash flows than both FI and SE2, indicating that both market participation and imbalance management are less financially attractive.

The NPV is then examined, which is illustrated in *Figure 55* at the defined EoL SoH for all scenarios. The trendline in the figure is based solely on the 0%, 30%, 70% and 100% imbalance management share scenarios.

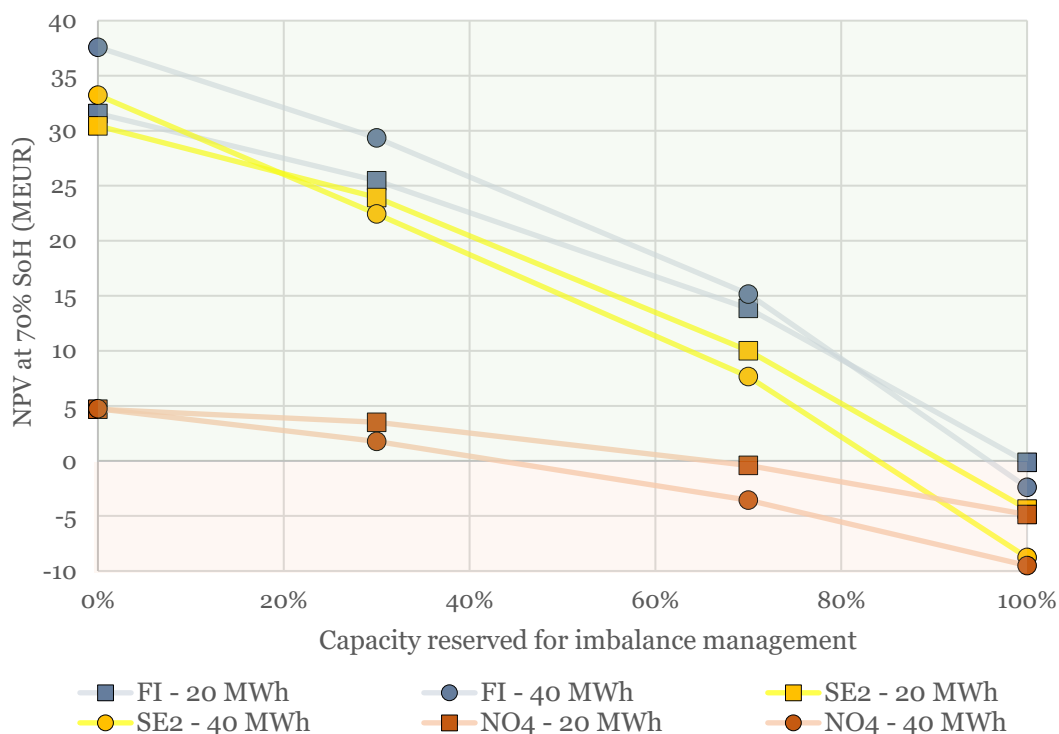


Figure 55, NPV for all scenarios

As demonstrated in the previous analysis of net cash flow, also the NPV for all scenarios declines as the share of capacity reserved for imbalance management increases. Furthermore, *Figure 55* indicates that this decline becomes more accelerated at higher imbalance shares. For FI and SE2, the results highlights the importance of market participation. However, a limited allocation, up to 70% to imbalance management can still provide diversification for value generation.

In FI, the gap between the NPVs of the 20 MWh and 40 MWh systems decreases as the imbalance management share increases. The 40 MWh system yields higher NPV across all scenarios except the 100% imbalance management scenario. For SE2, the 40 MWh system outperforms the 20 MWh system only in the scenario with solely market participation. Beyond that, it does not provide a substantial NPV advantage, likely due to the fact that a significant share of revenues is generated from capacity markets. In NO4, both system sizes result in nearly identical NPVs at 0% imbalance share, but as the share increases, the 20 MWh system performs better. Again, the results indicates that FI benefits more from increased system size than SE2 or NO4, primarily due to the greater contribution of energy-based revenues.

However, for all bidding zones, the 20 MWh system results in higher NPV than the corresponding 40 MWh system in the scenarios with solely imbalance management. The reduction in NPV for the larger system is a result of increased CAPEX and O&M costs, which are not sufficiently offset by additional cost savings at higher imbalance management shares.

FI shows the highest NPV across all scenarios when compared to the corresponding cases in SE2 and NO4, indicating the strongest economic potential for a BESS investment. However, in the 100% imbalance management scenarios with the 40 MWh system, the NPV turns negative, resulting in an unprofitable investment. In contrast, the 20 MWh system under the same condition results in a slightly positive NPV. All other FI scenarios result in positive NPVs, with the highest value achieved under full market participation. In SE2, both system sizes yield negative NPVs in the 100% imbalance management scenario, while the other scenarios exhibit positive values. NO4 presents the lowest NPVs overall, with only the 0% and 30% imbalance management scenarios resulting in positive NPVs, both below 5 MEUR.

Lastly, the PBT is examined, illustrated in *Figure 56* for those scenarios in which the system pays back within the BESS lifetime. The trendline in the figure is based solely on the simulated scenarios.

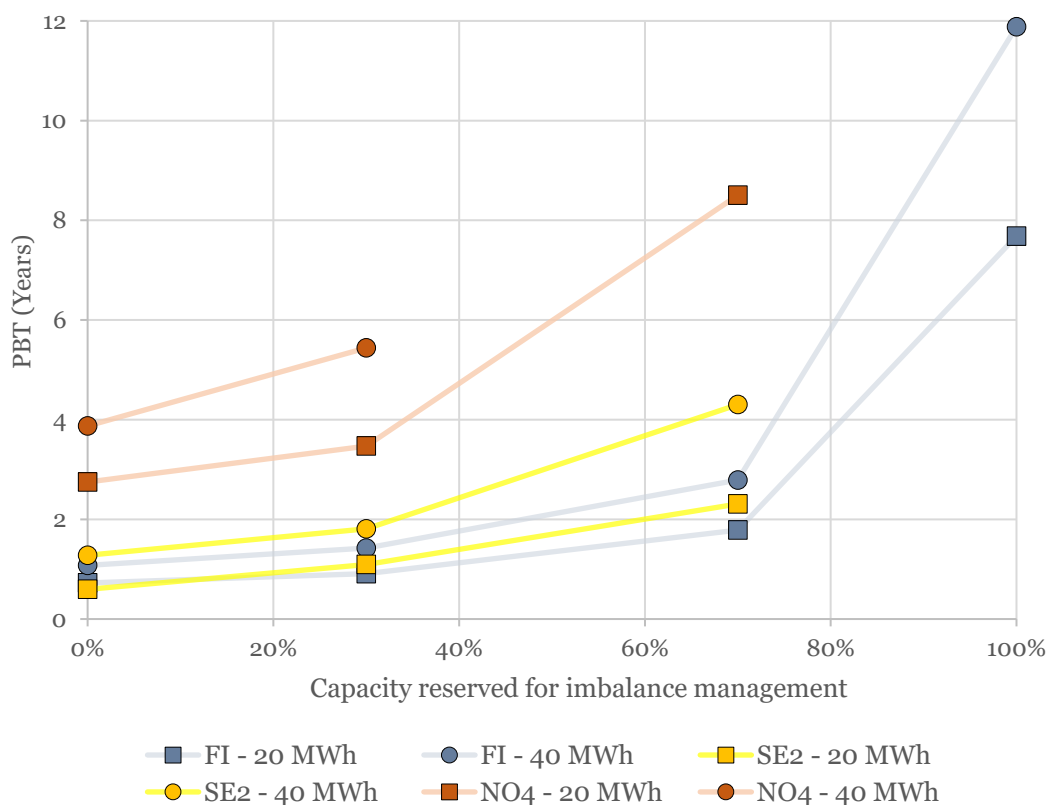


Figure 56, PBT for those scenarios with a defined PBT

The PBT analysis exhibits generally similar trends to those observed in the NPV and net cash flow assessments. As the share of capacity reserved for imbalance management increases, PBT also increases, which is an expected outcome given the corresponding decline in NPV and net cash flow. Additionally, as identified in the NPV analysis, PBT increases at an accelerated rate with an increasing imbalance share. This is more pronounced for the larger BESS size, indicating greater sensitivity of PBT to imbalance management in larger systems.

In the FI bidding zone, all scenarios result in payback periods within the operational lifetime of the BESS, indicating profitable investments. This contrasts with the NPV results for the 100% imbalance management scenarios, which showed negative or marginal profitability. This difference is a result of that PBT analysis does not consider the time value of money, whereas NPV discounts future revenues, making it less favourable for scenarios with longer lifetimes. In FI, the scenarios with 0%, 30% and 70% imbalance management shares all show fast payback times of under three years, with the shortest in the solely market participation scenario. These values are significantly below the simulated operational lifetimes of the systems.

For SE2 and NO4, the results similarly reflect the NPV findings, which resulted in that the scenarios based solely on imbalance management are unprofitable for both BESS sizes, as they do not achieve payback within the BESS lifetime. In SE2, all other scenarios yield PBTs below five years, which remains clearly inside the expected operation lifetimes. Although SE2 generally shows slightly longer PBTs than FI, the 20 MWh system with 0% imbalance management share performs marginally better. In contrast, NO4 exhibits the longest PBTs. Only the 0% and 30% imbalance management scenarios result in PBTs below six years, and only the 20 MWh system achieves payback in the 70% scenario with a PBT of 8.5 years. All other NO4 scenarios fail to earn back the investment within the systems lifetime. Even at low imbalance shares, NO4 maintains higher PBTs than FI and SE2, with its 0% imbalance scenario performing worse than the 70% scenarios in the other bidding zones.

Overall, the PBT analysis confirms same ranking as the NPV analysis, with FI offering the strongest economic cases for BESS investments, followed by SE2 and NO4. Notably, all scenarios with an imbalance management share of 70% or less, except for the 40 MWh system in NO4, achieve payback significantly earlier than the end of the asset's lifetime. Especially in FI and SE2, the PBTs are less than half of the operational lifetimes. The most favourable outcomes are seen in the market-only scenarios with a BESS size of 20 MWh, yielding PBTs of under one year in FI and SE2, and under three years in NO4.

7.3 Results of Imbalance Correction

In the previous chapter, the overall profitability of BESS investments was assessed, showing that lower capacity reserved for imbalance management led to higher profitability. However, this section further investigates how co-locating a BESS with the WPPs influences imbalance volumes and costs. As a reminder, the hourly-level imbalance data provided by Fortum have been anonymised with a random adjustment between -3% and 6% for each hourly value, meaning the results do not reflect the actual imbalance performance of the WPPs.

Figure 57 illustrates the hourly and cumulative imbalance costs for the Kalax WPP in the FI bidding zone during 2024, comparing scenarios with a 40 MWh BESS without imbalance correction and with 70% and 100% of the capacity reserved for imbalance management. Figure 58 presents similar results for SE2, comparing 20 MWh and 40 MWh BESS systems with a 70% imbalance management share. In the uncorrected scenarios, imbalance costs consists only of imbalance prices, whereas in the corrected scenarios, cost reductions are aggregated from savings in imbalance prices as well as savings in imbalance and transmission fees.

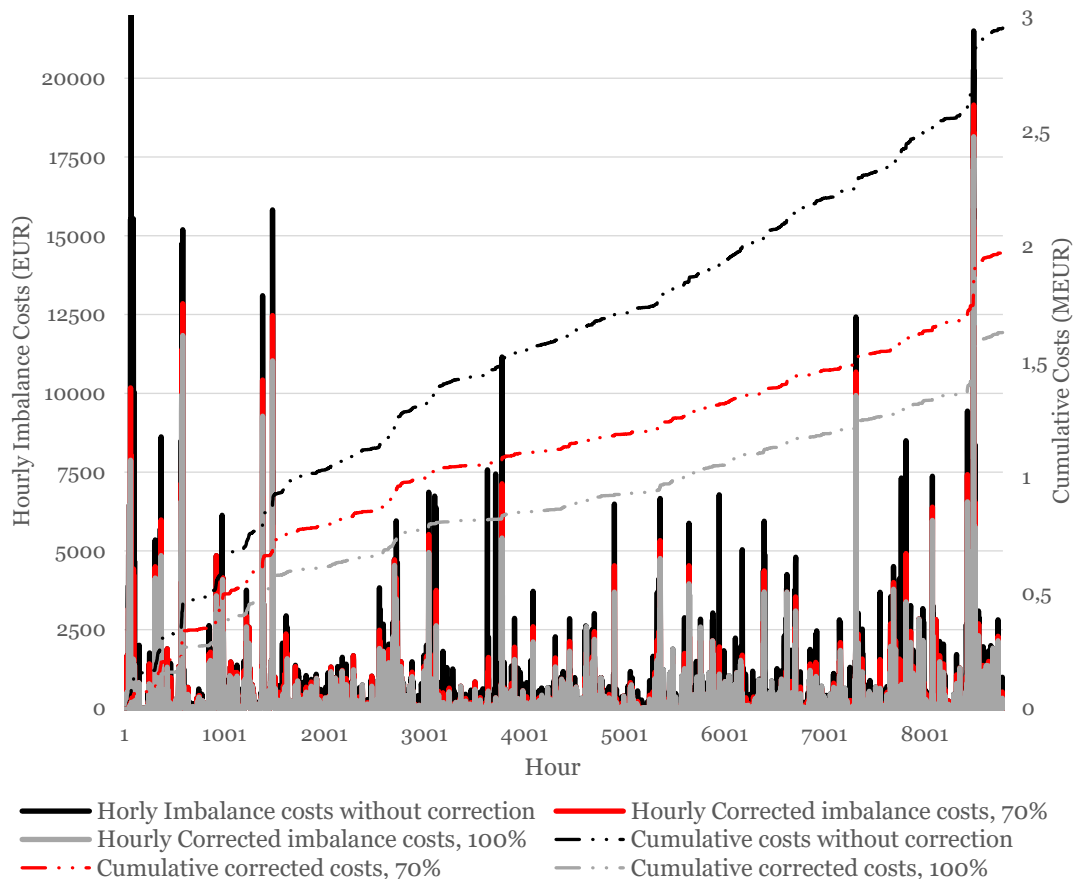


Figure 57, Hourly and cumulative imbalance costs for Kalax WPP in 2024 with and without 40 MWh BESS correction

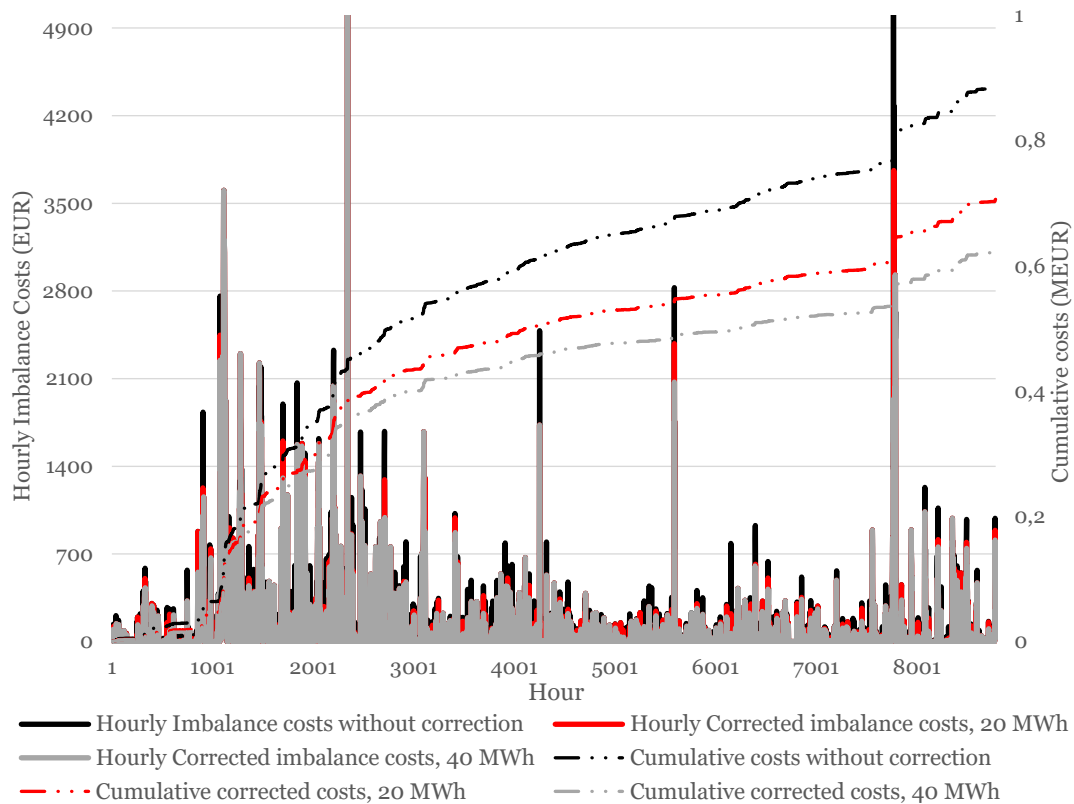


Figure 58, Hourly and cumulative imbalance costs for Solberg WPP in 2024 without and with a BESS with 70% imbalance management share

The figures show that reserving 70% of BESS capacity for imbalance management is sufficient to significantly reduce extreme imbalance cost spike hours. This is particularly pronounced for the Kalax WPP in FI, where high-cost imbalance hours are notably more frequent than for SE2 and NO4. In 2024, Kalax had 80 hours with imbalance costs exceeding 5000 EUR per hour, comparable to only 2 such hours for Solberg and none for Sør fjord. This difference is primarily driven by the higher imbalance prices in FI. Furthermore, the scenario with 100% capacity reserved for imbalance management in FI can mitigate these cost spikes even more effectively.

In SE2, the 40 MWh system have greater imbalance cost reductions compared to the smaller 20 MWh system. However, this is less pronounced during cost spike hours than the reduction difference observed between the 70% and 100% imbalance share scenarios in FI. This is primarily due to the same 10 MW power rating for both BESS configurations, which limits the maximum charge and discharge capacity per hour regardless of energy capacity. While increasing the energy capacity does not affect the possible hourly output and input, it enhances its ability to manage imbalances over consecutive hours, offering better flexibility.

The significant reduction in imbalance cost spikes compared to other hours indicate that BESS operation is most impactful during periods of high imbalance related costs, which occur when imbalance volumes and prices are high. For instance, in *Figure 57* for Kalax WPP, the period between hours 60 to 68 shows exceptionally high imbalance costs. Within this range, the highest single hour cost reaches 28070 EUR, which is considerably reduced in both BESS scenarios. The costs are reduced to 8025 EUR with a 70% imbalance management share and to 1276 EUR in the 100% scenario. Since the optimisation prioritises allocating BESS capacity to this critical hour, the surrounding high-cost hours receive less correction. Additionally, significant reductions can also be observed at hour 3712, where the costs are reduced from 7440 EUR to 338 EUR in both the 70% and 100% scenarios.

Imbalance mitigation during non-spike hours is notably less significant. For instance, in Kalax, from hour 1600 to 3000, cost reduction are modest in both 70% and 100% scenarios, especially when compared to reductions during cost spikes. During these 1400 hours, the cost savings are 76191 EUR for the 70% scenario, and 123992 EUR for the 100% scenario. In SE2, the difference between the 20 MWh and 40 MWh systems is minor during low-cost periods, such as hours 3800 to 4800 in *Figure 58*. Cost savings for the 20 MWh system is 20390 EUR, and for the 40 MWh system 29065 EUR for these 1000 hours, resulting in slightly improved cost reductions for the larger system.

Reserving a fixed share of BESS capacity for imbalance management proves effective reduction in cost spikes during high-cost hours, but offers limited value during periods with low imbalance costs. Because the reserved capacity is fixed, it remains allocated to imbalance management even when the economic value is minimal, resulting in underutilisation of the BESS during low-value hours for imbalance management. A more dynamic operation strategy, where capacity is allocated based on market conditions instead of fixed shares, could enhance overall performance. This approach would allow the BESS to respond to high-cost imbalance hours, without reserving fixed capacities for imbalance management for low-cost hours.

A summary of imbalance correction results for each scenario is presented in *Table 22*. It provides the percentages of imbalance volumes and costs remaining relative to the uncorrected values. These percentages indicates how much of the original imbalance volumes or costs remain after correction.

*Table 22, Remaining imbalance volumes and costs after correction
(% of uncorrected values)*

		30%			70%			100%		
		FI	SE2	NO4	FI	SE2	NO4	FI	SE2	NO4
20 MWh	Positive imbalance volume (%)	95.5	97.7	99.0	93.2	95.6	97.8	95.2	95.3	97.0
	Negative imbalance volume (%)	92.2	90.7	93.7	86.9	85.1	90.8	78.3	74.1	84.8
	Imbalance costs (%)	85.5	87.5	91.5	74.6	79.6	86.9	65.2	65.5	79.0
40 MWh	Positive imbalance volume (%)	93.0	96.5	98.1	89.2	93.3	96.2	92.4	92.9	95.4
	Negative imbalance volume (%)	87.9	84.0	89.4	80.4	76.9	85.5	68.7	63.1	77.3
	Imbalance costs (%)	80.7	80.2	86.5	67.0	70.3	80.4	55.2	53.6	70.0

As the share of capacity reserved for imbalance management increases, positive corrected imbalance volumes show only minor changes across both BESS sizes. The largest change occurs in the 40 MWh system for FI, where the positive imbalance volumes decrease by 3.8 percentage points when increasing the reserved share from 30% to 70%. Increasing the energy capacity from 20 MWh to 40 MWh leads similarly to only slight improvements in correcting positive imbalance volumes. In contrast, negative corrected imbalance volumes are significantly more affected by both increased imbalance management share and larger energy capacity. In all scenarios, negative imbalance volumes are reduced, with the most notable improvements occurring when the reserved share increases from 70% to 100%. When comparing the WPPs, Kalax experiences greater reductions in positive imbalance volumes than Solberg or Sør fjord across all scenarios. Solberg shows the largest reductions in negative imbalance volumes.

The optimiser prioritises reducing negative imbalance volumes by discharging rather than positive imbalance volumes by charging, primarily due to the higher cost-saving potential associated with negative imbalances. For Kalax, 88.8% of the total imbalance costs result from negative imbalances in the uncorrected case. The share for Solberg and Sør fjord are even higher, at 92.0% and 97.5%, respectively. Therefore, negative imbalance volumes, combined with their associated prices, lead to significantly higher costs than positive imbalances.

Across all scenarios, the results show that increasing the share of BESS capacity reserved for imbalance management leads to greater reductions in imbalance-related costs. Importantly, the cost reductions are greater than the reductions in imbalance volumes. This is because the optimiser prioritises reducing costs rather than imbalance volumes. As a result, even small reductions in volume during peak pricing periods can lead to significant cost savings.

The cost reduction results vary between bidding zones. In FI, the largest cost reductions occurs for the 40 MWh system when the reserved capacity increases from 30% to 70%, resulting in 13.7 percentage point reduction. The increase from 70% to 100% results in a slightly smaller reduction of 11.8 percentage points. In contrast, in SE2 and NO4, the opposite trend is observed, where the most significant improvements occur when increasing the imbalance share from 70% to 100%. The highest cost reduction ratio for all scenarios and bidding zones is for SE2, under the 100% imbalance management scenario with the 40 MWh system, where costs are reduced to 53.6% of the uncorrected values. However, as discussed in *Chapter 7.2.2*, this scenario is not the most profitable in terms of monetary value, as FI shows greater overall monetary savings despite slightly higher remaining cost ratios.

When comparing system sizes, the 40 MWh BESS consistently outperforms the 20 MWh system. Moreover, the gap in cost savings between the two sizes increases as the imbalance management share increases. For instance, in the FI 70% scenario, the 40 MWh system achieves a 7.6 percentage point greater reduction in costs than the 20 MWh system. The improved performance of the larger system is primarily due to its greater energy capacity, which enables it to handle longer or more frequent imbalance volumes. Overall, the best relative cost savings are achieved in FI and SE, while NO4 shows more modest reductions across all scenarios.

Imbalance prices play a critical role in determining the overall profitability of a BESS investment, which has explained why imbalance management has been more profitable in the simulated FI scenarios than in SE2 or NO4. These simulations have used imbalance price data exclusively for the year 2024, and results may vary if data from other years were considered. A comparison with 2023 shows that average positive imbalance prices were slightly lower in FI, while they were 45% higher in SE2, and 30% higher in NO4. The corresponding absolute values of average negative imbalance prices in 2023 were significantly higher with increases of 38% in FI, 167% in SE2, and 203% in NO4.

By comparison with 2025 prices, based on data available until August 4th, the average positive imbalance prices were 20% higher in FI compared to the same period in 2024, while SE2 and NO4 experienced slightly lower averages. However, negative imbalance prices increased considerably, with absolute values rising by 120% in FI, 257% in SE2 and 137% in NO4. The future variations in imbalance prices will have a significant influence on how BESS should be operated for imbalance management. *Chapter 7.4* will explore this further through sensitivity analysis, focusing on how changes in imbalance prices and market prices affect BESS profitability.

7.4 Sensitivity Analysis

This sensitivity analysis investigates how variations in imbalance prices and market prices affects the NPV of the scenarios. These factors are analysed, as they are uncertain and volatile, which affect the potential profitability and risks associated with BESS investments. In contrast, key BESS parameters such as CAPEX, efficiency, and EoL SoH have shown steady improvements over time, and are therefore considered more predictable. The impact of energy capacity has already been assessed through a comparison between the 20 MWh and 40 MWh BESS sizes. *Figure 59* presents the results of the sensitivity analysis on imbalance prices, showing how an increase, up to 100%, impacts the NPV of scenarios involving solely imbalance management.

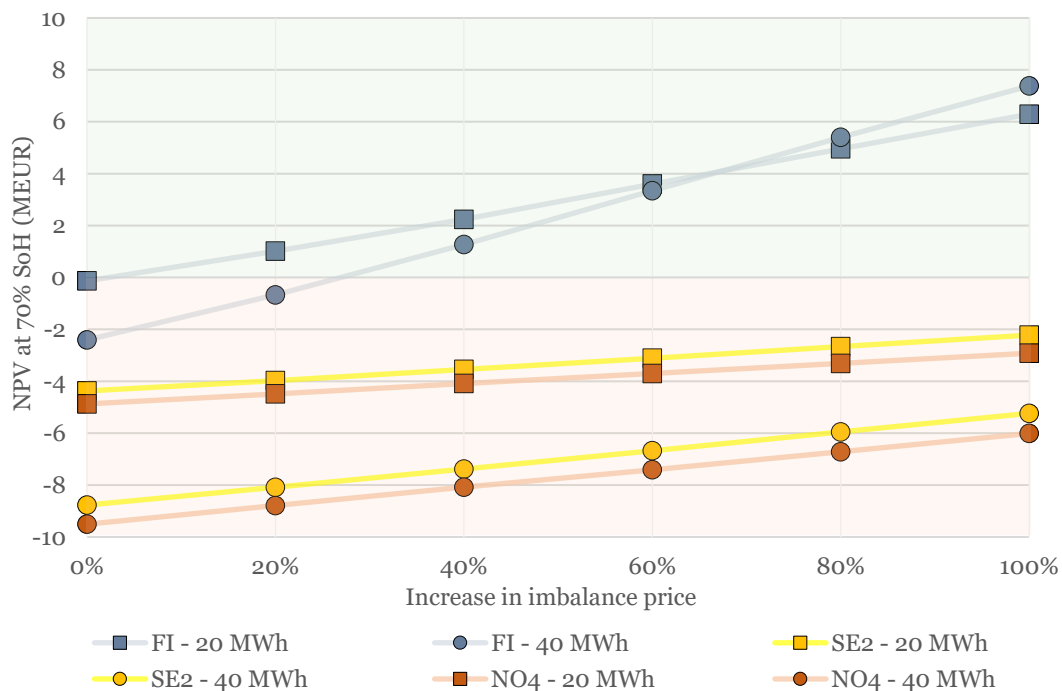


Figure 59, Impact of increased imbalance prices on NPV for scenarios with solely imbalance management

For all bidding zones and BESS sizes, the results show a clear linear increase in NPV as the imbalance prices are increased. The 40 MWh BESS shows a steeper growth in NPV compared to the 20 MWh system, indicating an enhanced benefit of increased prices for larger BESS sizes. FI bidding zone exhibits the most notable improvement compared to SE2 and NO4, due to its high starting imbalance prices. In the FI scenario with a 20 MWh system, the NPV is only slightly negative at the base price level, and even a small price increase results in a positive value. For the 40 MWh system, the NPV turns positive at approximately 27% increase in imbalance prices. The highest NPV in FI is achieved with the 40 MWh system and a 100% price increase, reaching nearly 8 MEUR.

SE2 and NO4 show similar trends, with significantly smaller increases in NPV compared to FI. In all scenarios, the NPV remains negative. The highest NPV for SE2, at below -2 MEUR, is achieved with the 20 MWh scenario, at a 100% increase in imbalance prices. These results indicates that even a major increase in imbalance prices in SE2 and NO4 would not be sufficient to make solely imbalance management a profitable investment in these scenarios.

A change in market prices presents a major risk to the profitability of a BESS investment. The impact of decreased market prices on NPV will be evaluated for the 40 MWh scenarios, where 30% of the capacity is reserved for imbalance management. The sensitivity analysis focuses exclusively on the capacity markets, while the energy market prices and imbalance prices remain unchanged. The reason for only decreasing capacity market prices, is due to their higher significance on overall net cash flow, and to achieve a more varying market allocation across scenarios. A gradual price reduction of up to 50% is considered. *Figure 60* presents the results, illustrating how decreasing capacity market prices affect the NPV under these conditions.

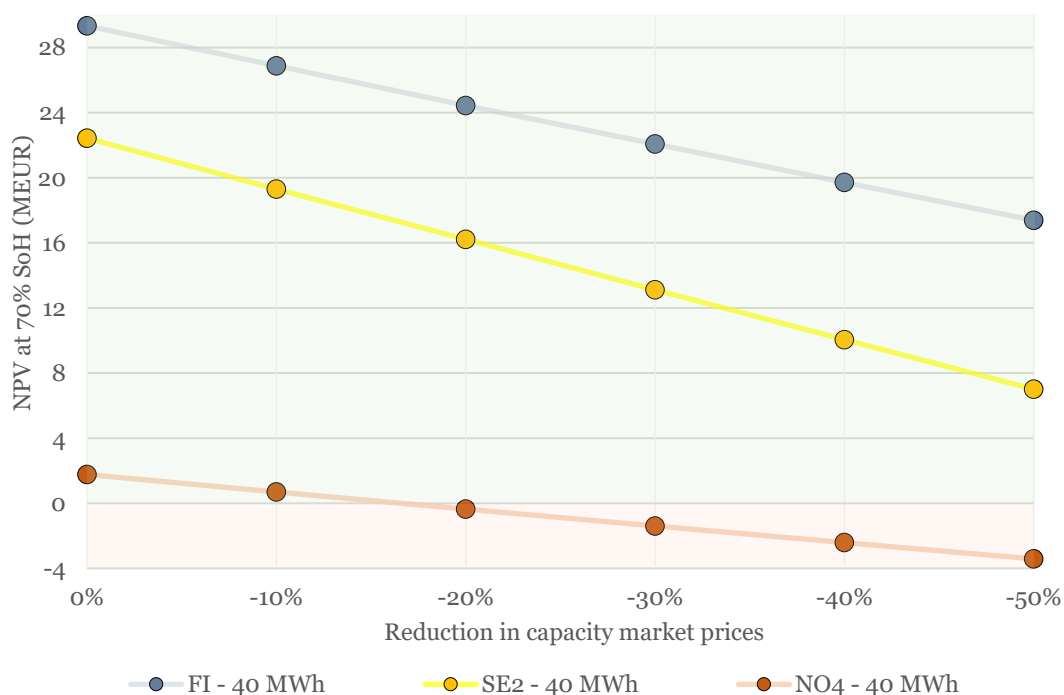


Figure 60, Impact of decreased capacity market prices on NPV for the 30% imbalance share scenarios with 40 MWh BESS

A reduction in capacity market prices results to approximately a linear decline in NPV across all scenarios. The most notably decline is observed in SE2, highlighting the high revenue share from capacity markets. In contrast, NO4 shows the mildest decrease, due to the already low starting point prices. The impact on FI is milder than in SE2, as a high share of its value is also generated from energy-based markets and imbalance management. Even though the decrease, both FI and SE show positive NPVs across the range of this sensitivity analysis, even with a 50% reduction in capacity market prices. At this level of price reduction, the NPV decreases in FI by 40.7%, while SE2 shows a larger drop of 68.8%. In NO4, the initial NPV of 1.8 MEUR turns negative when the capacity market prices are reduced by more than 17%. At 50% price reduction, NO4 reaches a negative NPV of -3.4 MEUR.

This sensitivity analysis highlights that when the majority of value is generated from a specific source, such as capacity markets or imbalance management, the investment becomes more sensitive to fluctuations in that specific market. In contrast, by allocating value creation across multiple revenue streams helps mitigate the risks associated with price uncertainty. This highlights the importance of diversifying value across different sources, as it improves investment stability and reduces dependency on single markets.

8 Conclusions and Future Research

In the Nordic countries, the growing share of wind power in the electricity mix increases system imbalances, as actual production and forecasted production of wind power are not aligned. At the same time, the trend of declining battery system costs have supported more BESS investments, particularly for operation in electricity and reserve markets. However, BESS can also be used for imbalance management for individual WPPs, reducing overall system imbalances and potentially improving WPP profitability by mitigating imbalance-related costs. Regardless of this potential, little public research has examined the simultaneous operation of BESS for both imbalance management and market participation within the Nordic market environment.

This thesis researched the investment potential of co-located BESS by analysing operation in multi-market optimisation, while also providing imbalance management for a WPP. The primary objective was to determine the optimal BESS capacity allocation between imbalance management and market participation to achieve the highest profitability. In other words, the influence of imbalance management on BESS profitability was examined. Secondary objectives included identifying the most value generating markets, and assessing if imbalance management alone could be profitable without market participation.

The empirical study was conducted as a quantitative mathematical simulation model using a mixed-integer programming optimiser implemented in Python. Simulations were performed for the FI, SE2, and NO4 bidding zones, with representative WPPs of Kalax, Solberg, and Sørkjord, respectively. Each site was modelled with 10 MW BESS, and energy capacities of 20 MWh and 40 MWh. Scenarios with BESS capacity reserved for imbalance management at 0%, 30%, 70%, and 100% shares were assessed, with the remaining share allocated to market participation. Markets considered included DA, ID, FCR-N, FCR-D, aFRR CM and EAM, as well as mFRR CM and EAM. Long-term profitability was evaluated utilising 2024 market data. The model included a Li-Ion battery, considering battery degradation and other technical characteristics. Cost components included transmission and imbalance fees, CAPEX, and O&M costs.

The results presented in this thesis indicate that operating a BESS simultaneously in imbalance management and market participation leads to decreased imbalance-related cost as the capacity reserved for imbalance management increases. However, the trade-off of reduced capacity available for market participation results in a greater loss of market revenues, which is not fully compensated by imbalance cost savings, suggesting that market revenues remain overall more financially attractive than imbalance cost savings. The findings in this thesis suggest that reserving less capacity for imbalance

management improves profitability. The highest NPV for each bidding zone and BESS size was observed in scenarios where all capacity was allocated to market participation. Additionally, NPV showed accelerated decline rate as the share of imbalance management increased. However, scenarios with 30% and 70% reserved capacities in FI and SE2 bidding zones still proved favourable NPVs. This indicates that although reserving a fixed share of BESS capacity for imbalance management reduces potential profitability, the investment can still remain financially viable.

The analysis of managing imbalances for the WPPs showed that a BESS has most potential to reduce imbalance cost spikes, which occur during periods of high imbalance prices. However, less value was generated during periods without cost spikes. This resulted in limited overall value generation, as reserving fixed capacity for imbalance management during low imbalance cost periods reduced the capacity available for market participation, which generally offered better value. Among the bidding zones, FI showed the greatest value for managing imbalances, followed by SE2, while NO4 showed the lowest profitability. In all scenarios where 100% of the capacity was reserved for imbalance management resulted in negative NPVs, except for the 20 MWh system in FI, which showed only slightly positive NPV. Therefore, solely relying on imbalance management proved to be unprofitable within the scope of this thesis.

The analysis of market-specific cash flows revealed that most value was generated in capacity markets, although the dominant markets varied across bidding zones. In SE2, the FCR-D down-regulation market contributed the largest share of net cash flow, while in NO4, the FCR-N market was the most dominant. Both bidding zones showed low diversification of value generation, as these specific markets accounted for the majority of revenues. In contrast, FI demonstrated a more even distribution of net cash flow, with no single market excessively dominating. Such diversification of revenue streams reduces the risk of profitability loss due to specific market saturation or price declines, making FI in comparison less risky for BESS investments.

By comparing the 20 MWh and 40 MWh systems showed that the larger system achieved greater value generation in energy-based markets and imbalance management. Its advantage over the 20 MWh system increased as less capacity was reserved for imbalance management. Conversely, the profitability of the 20 MWh system exceeded that of the 40 MWh system, as a larger share of capacity was allocated to imbalance management. From an operational perspective, increasing the capacity reserved for imbalance management reduced the number of charging-discharging cycles, thereby decreasing battery degradation and extending the operational lifetime.

This thesis has certain methodological limitations. The primary limitation is the deterministic approach, in which all market prices and volumes were known in advance, which does not accurately reflect the real-world conditions. An improvement to the simulation would involve using historical forecasted market data for bidding BESS capacity, while relying actual activations and cash flows according to historical realised prices and volumes. This approach would provide a more realistic evaluation of profitability by accounting for capacities that are not accepted in the markets, resulting in lost revenue opportunities, as well as potential penalties for non-deliveries. In other words, bids would be made based on forecasted data, whereas realised prices and volumes would reflect actual market outcomes. The deterministic approach in this thesis estimates the maximum possible value, assuming perfect foresight of prices and volumes.

Another key limitation includes the reliance on 2024 data applied in a repeatable manner. Consequently, the results presented reflect only to the performance in 2024 and may not represent the future value of BESS without utilising long-term data or forecasts. Furthermore, the simulation assumes a one-hour MTU for simplification, while some markets in 2024 operated with a 15-minute interval. In future, most markets will operate with the shorter MTU, which allows for further research when 15-minute market data becomes available for longer periods. This ongoing transition may influence the attractiveness of certain markets, and change strategies for multi-market optimisation. Additionally, the simulation does not consider FCR-D activations affecting the SoC, although in reality, these small activations would have impact on the SoC.

For future research, a similar study could be conducted with modifications to the simulation. Unlike this study, which used fixed reserved capacities for imbalance management that cannot be used in market participation, a more realistic approach would allow dynamic capacity allocation. This approach allocates capacity based on the expected value of each market or imbalance management, without fixed reservations.

Additionally, this simulation performed optimisation on a daily basis without accounting for following days. An improvement would be to extend the optimisation horizon to longer periods, such as few days or one week. Furthermore, with the expected increase in imbalance volumes in the system, annual fluctuations in imbalances and market prices, and the continuing decline in BESS costs attracting greater interest from investors, these factors highlight the need for updated research using recent data to provide accurate and updated insights into BESS profitability.

References

Ali, H., Beltran, H., Lindsey, N.J. and Pecht, M. (2023). *Assessment of the calendar aging of lithium-ion batteries for a long-term—Space missions*. *Frontiers in Energy Research*, 11. doi:<https://doi.org/10.3389/fenrg.2023.1108269>

Ampowr. (2025). *Battery Energy Storage Systems for Wind Turbines*. Ampowr. [online] Available at: https://ampowr.com/energy-storage-systems-wind-turbines/#toc_Compressed_Air_Energy_Storage [Accessed 22 May 2025]

Andersen, L. (2025). *E-mail conversation*. Statnett. 4 April 2025

Andrew, J. (2019). *Fundamentals of wind turbines*. Available at: https://energycentral.com/system/files/ece/nodes/375803/tlt_08-19_webinars.pdf [Accessed 4 June 2025]

Apata, O. (2023). *Overview of Current Development and Research Trends in Energy Storage Technologies*. pp.1–22. In: *Energy Storage Technologies in Grid Modernization*. doi:<https://doi.org/10.1002/9781119872146.ch1>

Aurora. (2025). *Nordic battery boom: Powering growth amid saturation risks*. Online Report. Available at: <https://auroraer.com/resources/webinar/nordics-battery-boom> [Accessed 22 May 2025]

Battery University. (2023). *BU-205: Types of Lithium-ion*. Battery University. [online] Available at: <https://batteryuniversity.com/article/bu-205-types-of-lithium-ion> [Accessed 28 April 2025]

Bhutada, G. (2023). *The Six Major Types of Lithium-ion Batteries: A Visual Comparison*. Elements by Visual Capitalist. [online] Available at: <https://elements.visualcapitalist.com/the-six-major-types-of-lithium-ion-batteries/> [Accessed 29 April 2025]

Bjellerup, V. (2025). *E-mail conversation*. Svenska Kraftnät. 9 April 2025

Blake Clough Consulting. (2025). *Co-Located BESS and Renewables - Advantages and Risks*. Blake Clough Consulting. [online]. Available at: <https://www.blakeclough.com/co-located-bess-and-renewables-advantages-and-risks/> [Accessed 23 May 2025]

Bush, J. (2023). *Trading in the continuous intraday market: how does it work?*. Modo Energy. [online] Available at: <https://modoenergy.com/research/continuous-intraday-trading-wholesale-epex-n2ex-volume-battery-energy-storage-prices> [Accessed 11 March 2025]

Charles River Associates. (2023). *Unlocking the Potential: Navigating Key Considerations in Battery Energy Storage System for Business Cases*. CRA. Available at: https://media.crai.com/wp-content/uploads/2023/10/28100955/20230921_BESS-Business-Case-and-Revenue-Generation_FINAL.pdf [Accessed 9 May 2025]

Chen, Z., Li, Z., and Chen, G. (2023). *Optimal configuration and operation for user-side energy storage considering lithium-ion battery degradation*. International Journal of Electrical Power & Energy Systems. 145, pp.108621–108621. doi:<https://doi.org/10.1016/j.ijepes.2022.108621>

Choi, D., et al. (2021). *Li-ion battery technology for grid application*. Journal of Power Sources. 511, p.230419. doi:<https://doi.org/10.1016/j.jpowsour.2021.230419>

Claire, A. (2025). *Understanding BESS Specifications: Key Factors to Consider*. Sinovoltaics.com. [online] Available at: <https://sinovoltaics.com/energy-storage/storage/understanding-bess-specifications-key-factors-to-consider/> [Accessed 6 May 2025]

Collath, N., Tepe, B., Englberger, S., Jossen, A. and Hesse, H. (2022). *Aging aware operation of lithium-ion battery energy storage systems: A review*. Journal of Energy Storage, [online] 55, p.105634. doi:<https://doi.org/10.1016/j.est.2022.105634>

Cristea, M., Tîrnovan, R.-A., Cristea, C. and Făgărășan, C. (2022). *Levelized cost of storage (LCOS) analysis of BESSs in Romania*. Sustainable Energy Technologies and Assessments, 53, p.102633. doi:<https://doi.org/10.1016/j.seta.2022.102633>

Dai, H., Li, N., Wang, Y. and Zhao, X. (2022). *The Analysis of Three Main Investment Criteria: NPV IRR and Payback Period*. [online] Advances in Economics, Business and Management Research. doi:<https://doi.org/10.2991/aebmr.k.220307.028>

de Siqueira, L.M.S. and Peng, W. (2021). *Control strategy to smooth wind power output using battery energy storage system: A review*. Journal of Energy Storage, 35, p.102252. doi:<https://doi.org/10.1016/j.est.2021.102252>

Dhananjay, K.R., et al. (2023). *Performance Analysis of Lithium-Ion Battery Considering Round Trip Efficiency*. IEEE 2nd International Conference on Industrial Electronics. doi:<https://doi.org/10.1109/icidea59866.2023.10295170>

ECA. (2021). *Fast & furious: fast frequency response services as the key to rev up battery investments*. ECA UK - Economic Consulting Associates. Eca-uk.com. [online]. Available at: <https://www.eca-uk.com/2021/11/29/fast-furious-fast-frequency-response-services-as-the-key-to-rev-up-battery-investments/> [Accessed 22 May 2025]

ECB. (2025). *Currency converter*. ECB Data Portal. [online] Available at: <https://data.ecb.europa.eu/currency-converter>

Edge, J.S., et al. (2021). *Lithium ion battery degradation: what you need to know*. Physical Chemistry Chemical Physics. 23(14), pp.8200–8221. doi:<https://doi.org/10.1039/d1cp00359c>

Energiategollisuus. (2024). *Sähkön hintatilasto*. [online] Available at: <https://energia.fi/tilastot/sahkotilastot/sahkon-hintatilasto/> [Accessed 12 August 2025]

Energiategollisuus. (2025). *Sähköä riittää, talouskasvua ei kannata pelätä*. [online] Available at: <https://energia.fi/tiedotteet/sahkoa-riittaa-talouskasvua-ei-kannata-pelata/> [Accessed 12 August 2025]

Energiforsk. (2025). *Så får industrin tillräckligt med el till 2035*. [online] ISBN: 978-91-89918-16-0. Available at: <https://energiforsk.se/media/34416/2025-1113-sa-far-industrin-tillrackligt-med-el-till-2035.pdf> [Accessed 12 August 2025]

Energinet., et al. (2023). *Wind and Solar in the Nordic Reserve Markets – Challenges and Possibilities of Weather Dependent Production*. Available at: <https://www.statnett.no/globalassets/for-aktorer-i-kraftsystemet/market/reservemarkeder/nordic-wind-and-solar-publication-.pdf> [Accessed 31 March 2025]

ENTSO-E. (2019). *Fast Frequency Reserve – Solution to the Nordic inertia challenge*. Available at: <https://www.epressi.com/media/userfiles/107305/1576157646/fast-frequency-reserve-solution-to-the-nordic-inertia-challenge-1.pdf> [Accessed 3 April 2025]

ENTSO-E. (2021). *Technical Requirements for Fast Frequency Reserve Provision in the Nordic Synchronous Area – External document*. Version 1.1. Available at: <https://www.svk.se/siteassets/english/stakeholder-portal/prequalification/technical-requirements-for-ffr-v1.1.pdf> [Accessed 3 April 2025]

ENTSO-E. (2023a). *Technical Requirements for Frequency Containment Reserve Provision in the Nordic Synchronous Area*. Available at: <https://www.svk.se/siteassets/aktorsportalen/bidra-med-reserver/om-olika-reserver/fcr/fcr-technical-requirements-may-23.pdf> [Accessed 30 March 2025]

ENTSO-E. (2023b). *Imbalance: Imbalance Volumes and Prices*. [online] Available at: https://transparency.entsoe.eu/content/static_content/Static%20content/knowledge%20base/data-views/balancing/Data-view%20Imbalance.html [Accessed 17 April 2025]

ENTSO-E. (2024a). *Overview of Frequency Control in the Nordic Power System*. Available at: https://eepublicdownloads.blob.core.windows.net/public-cdn-container/clean-documents/SOC%20documents/Nordic/2024/Overview_of_Frequency_Control_in_the_Nordic_Power_System.pdf [Accessed 30 March 2025]

ENTSO-E. (2024b). *Nordic Balancing Philosophy*. Available at: <https://www.fingrid.fi/globalassets/dokumentit/fi/tiedotteet/ajankoh-taista/nordic-balancing-philosophy-may24.pdf> [Accessed 8 April 2025]

ENTSO-E. (2024c). *Automatic Frequency Restoration Reserve Process – Implementation Guide*. Version 1.2. Available at: https://eepublicdownloads.entsoe.eu/clean-documents/EDI/Library/ERRP/Automatic_Frequency_Restoration_Reserve_Process_v1.2.pdf [Accessed 9 April 2025]

ENTSO-E. (2024d). *Common Platform for manually activated frequency restoration reserves- Implementation Guide*. Version 1.7. Available at: https://eepublicdownloads.entsoe.eu/clean-documents/EDI/Library/ERRP/Common_Platform_for_manually_activated_restoration_reserves_IG_v1.7.pdf [Accessed 9 April 2025]

ENTSO-E. (2025a). *ENTSO-E Transmission System Map*. [online] Available at: <https://www.entsoe.eu/data/map/> [Accessed 28 February 2025]

ENTSO-E. (2025b) *Single Intraday Coupling (SIDC)*. [online] Available at: https://www.entsoe.eu/network_codes/cacm/implementation/sidc/ [Accessed 11 March 2025]

ENTSO-E. (2025c). *The Nordic aFRR capacity markets*. [online] Available at: https://www.entsoe.eu/network_codes/eb/nordic-afrr-capacity-markets/ [Accessed 9 April 2025]

ENTSO-E. (2025d). *Actual Generation per Production Type*. Open Data. [online] Available at: <https://transparency.entsoe.eu/generation/r2/actualGenerationPerProductionType/show> [Accessed 4 June 2025]

ENTSO-E. (2025e). *Generation Forecasts for Wind and Solar*. Open Data. [online] Available at: <https://transparency.entsoe.eu/generation/r2/dayAhead-GenerationForecastWindAndSolar/show> [Accessed 4 June 2025]

ENTSO-E. (2025f.) *Accepted Offers and Activated Balancing Reserves (legacy)*. Open Data. [online] Available at: <https://transparency.entsoe.eu/balancing/r2/activationAndActivatedBalancingReserves/show> [Accessed 19 June 2025]

EPEX Spot. (2025a). *15-minute products in Market Coupling*. Epexspot.com [online] Available at: <https://www.epexspot.com/en/15-minute-products-market-coupling> [Accessed 15 August 2025]

EPEX Spot. (2025b). *Trading Products*. Epexspot.com [online] Available at: <https://www.epexspot.com/en/tradingproducts#intraday-trading> [Accessed 12 March 2025]

Erdozia, A., and Ferraris, A. (2017). *Benefit and value of Li-ion batteries in combination with large-scale renewable energy sources*. Aalto.fi. [online] Available at: <https://aaltodoc.aalto.fi/items/6f22410e-285a-45a1-a541-a20d72956ab5> [Accessed 22 May 2025]

eSett. (2021). *Single Balance Commissioning Plan*. Version 1.5. Available at: https://www.esett.com/app/uploads/2021/09/esett_single_balance_commissioning_plan_28.9.2021.pdf [Accessed 17 April 2025]

eSett. (2024). *Nordic Imbalance Settlement Handbook*. eSett.com. [online] Available at: <https://www.esett.com/handbook/> [Accessed 17 April 2025]

eSett. (2025a). *mFRR EAM*. eSett.com. [online] Available at: <https://www.esett.com/mfrr-eam/> [Accessed 9 April 2025]

eSett. (2025b). *eSett in Brief*. eSett.com. [online] Available at: <https://www.esett.com/about/esett-in-brief/> [Accessed 17 April 2025]

eSett. (2025c). *New Market Participants*. eSett.com. [online] Available at: <https://www.esett.com/customers/new-market-participants/> [Accessed 17 April 2025]

eSett. (2025d). *Imbalance Prices*. eSett.com. Open Data. [online] Available at: https://opendata.esett.com/prices_single [Accessed 4 May 2025]

eSett. (2025e). *Fees*. eSett.com. Open Data. [online] Available at: <https://opendata.esett.com/fees> [Accessed 4 June 2025]

Fan, F., et al. (2021). *Sizing and Coordination Strategies of Battery Energy Storage System Co-Located with Wind Farm: The UK Perspective*. *Energies*, 14(5), p.1439. doi:<https://doi.org/10.3390/en14051439>

Feehally., et al. (2018). *Efficiency Analysis of a High Power Grid-connected Battery Energy Storage System*. *Materials Today: Proceedings*, 5(11), pp.22811–22818. doi:<https://doi.org/10.1016/j.matpr.2018.07.095>

Fingrid. (2016). *Electricity market needs fixing – What can we do?*. Available at: <https://www.fingrid.fi/globalassets/dokumentit/en/electricity-market/development-projects/fingrid-electricity-market-needs-fixing-2016-web.pdf> [Accessed 7 March 2025]

Fingrid. (2022). *Tuulivoiman osallistuminen reservimarkkinoille*. Available at: <https://www.fingrid.fi/globalassets/dokumentit/fi/sahkomarkkinat/reservit/tuulivoima-reservimarkkinoilla.pdf> [Accessed 19 May 2025]

Fingrid. (2024a). *Bidding FCR, Implementation guide*. Version 2.16. Available at <https://www.fingrid.fi/globalassets/dokumentit/fi/sahkomarkkinat/reservit/implementation-guide-fcr-2.16.pdf> [Accessed 31 March 2025]

Fingrid. (2024b). *Ehdot ja edellytykset nopean taajuusreservin (FFR) toimittajalle*. Available at: <https://www.fingrid.fi/globalassets/dokumentit/fi/sahkomarkkinat/reservit/reservitoimittajien-FFR-ehdot-ja-edellytykset.pdf> [Accessed 4 April 2025]

Fingrid. (2024c). *BSP – Implementation Guide – aFRR energy market*. Version 1.1 Available at: <https://www.fingrid.fi/globalassets/dokumentit/fi/sahkomarkkinat/reservit/implementation-guide-afrr-energy-activation-market.pdf> [Accessed 11 April 2025]

Fingrid. (2025a). *Part of the Nordic power system*. Fingrid.fi. [online] Available at: <https://www.fingrid.fi/en/grid/development/part-of-the-nordic-power-system/> [Accessed 28 February 2025]

Fingrid. (2025b). *Inertia of the Nordic power system*. Fingrid.fi. [online] Available at: <https://www.fingrid.fi/en/electricity-market-information/InertiaofNordicpowersystem/> [Accessed 28 February 2025]

Fingrid. (2025c). *Markkinapaikat*. Fingrid.fi. [online] Available at: <https://www.fingrid.fi/sahkomarkkinat/markkinoiden-yhtenaisyyys/johdanto-sahkomarkkinoihin/> [Accessed 7 March 2025]

Fingrid. (2025d). *FCR, Taajuusohjattu käyttö- ja häiriöreservi*. Fingrid.fi. [online] Available at: <https://www.fingrid.fi/sahkomarkkinat/reservit-ja-saatosahko/taajuusohjattu-kaytto--ja-hairioreservi/> [Accessed 30 March 2025]

Fingrid. (2025e). *Ehdot ja edellytykset taajuuden vakautusreservin (FCR) toimittajalle*. Available at: https://www.fingrid.fi/globalassets/dokumentit/fi/sahkomarkkinat/reservit/liite-1-fcr-ehdot-2025_2.pdf [Accessed 31 March 2025]

Fingrid. (2025f). *Taajuusohjattu käyttö- ja häiriöreservi (FCR-N, FCR-D ylös ja FCR-D alas), vuosimarkkinahankinta ja toteutuneet tuntikaupat*. Fingrid.fi. [online] Available at: <https://www.fingrid.fi/sahkomarkkinainformaatio/reservimarkkinainformaatio/Taajuusohjattu-kaytto-ja-hairioreservi-vuosimarkkinahankinta-ja-toteutuneet-tuntikaupat/> [Accessed 31 March 2025]

Fingrid. (2025g). *FFR, Nopea taajuusreservi*. Fingrid.fi. [online] Available at: <https://www.fingrid.fi/sahkomarkkinat/reservit-ja-saatosahko/nopea-taajuusreservi/> [Accessed 3 April 2025]

Fingrid. (2025h). *aFRR-reservin eurooppalainen markkinapaikka PICASSO*. Fingrid.fi. [online] Available at: <https://www.fingrid.fi/sahkomarkkinat/markkinoiden-yhtenaisyyys/pohjoismainen-tasehallinta/picasso/> [Accessed 11 April 2025]

Fingrid. (2025i). *mFRR, manuaalinen taajuuden palautusreservi*. Fingrid.fi. [online] Available at: <https://www.fingrid.fi/sahkomarkkinat/reservit/reservituotteet-ja-markkinoille-osallistuminen/mfrr-manuaalinen-taajuuden-palautusreservi/> [Accessed 14 April 2025]

Fingrid. (2025j). *Description of balance model*. Fingrid.fi. [online] Available at: <https://www.fingrid.fi/en/electricity-market/balance-service/description-of-balance-model/> [Accessed 17 April 2025]

Fingrid. (2025k). *Wind power generation*. Fingrid.fi. [online] Available at: <https://www.fingrid.fi/en/electricity-market-information/wind-power-generation/> [Accessed 19 May 2025]

Fingrid. (2025l). *Datasets / Download datasets*. Fingrid.fi. Datasets. [online] Available at: <https://data.fingrid.fi/en/data>

Fingrid. (2025m). *Main grid contract and service fees*. Fingrid.fi. [online] Available at: <https://www.fingrid.fi/en/grid/grid-connection-agreement-phases/main-grid-contract-and-service-fees/#service-fees> [Accessed 23 June 2025]

Fortum. (2025a). *Electricity derivatives markets*. Fortum.com [online] Available at: <https://www.fortum.com/news-and-publications/fact-sheets/electricity-derivatives-markets> [Accessed 3 March 2025]

Fortum. (2025b). *The Power of Nordic Energy - A great place for industrial decarbonisation*. Whitepaper. Retrieved from: <https://www.fortum.com/services/power-trading-and-energy-supply/fortum-insights/nordics-great-place-industrial-decarbonisation> [Accessed 12 March 2025]

Fortum. (2025c). *Kalax wind farm*. Fortum.com. [online] Available at: <https://www.fortum.com/energy-production/wind-power/farms/kalax-wind-farm> [Accessed 2 May 2025]

Fortum. (2025d). *Solberg wind farm*. Fortum.com. [online] Available at: <https://www.fortum.com/energy-production/wind-power/farms/solberg-wind-farm> [Accessed 2 May 2025]

Fortum. (2025e). *Sørfjord wind farm*. Fortum.com. [online] Available at: <https://www.fortum.com/energy-production/wind-power/farms/sorfjord-wind-farm> [Accessed 2 May 2025]

Gasum. (2025). *Kaupankäynti päivänsisäisellä Intraday-markkinalla*. Gasum.com [online] Available at: <https://www.gasum.com/fi/energia-yrityksille/energiamarkkinapalvelut/valvomo/intraday-kaupankaynti/> [Accessed 11 March 2025]

He, G., Chen, Q., Kang, C., Xia, Q. and Poola, K. (2017). *Cooperation of Wind Power and Battery Storage to Provide Frequency Regulation in Power Markets*. IEEE Transactions on Power Systems, 32(5), pp.3559–3568. doi:<https://doi.org/10.1109/tpwrs.2016.2644642>

Hemmati, M., Bayati, N. and Ebel, T. (2024). *Life Cycle Assessment and Costing of Large-Scale Battery Energy Storage Integration in Lombok's Power Grid*. Batteries, [online] 10(8), pp.295–295. doi:<https://doi.org/10.3390/batteries10080295>

Hepworth, H. (2025). *Svensk elproduktion och installerad effekt 2024 – en regional översikt*. Energiföretagen Sverige. [online] Available at: <https://www.energiforetagen.se/medlemsportalen/medlemsnyheter/2025/mars/svensk-elproduktion-och-installerad-effekt-2024--en-regional-oversikt2/> [Accessed 19 May 2025]

Hossain, E., Faruque, H.M.R., Sunny, Md.S.H., Mohammad, N. and Nawar, N. (2020). *A Comprehensive Review on Energy Storage Systems: Types, Comparison, Current Scenario, Applications, Barriers, and Potential Solutions, Policies, and Future Prospects*. Energies, 13(14), p.3651. doi:<https://doi.org/10.3390/en13143651>

Hukkinen, O. (2024). *Business case analysis of a battery energy storage system co-located with a wind park: A Finnish case study*. Aalto.fi. [online] Available at: <https://aaltodoc.aalto.fi/items/606288c5-803e-4170-942d-e78dae83d97d> [Accessed 15 February 2025]

Huvilinna, J. (2015). *Value of Battery Energy Storage at Ancillary Service Markets*. Aalto.fi. [online] Available at: <https://aalto-doc.aalto.fi/items/78a68b74-a7a4-4497-aa5f-4da3839b8181> [Accessed 22 May 2025]

IEA. (2025). *Norway*. IEA.org. [online] Available at: <https://www.iea.org/countries/norway/electricity> [Accessed 19 May 2025]

IEA Wind TCP. (2022). *Wind Energy in Norway*. IEA-wind.org. [online] Available at: <https://iea-wind.org/about-iea-wind-tcp/members/norway/> [Accessed 19 May 2025]

Ikäheimo, S., Malmi, T., Walden, R. (2024). *Yrityksen laskentatoimi*. 9th edition. Alma Insight Helsinki 2024. ISBN 978-952-14-5234-5

Ilyukhin, S. and Sainio, J. (2024). *Recipe for successful PPA, with wind and solar power as ingredients*. Fortum.com. [online] Available at: <https://www.fortum.com/news-and-publications/forthedoers-blog/recipe-successful-ppa> [Accessed 3 March 2025]

IRENA. (2015). *Battery Storage for Renewables: Market Status and Technology Outlook*. International Renewable Energy Agency. Available at: https://www.irena.org/-/media/Files/IRENA/Agency/Publication/2015/IRENA_Battery_Storage_report_2015.pdf [Accessed 24 April 2025]

IRENA. (2017). *Electricity Storage and Renewables: Costs and Markets to 2030*. International Renewable Energy Agency. ISBN 978-92-9260-038-9. Available at: https://www.irena.org/-/media/Files/IRENA/Agency/Publication/2017/Oct/IRENA_Electricity_Storage_Costs_2017.pdf [Accessed 6 May 2025]

IRENA. (2020). *Electricity Storage Valuation Framework: Assessing system value and ensuring project viability*. International Renewable Energy Agency. ISBN 978-92-9260-161-4. Available at: https://www.irena.org/-/media/Files/IRENA/Agency/Publication/2020/Mar/IRENA_storage_valuation_2020.pdf [Accessed 10 May 2025]

IRENA. (2024). *Renewable power generation costs in 2023*. International Renewable Energy Agency. ISBN: 978-92-9260-621-3. Available at: <https://www.irena.org/Publications/2024/Sep/Renewable-Power-Generation-Costs-in-2023> [Accessed 15 May 2025]

Jaakamo, N. (2020). *Impact of the 15-Minute Imbalance Settlement Period and Electricity Storage on an Independent Wind Power Producer*. Aalto.fi. [online] Available at: <https://aalto-doc.aalto.fi/items/153f7ad6-97c6-4024-99e5-ee425e33309d> [Accessed 15 February 2025]

Jimenez, D., Ortiz-Villalba, D., Perez, A. and Orchard, M.E. (2018). *Lithium-ion Battery Degradation Assessment in Microgrids*. IEEE International Autumn Meeting on Power, Electronics and Computing (ROPEC). doi:<https://doi.org/10.1109/ropec.2018.8661410>

Joshi, P. and Gokhale-Welch, C. (2022). *Fundamentals of Wind Energy*. National Renewable Energy Laboratory. Available at: <https://docs.nrel.gov/docs/fy23osti/84501.pdf> [Accessed 14 May 2025]

Kalmikov, A. (2017). *Wind Power Fundamentals*. Wind Energy Engineering, pp.17–24. doi:<https://doi.org/10.1016/b978-0-12-809451-8.00002-3>

Ke, X., Lu, N. and Jin, C. (2015). *Control and Size Energy Storage Systems for Managing Energy Imbalance of Variable Generation Resources*. IEEE Transactions on Sustainable Energy, 6(1), pp.70–78. doi:<https://doi.org/10.1109/tste.2014.2355829>

Kebede, A.A., Kalogiannis, T., Van Mierlo, J. and Bercibar, M. (2022). *A comprehensive review of stationary energy storage devices for large scale renewable energy sources grid integration*. Renewable and Sustainable Energy Reviews, [online] 159(112213). doi:<https://doi.org/10.1016/j.rser.2022.112213>

Laine-Ylijoki, J. (2024). *Techno-Economic Analysis of Battery Energy Storage Systems in Wind Power Plants and Reserve Markets*. Aalto.fi. [online] Available at: <https://aaltodoc.aalto.fi/items/1b8554bf-30d2-4a92-936b-0b621a656659> [Accessed 13 February 2025]

Laukkanen, J. (2023). *Akustot ja muut energiavarastot välttämätön osa uusittuvan energian tehokasta käyttöä*. Sweco.fi. [online] Available at: <https://www.sweco.fi/blog/akustot-energian-varastointiin/> [Accessed 22 May 2025]

Leinonen, P. (2018). *What is inertia?*. Fingridlehti. [online] Available at: <https://www.fingridlehti.fi/en/what-is-inertia/#b1688b08> [Accessed 28 February 2025]

Li, J., Wang, C. and Wang, H. (2023). *Optimal Energy Storage Scheduling for Wind Curtailment Reduction and Energy Arbitrage: A Deep Reinforcement Learning Approach*. arXiv (Cornell University) doi:<https://doi.org/10.48550/arXiv.2304.02239>

Lieskoski, S., Koskinen, O., Tuuf, J. and Björklund-Sänkiaho, M. (2024). *A review of the current status of energy storage in Finland and future development prospects*. Journal of energy storage, 93, pp.112327–112327. doi:<https://doi.org/10.1016/j.est.2024.112327>

Lundström, M. (2024). *Has the Nordic-Baltic wind power success story come to an end?* Nordic Investment Bank. [online] Available at: <https://www.nib.int/cases/has-the-nordic-baltic-wind-power-success-story-come-to-an-end> [Accessed 19 May 2025]

Mahesh, M., Bhaskar, D.V., Jisha, R.K., Krishan, R. and Gnanadass, R. (2021). *Lifetime estimation of grid connected LiFePO₄ battery energy storage systems*. Electrical Engineering. doi:<https://doi.org/10.1007/s00202-021-01371-w>

Miettinen, J. and Holttinen, H. (2019). *Impacts of wind power forecast errors on the real-time balancing need: a Nordic case study*. IET Renewable Power Generation, 13(2), pp.227–233. doi:<https://doi.org/10.1049/iet-rpg.2018.5234>

Mimer. (2025). *Statistik*. Svenska Kraftnät. Open Data. [online] Available at: <https://mimer.svk.se/ProductionConsumption/ProductionIndex>

Mitali, J., Dhinakaran, S. and Mohamad, A.A. (2022). *Energy storage systems: A review*. Energy Storage and Saving, 1(3). doi:<https://doi.org/10.1016/j.enss.2022.07.002>

Modig, N., et al. (2022). *Overview of Frequency Control in the Nordic Power System*. ENTSO-E. Available at: <https://www.epressi.com/media/userfiles/107305/1648196866/overview-of-frequency-control-in-the-nordic-power-system-1.pdf> [Accessed 28 February 2025]

Mouais, T. and Qaisar, S.M. (2023). *A Comprehensive Review of the Li-Ion Batteries Fast-Charging Protocols*. In: Dhundhara, S., Verma Y.P, and Kumar, A. *Energy Storage Technologies in Grid Modernization*. Wiley. doi: <https://doi.org/10.1002/9781119872146.ch2>

Muikku, J. (2025). *E-mail conversation*. Fingrid. 16 April 2025

Määttänen, M. (2023). *Kuinka sähkö kulkee?* Fingridlehti. [online] Available at: <https://www.fingridlehti.fi/kuinka-sahko-kulkee/> [Accessed 28 February 2025]

Nano Energies. (2025). *Automatic Frequency Restoration Reserve (aFRR)*. Available at: <https://nanoenergies.eu/knowledge-base/automatic-frequency-restoration-reserve-afrr> [Accessed 8 April 2025]

Naumann, M., Spingler, F.B. and Jossen, A. (2020). *Analysis and modeling of cycle aging of a commercial LiFePO₄/graphite cell*. Journal of Power Sources, 451, p.227666. doi:<https://doi.org/10.1016/j.jpowsour.2019.227666>

NEMO Committee. (2024). *Information Package About Intraday Auction*. Available at: <https://www.nemo-committee.eu/assets/files/information-package-about-intraday-auction.pdf> [Accessed 12 March 2025]

Next Kraftwerke. (2025). *What does intraday trading mean?*. Next-kraftwerke.com. [online] Available at: <https://www.next-kraftwerke.com/knowledge/intraday-trading> [Accessed 11 March 2025]

Nord Pool. (2024). *Intraday Market Regulations*. Available at: <https://www.nordpoolgroup.com/49c3b9/globalassets/download-center/rules-and-regulations/intraday-market-regulations--13.06.24.pdf> [Accessed 12 March 2025]

Nord Pool. (2025a). *Market members*. Nordpool.com. [online] Available at: <https://www.nordpoolgroup.com/en/the-power-market/The-market-members/> [Accessed 28 February 2025]

Nord Pool. (2025b). *Bidding areas*. Nordpool.com. [online] Available at: <https://www.nordpoolgroup.com/en/the-power-market/Bidding-areas/> [Accessed 28 February 2025]

Nord Pool. (2025c). *Price formation*. Nordpool.com. [online] Available at: <https://www.nordpoolgroup.com/en/the-power-market/Day-ahead-market/Price-formation/> [Accessed 6 March 2025]

Nord Pool. (2025d). *Day-ahead market*. Nordpool.com. [online] Available at: <https://www.nordpoolgroup.com/en/the-power-market/Day-ahead-market/> [Accessed 6 March 2025]

Nord Pool. (2025e). *Product Specifications: Nordic / Baltic Market Areas*. Available at: <https://www.nordpoolgroup.com/49314f/globalassets/download-center/rules-and-regulations/product-specifications---nordic-and-baltic-market-areas-valid-from-18.03.2025.pdf> [Accessed 12 March 2025]

Nord Pool. (2025f). *About the SIDC Intraday Auctions (IDAs)*. Nordpool.com. [online] Available at: <https://support.nordpoolgroup.com/support/solutions/articles/8000111575> [Accessed 12 March 2025]

Nord Pool. (2025g). *Reports*. Nordpool.com. Data Portal. [online] Available with license at: <https://data.nordpoolgroup.com/reports>

Nordic Balancing Model. (2019). *Roadmap Report*. Available at: <https://nordic-balancingmodel.net/wp-content/uploads/2019/11/NBM-Roadmap-Report-updated-after-consultation.pdf> [Accessed 17 April 2025]

Nordic Balancing Model. (2021). *Single price-single position implemented on 1 November in the Nordic countries*. nordicbalancingmodel.net. [online] Available at: <https://nordicbalancingmodel.net/single-price-single-position-implemented-on-1-november-in-the-nordic-countries/> [Accessed 17 April 2025]

Nordic Balancing Model. (2024a). *Market Handbook – Nordic FFR capacity markets*. Version 2.0. Available at: <https://nordicbalancingmodel.net/wp-content/uploads/2024/12/Market-handbook-FFR-CM-Version-2.0.pdf> [Accessed 10 April 2025]

Nordic Balancing Model. (2024b). *Explanatory document to the proposal for the establishment of common and harmonised rules and processes for the exchange and procurement of mFRR balancing capacity between the bidding zones of Denmark, Finland, and Sweden*. Available at: <https://nordicbalancingmodel.net/wp-content/uploads/2024/02/Explanatory-document-to-proposal-for-methodologies-referring-to-EBGL-article-33-and-38-%E2%80%93-trilateral-mFRR-CM.pdf> [Accessed 9 April 2025]

Nordic Balancing Model. (2024c). *Trilateral capacity market for mFRR is live*. nordicbalancingmodel.net. [online] Available at: <https://nordicbalancingmodel.net/trilateral-capacity-market-for-mfrr-is-live/> [Accessed 9 April 2025]

Nordic Balancing Model. (2024d). *BSP – Implementation Guide – mFRR energy activation market*. Available at: <https://nordicbalancingmodel.net/wp-content/uploads/2024/09/Implementation-Guide-mFRR-energy-activation-market-BSP-v116.pdf> [Accessed 14 April 2025]

Nordic Balancing Model. (2025a). *Roadmap and Projects*. nordicbalancingmodel.net. [online] Available at: <https://nordicbalancingmodel.net/roadmap-and-projects/> [Accessed 9 April 2025]

Nordic Balancing Model. (2025b). *Nordic mFRR capacity market*. nordicbalancingmodel.net. [online] Available at: <https://nordicbalancingmodel.net/roadmap-and-projects/nordic-mfrr-capacity-market/> [Accessed 9 April 2025]

Nordic Balancing Model. (2025c). *Automated mFRR energy activation market*. nordicbalancingmodel.net. [online] Available at: <https://nordicbalancingmodel.net/roadmap-and-projects/automated-nordic-mfrr-energy-activation-market/> [Accessed 9 April 2025]

Nordic Balancing Model. (2025d). *15 min Imbalance Settlement Period*. nordicbalancingmodel.net. [online] Available at: <https://nordicbalancingmodel.net/roadmap-and-projects/15-min-time-resolution/> [Accessed 17 April 2025]

NordREG. (2019). *An overview of the Nordic electricity market*. [online] Available at: <https://www.nordicenergyregulators.org/about-nordreg/an-overview-of-the-nordic-electricity-market/> [Accessed 28 February 2025]

Norwegian Ministry of Energy. (2024a). *The Electricity Grid*. Energy Facts Norway. Energifaktanorge.no. [online] Available at: <https://energifaktanorge.no/en/norsk-energiforsyning/kraftnett/> [Accessed 28 February 2025]

Norwegian Ministry of Energy. (2024b). *The power market*. Energy Facts Norway. Energifaktanorge.no. [online] Available at: <https://energifaktanorge.no/en/norsk-energiforsyning/kraftmarkedet/> [Accessed 6 March 2025]

Noyanbayev, N.K., Forsyth, A.J. and Feehally, T. (2018). *Efficiency analysis for a grid-connected battery energy storage system*. Materials Today: Proceedings, 5(11), pp.22811–22818. doi:<https://doi.org/10.1016/j.matpr.2018.07.095>

NREL. (2024). *Utility-Scale Battery Storage*. atb.nrel.gov. [online] Available at: https://atb.nrel.gov/electricity/2024/utility-scale_battery_storage [Accessed 9 May 2025]

NVE. (2025). *Data for utbygde vindkraftverk i Norge*. nve.no. [online] Available at: <https://www.nve.no/energi/energisystem/vindkraft-paa-land/data-for-utbygde-vindkraftverk-i-norge/> [Accessed 19 May 2025]

Othman, H. (2022). *Energy Storage Applications in Transmission and Distribution Grids*. Cambridge University Press & Assessment. ISBN: 9781009014038. Available at: <https://www.cambridge.org/us/university-press/subjects/engineering/energy-technology/energy-storage-applications-transmission-and-distribution-grids?format=PB&isbn=9781009014038> [Accessed 9 May 2025]

Ovaskainen, M., Paakkunainen, T., and Barcón, S. (2023). *Main characteristics to consider in a BESS during the design process*. 2022 IEEE International Autumn Meeting on Power, Electronics and Computing (ROPEC), [online] pp.1–9. doi:<https://doi.org/10.1109/ropec58757.2023.10409379>.

O'Malley, M., et al. (2024). *Grand challenges of wind energy science – meeting the needs and services of the power system*. Wind energy science, 9(11), pp.2087–2112. doi:<https://doi.org/10.5194/wes-9-2087-2024>

Pantzar, M. (2024). *Sähköön kulutus hurjassa kasvussa – Fingrid: ”Kaksinkeräistäuu 10 vuodessa*. yle.fi. [online] Available at: <https://yle.fi/a/74-20130045> [Accessed 12 August 2025]

Pinto, G.X.A., Napolini, H.F. and Rütther, R. (2024). *Assessing the economic viability of BESS in distributed PV generation on public buildings in Brazil: A 2030 outlook*. Renewable Energy, [online] 225, p.120252. doi:<https://doi.org/10.1016/j.renene.2024.120252>

Pusceddu, E., Zakeri, B. and Castagneto Gisse, G. (2021). *Synergies between energy arbitrage and fast frequency response for battery energy storage systems*. *Applied Energy*, 283, p.116274. doi:<https://doi.org/10.1016/j.apenergy.2020.116274>

Renewables Finland. (2024). *Tuulivoima Suomessa 31.12.2024*. Available at: https://suomenuusiutuivat.fi/media/tuulivoima_vuositilastot-2024-1.pdf [Accessed 19 May 2025]

Rystad Energy. (2023). *Five key parameters of BESS capex*. Whitepaper. Retrieved from: <https://www.rystadenergy.com/insights/five-key-parameters-of-bess-capex> [Accessed 9 May 2025]

Saulny, N. (2017). *Operation and Profitability of Batteries in Electricity Reserve Markets*. Aalto.fi. [online] Available at: <https://aaltodoc.aalto.fi/items/be2boec9-ab08-4777-a01d-4b8bde2344be> [Accessed 24 April 2025]

Sheridan, C. and Conlon, M. (2021). *A Techno-Economic Evaluation of Battery Energy Storage Systems co-located with Wind in the Irish Integrated Electricity Market*. doi:<https://doi.org/10.1109/upec50034.2021.9548207>

SKGS. (2024). *The Swedish Industry's Demand for Electricity up to 2035*. Version 3. Available at: <https://skgs.org/app/uploads/sites/2/2024/09/Swedish-Industries-Electricity-Demand-SKGS-2024.pdf> [Accessed 12 August 2025]

Solovian, A. (2019). *Impact of quarter hourly imbalance settlement period on the Nordic physical electricity market*. Aalto.fi. [online] Available at: <https://aaltodoc.aalto.fi/items/1ea3b1e3-76b6-4718-a041-14b6aefdb8b2> [Accessed 10 March 2025]

Standard Renewables. (2023). *How BESS Can Boost Financial Margins for Wind Farms*. standardrenewables.com. [online]. Available at: <https://standardrenewables.com/how-bess-can-boost-financial-margins-for-wind-farms/> [Accessed 22 May 2025]

Statnett. (2018). *How the power system works*. Statnett.no. [online] Available at: <https://www.statnett.no/en/about-statnett/The-power-system/how-the-power-system-works/> [Accessed 28 February 2025]

Statnett. (2022). *Quarterly resolution and the energy markets*. Statnett.no. [online] Available at: <https://www.statnett.no/en/for-stakeholders-in-the-power-industry/system-operation/the-power-market/quarterly-resolution-and-the-energy-markets/> [Accessed 17 April 2025]

Statnett. (2024a). *Primærreserver – FCR*. Statnett.no. [online] Available at: <https://www.statnett.no/for-aktorer-i-kraftbransjen/systemansvaret/kraft-markedet/reservemarkeder/primarreserver/> [Accessed 31 March 2025]

Statnett. (2024b). *Raske frekvensreserver - FFR*. Statnett.no. [online] Available at: <https://www.statnett.no/for-aktorer-i-kraftbransjen/systemansvaret/kraft-markedet/reservemarkeder/ffr/> [Accessed 3 April 2025]

Statnett. (2024c). *Transmission grid tariffs for 2024*. Available at: <https://www.statnett.no/globalassets/for-aktorer-i-kraftsystemet/tariff/tariff-booklet-2024.pdf> [Accessed 23 June 2025]

Statnett. (2025a). *Sekundærreserver – aFRR*. Statnett.no. [online] Available at: <https://www.statnett.no/for-aktorer-i-kraftbransjen/systemansvaret/kraft-markedet/reservemarkeder/sekundarreserver/> [Accessed 11 April 2025]

Statnett. (2025b). *Tertiærreserver – mFRR*. Statnett.no. [online] Available at: <https://www.statnett.no/for-aktorer-i-kraftbransjen/systemansvaret/kraft-markedet/reservemarkeder/tertiarreserver/> [Accessed 14 April 2025]

Statnett. (2025c). *Last ned grunndata*. Statnett.no. Open Data. [online] Available at: <https://www.statnett.no/for-aktorer-i-kraftbransjen/tall-og-data-fra-kraftsystemet/last-ned-grunndata/>

Statnett. (2025d). *NettWeb – portal for tariffkunder*. Data portal. [online] Available at: <https://nettavregning.statnett.no/#/marginalloss/details>

Statnett., Fingrid., Energinet., Svenska Kraftnät. (2019). *Nordic Grid Development Plan 2019*. Available at: <https://www.statnett.no/contentassets/61e33bec85804310a0feef41387da2c0/nordic-grid-development-plan-2019-for-web.pdf> [Accessed 28 February 2025]

Suvic. (2025). *BESS solutions complement renewable energy construction*. Suvic.fi. [online] Available at: <https://www.suvic.fi/en/news/bess-systems-and-hybrid-parks-complement-renewable-energy-development> [Accessed 22 May 2025]

Svenska Kraftnät. (n.d.). *Villkor för Leverantör av FCR*. Bilaga till Avtal om leverans av Balanstjänster. Bilaga 2. Available at: <https://www.svk.se/49e793/siteassets/aktorsportalen/bsp-och-brp/kommande-avtal-bsp-och-brp/kommande-avtal-bsp/bilaga-2-villkor-fcr-5937-2.pdf> [Accessed 31 March 2025]

Svenska Kraftnät. (2024a). *Svenska kraftnät increases the FCR-D down procurement in 2025*. Svk.se. [online] Available at: <https://www.svk.se/en/about-us/news/news/svenska-kraftnat-increases-the-fcr-d-down-procurement-in-2025/> [Accessed 31 March 2025]

Svenska Kraftnät. (2024b). *Snabb frekvensreserv (FFR)*. Svk.se. [online] Available at: <https://www.svk.se/aktorsportalen/bidra-med-reserver/om-olika-reserver/ffr/> [Accessed 4 April 2025]

Svenska Kraftnät. (2024c). *Nordisk kapacitetsmarknad för aFRR*. Svk.se. [online] Available at: <https://www.svk.se/utveckling-av-kraftsystemet/systemansvar--elmarknad/ny-nordisk-balanseringsmodell-nbm/nordisk-kapacitetsmarknad-for-afrr/> [Accessed 11 April 2025]

Svenska Kraftnät. (2024d.) *Prislista 2024 för Transmissionsnätet*. Available at: <https://www.svk.se/siteassets/aktorsportalen/anslut-till-transmissionsnätet/transmissionsnatstariff/arkiverade-prislistor/prislista-2024-for-transmissionsnätet.pdf> [Accessed 23 June 2025]

Svenska Kraftnät. (2025a). *The control room*. Svk.se. [online] Available at: <https://www.svk.se/en/national-grid/the-control-room/> [Accessed 28 February 2025]

Svenska Kraftnät. (2025b). *Tariff, prislistor, avtal och abonnemang*. Svk.se. [online] Available at: <https://www.svk.se/aktorsportalen/anslut-till-transmissionsnätet/transmissionsnatstariffen/tariff-prislistor-avtal-abonnemang/> [Accessed 22 April 2025]

Svenska Kraftnät. (2025c). *Behov av reserver idag och i framtiden*. Svk.se. [online] Available at: <https://www.svk.se/aktorsportalen/bidra-med-reserver/behov-av-reserver-nu-och-i-framtiden/> [Accessed 11 April 2025]

Svenska Kraftnät. (2025d). *Automatisk frekvensåterställningsreserv (aFRR)*. Svk.se. [online] Available at: <https://www.svk.se/aktorsportalen/bidra-med-reserver/om-olika-reserver/afrr/> [Accessed 11 April 2025]

Svenska Kraftnät. (2025e). *Avropad volym och kostnader 2024 års upphandling*. Svk.se. [online] Retrieved from: <https://www.svk.se/aktorsportalen/bidra-med-reserver/om-olika-reserver/ffr/behov-av-ffr/> [Accessed 18 June 2025]

Ullah, F., et al. (2024). *A Comprehensive Review of Wind Power Integration and Energy Storage Technologies for Modern Grid Frequency Regulation*. *Heliyon*, 10(9), pp.e30466–e30466. doi:<https://doi.org/10.1016/j.heliyon.2024.e30466>

U.S Department of Energy. (2025). *How a Wind Turbine Works*. Energy.gov. [online] Available at: <https://www.energy.gov/eere/wind/how-wind-turbine-works-text-version> [Accessed 15 May 2025]

Vinci, G., Arangia, V, C., Ruggieri, R., Savastano, M. and Ruggeri, M. (2024). *Reuse of Lithium Iron Phosphate (LiFePO₄) Batteries from a Life Cycle Assessment Perspective: The Second-Life Case Study*. *Energies*, [online] 17(11), pp.2544–2544. doi:<https://doi.org/10.3390/en17112544>

Vold, E. (2025). *E-mail conversation*. Statnett. 15 April 2025

Volta Foundation. (2025). *Battery Report 2024*. Report. Retrieved from: <https://volta.foundation/battery-report-2024/download-the-2024-battery-report> [Accessed 23 April 2025]

Weaver, N. (2022). *Inertia (and rate of change of frequency): an introduction*. Modoenergy.com. [online] Available at: <https://modoenergy.com/research/system-inertia-grid-frequency-rocof-explainer> [Accessed 14 March 2025]

Xu, B., Oudalov, A., Ulbig, A., Andersson, G. and Kirschen, D.S. (2018). *Modeling of Lithium-Ion Battery Degradation for Cell Life Assessment*. *IEEE Transactions on Smart Grid*, 9(2), pp.1131–1140. doi:<https://doi.org/10.1109/tsg.2016.2578950>

Zhu, R., Das, K., Sørensen, P.E. and Hansen, A.D. (2023). *Optimal Participation of Co-Located Wind–Battery Plants in Sequential Electricity Markets*. *Energies*, 16(15), p.5597. doi:<https://doi.org/10.3390/en16155597>